

Winter 2011

Synthesis of 6-thiosubstituted pentacenes and study of an unexpected photorearrangement of 6-phenylthiopentacene dimer

Julia Y K Chan

University of New Hampshire, Durham

Follow this and additional works at: <https://scholars.unh.edu/thesis>

Recommended Citation

Chan, Julia Y K, "Synthesis of 6-thiosubstituted pentacenes and study of an unexpected photorearrangement of 6-phenylthiopentacene dimer" (2011). *Master's Theses and Capstones*. 678.
<https://scholars.unh.edu/thesis/678>

This Thesis is brought to you for free and open access by the Student Scholarship at University of New Hampshire Scholars' Repository. It has been accepted for inclusion in Master's Theses and Capstones by an authorized administrator of University of New Hampshire Scholars' Repository. For more information, please contact nicole.hentz@unh.edu.

SYNTHESIS OF 6-THIOSUBSTITUTED PENTACENES AND STUDY OF AN
UNEXPECTED PHOTOREARRANGEMENT OF 6-PHENYLTHIOPENTACENE
DIMER

BY

Julia Y. K. Chan
B.Sc. University of British Columbia, 2009

THESIS

Submitted to the University of New Hampshire
in Partial Fulfillment of
the Requirements for the Degree of

Master of Science
in
Chemistry

December, 2011

UMI Number: 1507816

All rights reserved

INFORMATION TO ALL USERS

The quality of this reproduction is dependent upon the quality of the copy submitted.

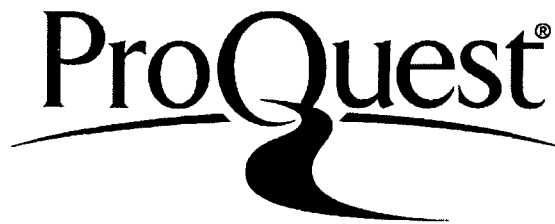
In the unlikely event that the author did not send a complete manuscript and there are missing pages, these will be noted. Also, if material had to be removed, a note will indicate the deletion.



UMI 1507816

Copyright 2012 by ProQuest LLC.

All rights reserved. This edition of the work is protected against unauthorized copying under Title 17, United States Code.



ProQuest LLC
789 East Eisenhower Parkway
P.O. Box 1346
Ann Arbor, MI 48106-1346

This thesis has been examined and approved.

Glen P. Miller, Thesis Director
Professor of Chemistry

Gary R. Weisman
Professor of Chemistry

Christopher F. Bauer
Professor of Chemistry

Samuel Pazicni
Assistant Professor of Chemistry

Date

"Dripping water can eat through a stone."

-Chinese Proverb

ACKNOWLEDGEMENTS

It is my pleasure to thank those who made this thesis possible. First and foremost, I would like to say a big thank you to my advisor Dr. Glen Miller for his guidance, enthusiasm, and optimism throughout my research. Through his genuine encouragement and support, both financially and intellectually, I was motivated to carry on my research during times when my reactions consistently failed to succeed and I was too emotionally frustrated to carry on my research any further. Through working with Dr. Miller, I learned how to become a better writer, presenter, and speaker!

I would also like to thank my committee members who took the time to proof read my thesis and for contributing in any way possible to make my experience in graduate school a positive learning experience. Dr. Weisman's NMR course has provided me with a lot of fundamental knowledge on how to interpret NMR. I also want to thank Dr. Bauer, Dr. Pazicni, and the rest of the Chemistry Education group for their continued intellectual support, consideration, understanding, and keeping me sane when my reactions kept failing!

I would like to thank the entire Miller group for all that they have taught me, not only in laboratory skills but also life skills. When I was frustrated, you were all kind and offered assistance and reminded me to "enjoy the journey" and focus less on the result. I want to thank Dr. Weimin Lin, Dr. Chandrani Pramanik, and Dr. Jennifer Hodgsons for spending time to proof read my thesis.

No acknowledgement is complete without thanking my family. I can never thank my parents, Sharon Chow and Raymond Chan, enough for convincing me to pursue in

graduate school and their endless support, advices, and daily encouragements! I want to also thank my brother, Richard Chan, for making me smile and sending me funny text messages during the stressful times.

I would like to thank the Chemistry Department for being so kind and generous to me. I would also like to thank the "National Science Foundation" and "Center for the High-Rate Nanomanufacturing" for funding me throughout my research.

Last but not least, I would like to thank God for giving me this wonderful opportunity of studying abroad and meeting new people. I would not have been able to walk this journey alone without your constant support and guidance.

Thank you for reading my thesis!

TABLE OF CONTENTS

| | |
|--|------|
| ACKNOWLEDGEMENTS..... | iv |
| LIST OF FIGURES..... | viii |
| LIST OF SCHEMES..... | x |
| LIST OF TABLES..... | xii |
| LIST OF NUMBERED STRUCTURES..... | xiii |
| ABSTRACT..... | xvi |
| CHAPTER 1: INTRODUCTION..... | 1 |
| 1.1 Acenes..... | 1 |
| 1.2 Pentacene..... | 4 |
| 1.2.1 Functionalization of pentacenes..... | 5 |
| 1.2.2 Stability of disubstituted pentacenes..... | 6 |
| 1.2.3 Stability of dithiosubstituted pentacenes..... | 8 |
| 1.2.4 Packing arrangement of thiosubstituted pentacenes..... | 10 |
| 1.3 Monosubstituted Pentacenes..... | 11 |
| 1.3.1 Applications of monosubstituted pentacenes..... | 14 |
| 1.4 Photodegradation of Acenes..... | 16 |
| 1.4.1 Photooxidation..... | 16 |
| 1.4.2 Photodimerization..... | 18 |
| CHAPTER 2: RESULTS AND DISCUSSION..... | 20 |
| 2.1 Synthesis of 6-organothio substituted pentacenes..... | 20 |
| 2.2 ¹ H NMR spectra of 6-organothio substituted pentacenes..... | 23 |
| 2.3 Investigations of photodegradation of monoadduct 26 and 27 | 27 |

| | | |
|-------------------------------|---|----|
| 2.3.1 | Monitoring photodegradation by UV-Vis spectrophotometry... | 27 |
| 2.3.2 | Scaling the photodegradation in a quartz vessel: formation of bisadduct 32 in 20% yield..... | 31 |
| 2.3.3 | Monitoring photodegradation of monoadduct 26 by NMR..... | 32 |
| 2.4 | DFT investigation of photodimerization..... | 37 |
| 2.4.1 | Substitution pattern and effects for dimerization..... | 37 |
| 2.4.2 | DFT investigation of photodimer products..... | 39 |
| 2.4.3 | Reaction pathways for dimerization and rearrangement of monoadduct 26 | 42 |
| 2.4.4 | Proposed mechanism for the photorearrangement of 6-phenylthiopentacene dimer..... | 45 |
| CHAPTER 3: CONCLUSIONS..... | | 48 |
| CHAPTER 4: EXPERIMENTALS..... | | 49 |
| 4.1 | General Methods..... | 49 |
| 4.2 | Column Chromatography..... | 51 |
| 4.3 | Solvents..... | 52 |
| 4.4 | Reagents..... | 52 |
| 4.5 | Syntheses..... | 53 |
| List of References..... | | 58 |
| Appendices..... | | 63 |

LIST OF FIGURES

| <u>Figure</u> | | <u>Page</u> |
|--|--|-------------|
| <u>CHAPTER 1: INTRODUCTION</u> | | |
| 1.1 | Acene series..... | 2 |
| 1.2 | Numbering scheme in anthracene, tetracene and pentacene..... | 3 |
| 1.3 | Substituted pentacene derivatives..... | 6 |
| 1.4 | Ethynyl substituted pentacenes..... | 7 |
| 1.5 | TIPS-pentacene functionalized at the 6,13 position, 4 , and 5,14 positions, 12 | 8 |
| 1.6 | 2-D network sheet of 6,13-bis(methylthio)pentacene in the crystal structure: (a) front and (b) top views..... | 11 |
| 1.7 | Monosubstituted pentacene derivatives..... | 12 |
| 1.8 | "Butterfly" dimers formed at the 6,13 positions and at the 5,14 positions..... | 19 |
| <u>CHAPTER 2: RESULTS AND DISCUSSION</u> | | |
| 2.1 | ¹ H NMR spectra of 6-phenylthiopentacene, 26 in CDCl ₃ | 24 |
| 2.2 | ¹ H NMR spectra of 6,13-bis(phenylthio)pentacene, 32 in CDCl ₃ | 25 |
| 2.3 | Stacked ¹ H NMR spectra of 6-acetylthiopentacene, 22 , in <i>d</i> ₆ -DMSO and <i>d</i> ₆ -benzene..... | 27 |
| 2.4 | UV-Vis study for the photodegradation of 6-phenylthiopentacene..... | 29 |
| 2.5 | UV-Vis study for the photodegradation of 6-acetylthiopentacene..... | 30 |
| 2.6 | Reaction setup for the photodegradation study of 26 dissolved in CDCl ₃ in a quartz round bottom flask under an Ar atmosphere and irradiation of a solution of 26 with 254 nm UV light..... | 32 |

| | | |
|------|---|----|
| 2.7 | Concentration-time profiles of 26 , 32 , 17 , and 33 , observed by ¹ H NMR spectroscopy over a nine day period during the photodegradation of 26 in a Pyrex® valve NMR tube. Time refers to the duration of 254 nm light irradiation..... | 34 |
| 2.8 | ¹ H NMR spectra over the course of a nine day period with intermittent irradiation of 254 nm UV light..... | 36 |
| 2.9 | Reaction pathway showing Gibbs free energies (298.15 K) for the endo anti dimerization of 26 | 42 |
| 2.10 | Reaction pathway showing Gibbs free energies (298.15 K) for intramolecular substituent transfer on the endo anti photodimer of 26 . Energies are relative to the combined energy of two separate molecules of 26 | 43 |

LIST OF SCHEMES

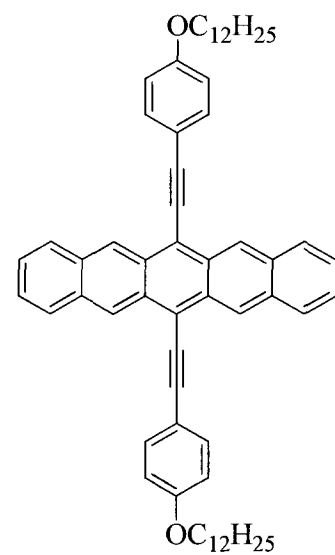
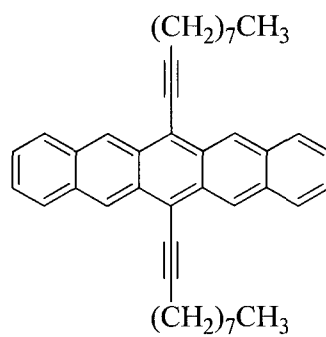
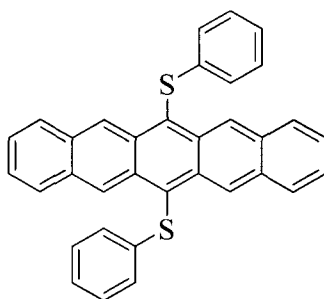
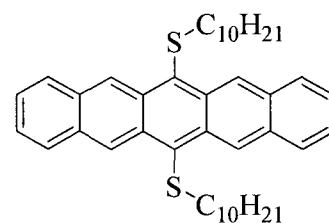
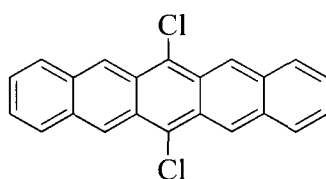
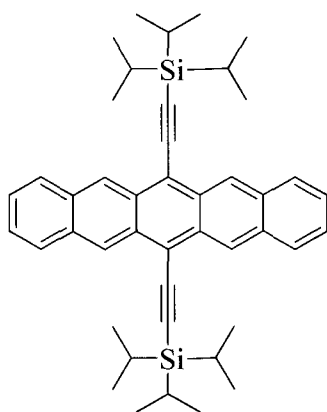
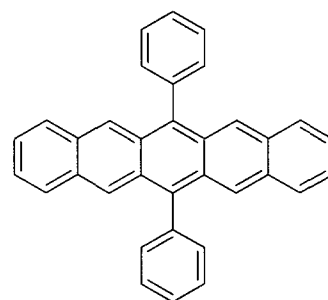
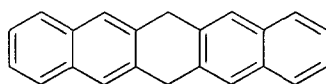
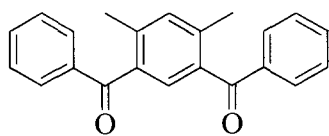
| <u>Scheme</u> | | <u>Page</u> |
|--|--|-------------|
| <u>CHAPTER 1: INTRODUCTION</u> | | |
| 1.1 | Synthesis of pentacene by Clar (1929)..... | 4 |
| 1.2 | Synthesis of 6-hydroxypentacene, 14 | 12 |
| 1.3 | Synthesis of 6-thien-2'-ylpentacene, 15 | 13 |
| 1.4 | Synthesis of other monoarylsubstituted pentacenes..... | 14 |
| 1.5 | Synthesis of 6-phenylpentacene, 16 | 14 |
| 1.6 | Photooxidation pathway for acenes..... | 16 |
| 1.7 | Formation for the endoperoxide of 2,3,9,10-tetrachloro-6,13-bis(2'6'-dimethylphenyl)pentacene on the 5 and 14 position..... | 17 |
| 1.8 | Formation of endoperoxide at the 6 and 13 position of central ring.... | 18 |
| 1.9 | Formation of centrosymmetric (exo) and planosymmetric (endo) photodimers from irradiation with UV light..... | 19 |
| <u>CHAPTER 2: RESULTS AND DISCUSSION</u> | | |
| 2.1 | Synthesis of 6,13-bisorganoothio-6,13-dihydropentacenes..... | 21 |
| 2.2 | Synthesis of pentacene monoadducts 26 and 27 | 23 |
| 2.3 | Proposed synthesis of monosubstituted pentacenes 26-28 using DBU..... | 23 |
| 2.4 | Products of the photodimerization of substituted pentacenes in the absence of oxygen..... | 38 |
| 2.5 | Relative Gibbs free energies (gas-phase at 298.15 K) for the dimerization products of 26 calculated at the M05-2X/6-311+G(d,p)//B3LYP/6-31G(d) level..... | 41 |

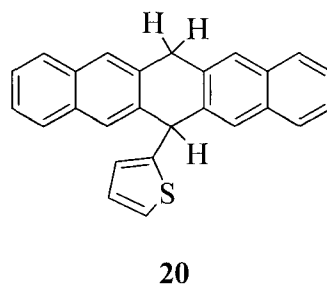
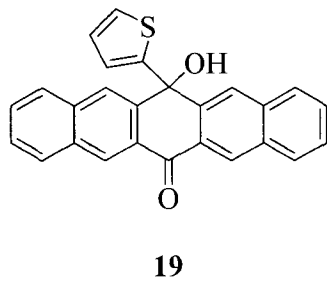
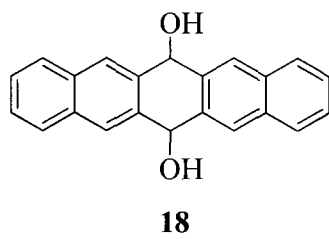
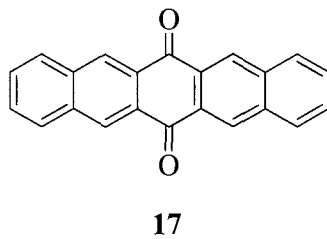
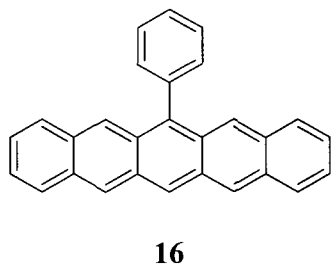
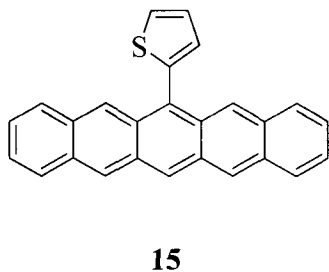
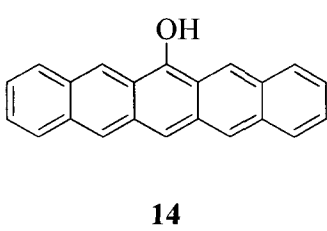
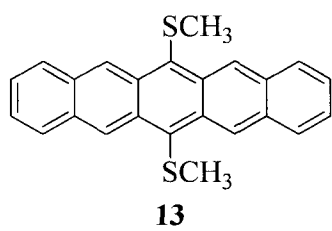
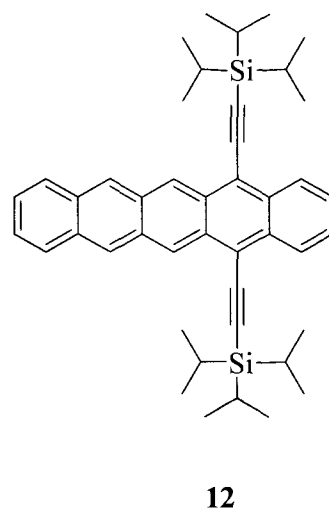
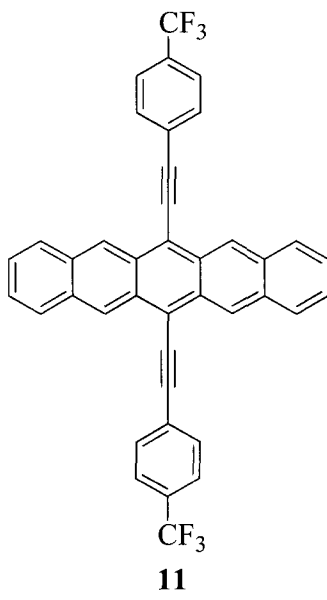
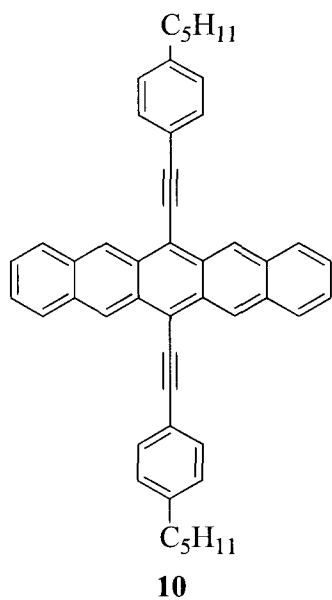
| | | |
|-----|--|----|
| 2.6 | Mechanism of the intramolecular photorearrangement of the endo anti photodimer of 26 showing M05-2X/6-311+G(d,p) charges (q) on the zwitterionic intermediates..... | 46 |
|-----|--|----|

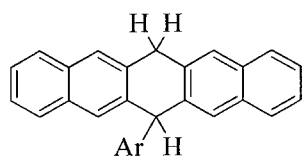
LIST OF TABLES

| <u>Table</u> | | <u>Page</u> |
|--|---|-------------|
| <u>CHAPTER 1: INTRODUCTION</u> | | |
| 1.1 | Electrochemical and optical properties of pentacene derivatives..... | 9 |
| <u>CHAPTER 2: RESULTS AND DISCUSSION</u> | | |
| 2.1 | Half-lives of monoadduct versus bisadduct..... | 31 |
| 2.2 | Relative concentrations of 26 , 32 , 17 , and 33 as measured from the crude ¹ H NMR spectra over a nine day period with intermittent irradiation of 254 nm UV light..... | 33 |
| 2.3 | Gibbs free energies (gas-phase at 298.15 K) for dimerization of substituted pentacenes calculated at the M05-2X/6-311+G(d,p)//B3LYP/6-31G(d) level..... | 38 |
| 2.4 | Relative enthalpies, entropies and Gibbs free energies (gas-phase at 298.15 K) of species along the reaction pathways of the endo anti dimerization of 26 and subsequent photorearrangement calculated at the M05-2X/6-311+G(d,p)//B3LYP/6-31G(d) level..... | 43 |
| 2.5 | Excited states calculated at the TD-M05-2X/6-311+G(d,p)//B3LYP/6-31G(d) level for the endo anti photodimer of 6-phenylthiopentacene..... | 47 |

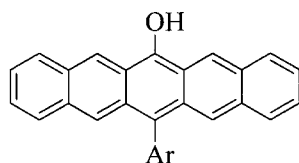
LIST OF NUMBERED STRUCTURES



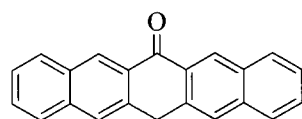
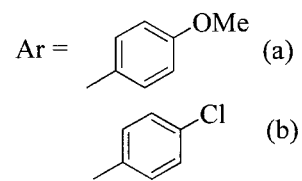




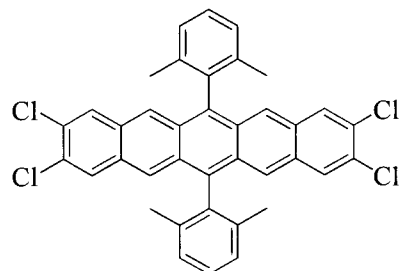
21



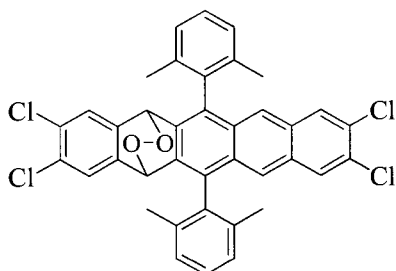
22



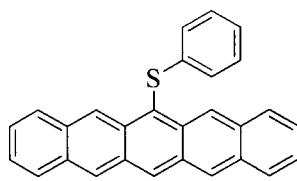
23



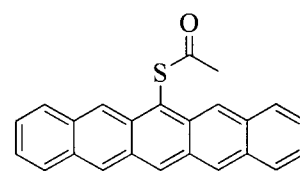
24



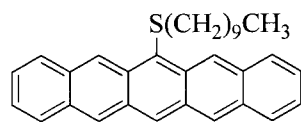
25



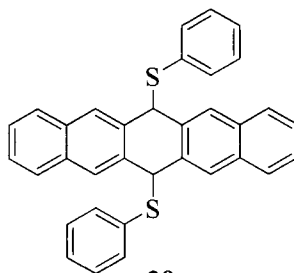
26



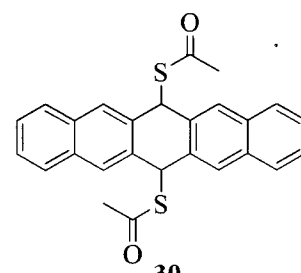
27



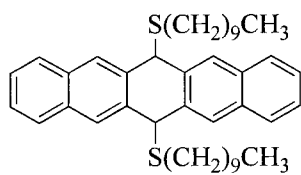
28



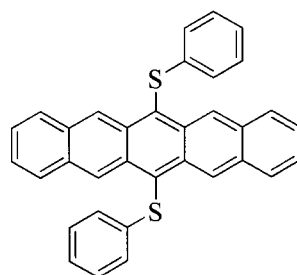
29



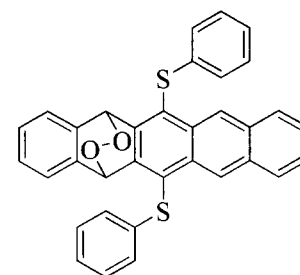
30



31



32



33

ABSTRACT

SYNTHESIS OF 6-THIOSUBSTITUTED PENTACENES AND STUDY OF AN UNEXPECTED PHOTOREARRANGEMENT OF 6-PHENYLTHIOPENTACENE DIMER

by

Julia Y. K. Chan

University of New Hampshire, May 2012

Two new monosubstituted pentacene derivatives, 6-phenylthiopentacene, **26**, and 6-acetylthiopentacene, **27**, have been prepared using a dehydrogenative aromatization and elimination reaction that utilizes 1,8-diazabicycloundec-7-ene (DBU) as reagent. Although many disubstituted pentacenes have been synthesized and characterized, monosubstituted pentacenes have received much less attention. While studying the photodegradation of **26** under ambient light and air conditions, an unexpected transformation to 6,13-bis(phenylthio)pentacene, **32**, was observed. The transformation requires short wavelength (254 nm) UV irradiation. Through a combined experimental and computational study, we have identified this transformation as a multi-step intramolecular process initiated by the photoexcitation of the endo anti dimer of **26**. The photoexcited dimer undergoes an intramolecular acid-base reaction which involves two proton transfers and nucleophilic substitution to form the rearranged photodimer which upon dissociation yields bisadduct **32**. Using 254 nm light and a quartz reaction vessel, bisadduct **32** has been isolated in 20% yield from monoadduct **26**.

CHAPTER 1: INTRODUCTION

1.1 Acenes

Acenes belong to a class of organic compounds known as polycyclic aromatic hydrocarbons (PAHs) which contain fused “alternant *cata*-annelated” benzenoid rings arranged in a linear fashion.¹ PAHs, more simply known as polyarenes, make up a large and diverse class of organic molecules and are commonly found in oil, coal, tar deposits, and are released through the burning of fossil fuels. They can also be found from anthropogenic sources such as vehicle emissions and from natural sources such as forest fires and volcanic activity.¹ In the past decade, there has been increased interest in the field of acene chemistry as these molecules hold promising electronic and optoelectronic properties, with applications in electronic devices, nanotechnology, and biomedical science.²

The term "acene" was first used by the father of modern PAH chemistry, Erich Clar, and was derived from one of the most common acenes, anthracene.³ Acenes contain anywhere from three to nine rings (Figure 1.1). The smallest acene is anthracene, which contains three fused benzene rings. Adjacent to anthracene in the acene series is tetracene, which contains four benzene rings. While anthracene can be isolated from natural petroleum oil or coal tar, tetracene can be found in diesel exhaust and from the combustion of organic products.⁴

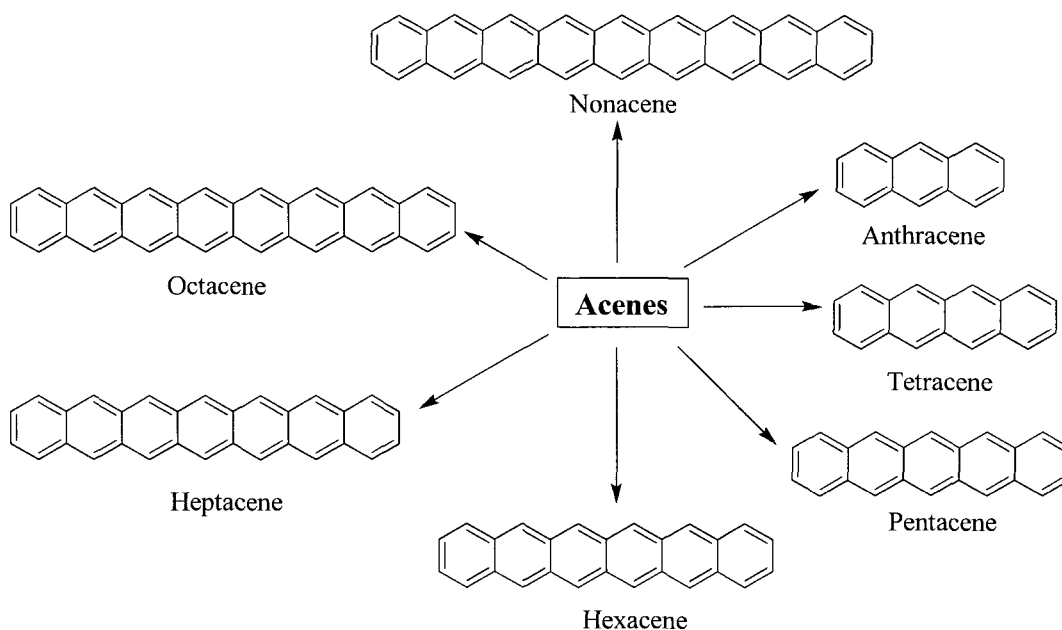


Figure 1.1: Acene series.

Larger acenes, containing five aromatic rings and beyond, are not found in nature but can be obtained via syntheses.² Their extended conjugation gives rise to smaller HOMO-LUMO gaps and higher charge carrier mobilities in semiconducting materials.⁵ However, despite showing desirable electronic properties, larger acenes are harder to isolate, characterize, and purify due to their increased reactivity.⁶ Furthermore, as acenes increase in size, they tend to decrease in solubility and stability.² Recently, Tonshoff and Bettinger successfully isolated octacene and nonacene, containing eight and nine benzene rings, respectively.⁷ Isolation of octacene and nonacene was performed using a Strating-Zwanenburg reaction in an argon matrix involving a photochemically induced decarbonylation of bridged α -diketones.^{7,8} To date, octacene and nonacene are the largest acenes known in the acene series.

Up until recently, research has mainly focused on smaller homologues of the acene series as they are more stable and more readily available in nature. To date, the largest acene most widely studied and characterized is pentacene, which consists of five fused benzene rings.⁴ Since its first synthesis in 1929 by Clar,⁹ more than 6000 journal articles containing the topic of pentacene have been published.¹⁰ Like tetracene and other larger acenes, pentacene is not isolated from petroleum sources. Instead, it can be found from the combustion of carbon-rich polymers¹¹ and in meteorites.¹² Figure 1.2 illustrates the numbering scheme used to label the carbon atoms in the first three members of the acene series.¹

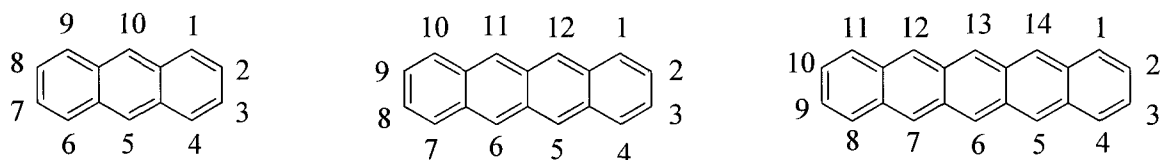


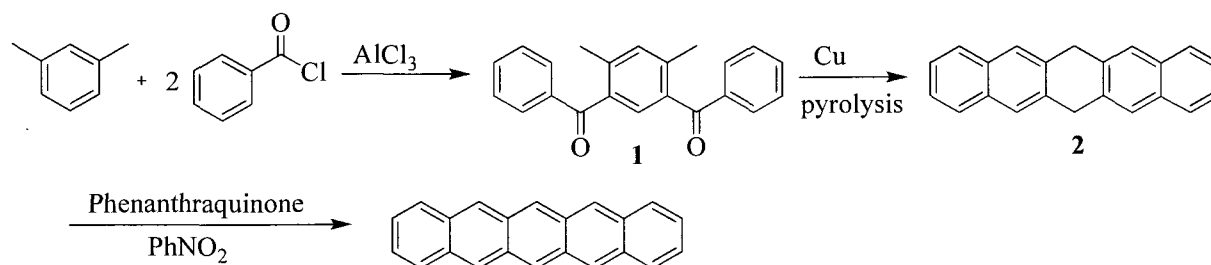
Figure 1.2: Numbering scheme in anthracene, tetracene and pentacene.¹

Acenes can act as organic semiconductors and be applied as active layers in electronic devices, such as organic field effect transistors (OFETs). OFETs have attracted considerable attention as an alternative to existing inorganic FETs which are made of single-crystal, polycrystalline or amorphous silicon chips.¹³ OFETs show advantages over inorganic FETs in that they are cheaper, lighter weight, and possess greater mechanical flexibility.^{14,15} Furthermore, the solubility of organic materials allows for better solution processibility and inexpensive thin film deposition. As organic semiconducting materials, acenes can be used and incorporated in many applications including flexible displays, low-cost electronic paper, memory chips and sensor elements in automotive and transportation industries.¹⁶

1.2 Pentacene

Pentacene is a deep blue, crystalline material that shows promising electronic and optoelectronic properties in devices.¹⁷ It possesses a high charge-carrier mobility that is comparable to amorphous silicon, exceeding $1 \text{ cm}^2/\text{Vs}$ in evaporated thin films.^{5,18} More recently, an even higher charge-carrier mobility of $5.5 \text{ cm}^2/\text{Vs}$ has been reported in pentacene FETs using surface modification techniques.¹⁹ These remarkable electronic properties of pentacene can be explained by its extended π -conjugated electronic structure, low HOMO-LUMO gap, and rigid planarity.²⁰

The first synthesis of pentacene by Clar (1929) is shown in Scheme 1.1 below.⁹ Starting with *m*-xylene and benzoyl chloride, two Friedel-Craft acylations were performed to generate dibenzoyl-*m*-xylene, **1**. Compound **1** was then subjected to pyrolysis conditions in the presence of copper to produce 6,13-dihydropentacene, **2**, which upon dehydrogenation afforded pentacene. Other approaches to synthesize pentacene have been reported by Ried and coworkers,²¹ Cava and coworkers,²² and Vets and workers.²³



Scheme 1.1: Synthesis of pentacene by Clar (1929).⁹

1.2.1 Functionalization of Pentacenes

One of the major drawbacks in the use of pentacene is its instability in light and air and facile photodegradation in solution.²⁴ Moreover, due to its low solubility in common organic solvents, solution processing such as spin-casting is made difficult.²⁵ To circumvent these problems, substituents that contribute to either improving stability or solubility have been introduced to the pentacene backbone.⁵ Several groups have introduced substituents such as phenyl groups,^{20,26,28} as shown for pentacene **3** (6,13-diphenylpentacene), and ethynyl groups,^{27,28,29} in particular silylethynyl derivatives, to the pentacene backbone (Figure 1.3). Of these silylethynyl derivatives, 6,13-bis(triisopropylsilylethynyl)pentacene or TIPS-pentacene, **4**, has been widely studied and is known for its high stability.³⁰ Other pentacene derivatives such as those bearing halogen groups such as 6,13-dichloropentacene, **5**, have been synthesized as well.³¹ Less widely studied are pentacene derivatives substituted with alkylthio groups such as pentacene **6** (6,13-bisdecylthiopentacene),³² and arylthio groups such as pentacene **7** (6,13-bis(phenylthio)pentacene).³³ In comparison with other substituted pentacenes, thiosubstituted pentacenes are amongst the longest lived in solution and exhibit excellent solubility in a variety of organic solvents.³² These properties make them promising candidates in electronic applications such as organic field-effect transistors (OFETs),³⁴ organic light emitting diodes (OLEDs),³⁵ organic photovoltaics (OPVs),³⁶ and flexible displays.³⁷

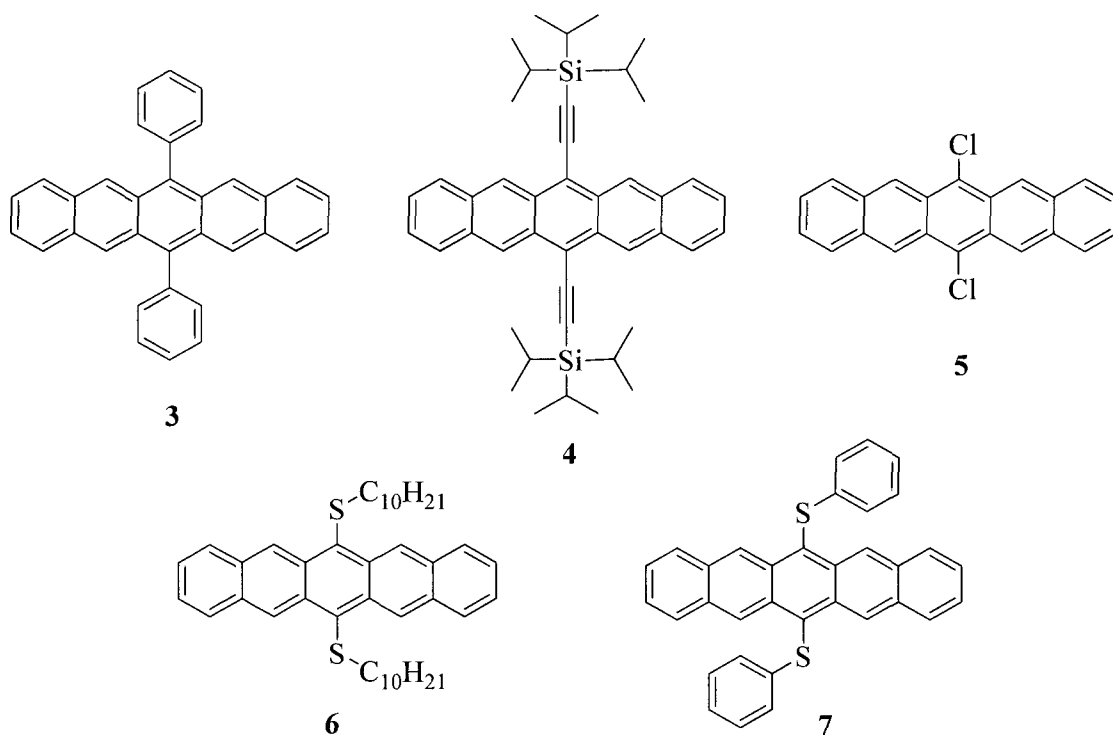


Figure 1.3: Substituted pentacene derivatives.

1.2.2 Stability of Disubstituted Pentacenes

Disubstituted pentacenes functionalized at the 6 and 13 positions have been widely synthesized and characterized.^{38,47} Since the center ring of the pentacene is most reactive towards light and oxygen, it is believed that substitution at these positions acts to enhance the stability of pentacenes and retard the rate of photooxidation.^{32,39,48} Hence, many groups have studied how substituting different moieties at these sites will affect the overall stability of pentacenes. For example, Anthony and co-workers showed that substituting a TIPS group at the 6,13 positions of pentacene increases stability³⁰ (see **4** in Table 1.1 and Section 1.2.4). It was reported that **4** has a charge mobility of 0.17 cm²/Vs in OTFTs.⁴⁰

In another study, Li and coworkers reported the synthesis of four different ethynyl substituted pentacene derivatives: 6,13-bis(1-decylethynyl)pentacene, **8**, 6,13-bis(4-dodecyloxyphenylethynyl)pentacene, **9**, 6,13-bis(4-pentylphenylethynyl)pentacene, **10**, and 6,13-bis(4-trifluoromethylphenylethynyl)pentacene, **11** (Figure 1.4).³⁸ Among these four substituted pentacenes, it was reported that **11** is the most stable ($t_{1/2}$ 9320 min) while **8** is the least stable ($t_{1/2}$ 540 min). The dramatic increase in stability for **11** can be explained by the presence of an extended π -electron delocalization and inductive electron-withdrawing effect provided by the trifluoromethyl group to the pentacene backbone. Pentacene **11** also shows the highest mobility (~ 0.42 cm²/Vs) and is soluble in a variety of solvents (toluene, chlorobenzene, dichlorobenzene) at elevated temperatures.³⁸

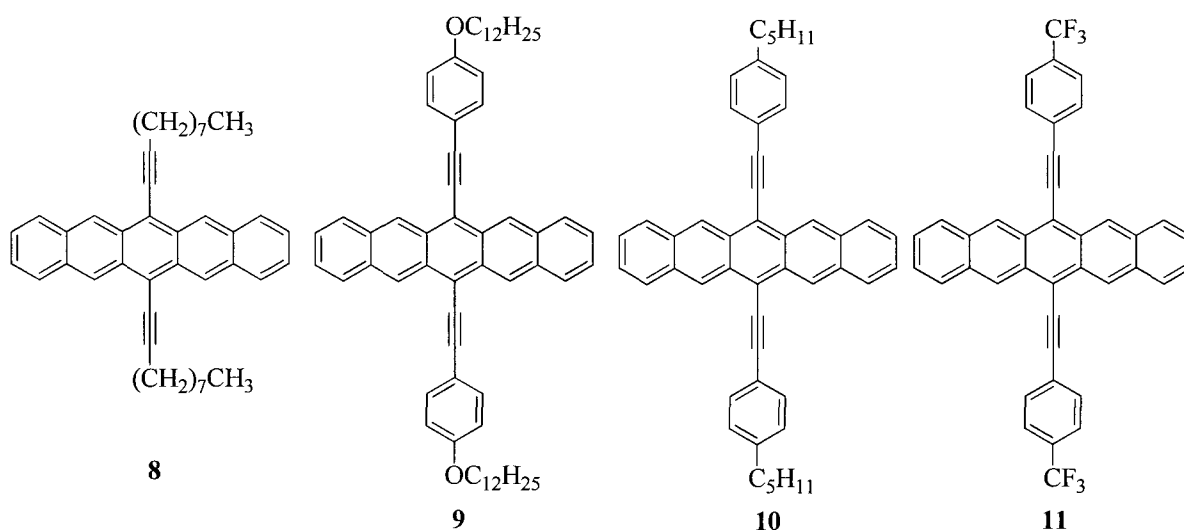


Figure 1.4: Ethynyl substituted pentacenes.³⁸

Anthony and coworkers have illustrated how functionalization at different positions on the pentacene affects intermolecular orbital overlap and packing in organic semiconductors. It was reported that symmetric TIPS-pentacene, **4**, functionalized at the

6,13 positions, stacks in a two-dimensional columnar array with significant π -overlap while asymmetric TIPS-pentacene functionalized at the 5 and 14 positions, **12**, stacks in a herringbone pattern, similar to that of unsubstituted pentacene.³⁰ Furthermore, **12** was shown to rapidly decompose on films upon exposure to air, supporting the fact that substitution at the most reactive sites of the pentacene backbone helps retard the rate of photooxidation.^{32,39,48}

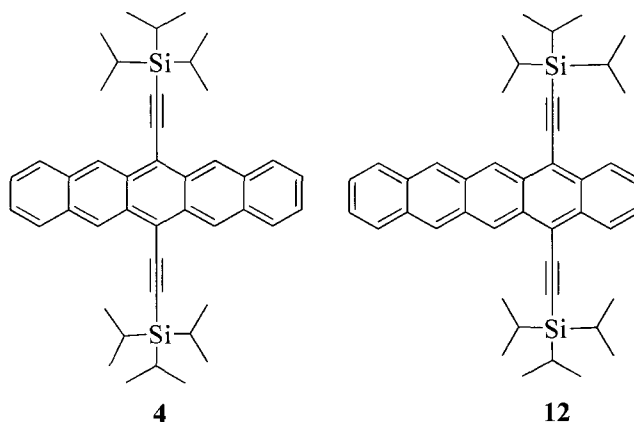


Figure 1.5: TIPS-pentacene functionalized at the 6, 13 position, **4**, and 5, 14 positions, **12**.

1.2.3 Stability of Dithiosubstituted Pentacenes

Through a combined experimental and computational study, Miller and co-workers observed that 6,13-dialkylthio and 6,13-diarylthio substituted pentacenes are amongst the longest lived pentacene derivatives known and they exhibit excellent solubility in a variety of organic solvents. Thiosubstituted pentacenes **6** and **7** (Figure 1.3) have considerably longer lifetimes than pentacenes **3** and **4** as shown in Table 1.1.³² The half-life of 6,13-bis(decylthio)pentacene, **6**, is 750 mins and that for 6,13-bis(phenylthio)pentacene, **7**, is even longer at 1140 mins. For pentacene **3**, a half-life of

only 8.5 mins was reported and as for compound **4**, a half-life of approximately 520 mins was reported.³² No half-life studies were conducted on pentacene **5**.

| Pentacene Derivatives | ($t_{1/2}$) mins | E_{HOMO} (eV) ^a | E_{LUMO} (eV) ^a | $E_{\text{g,Echem}}$ (eV) ^b | low-energy λ_{max} (nm) | $E_{\text{g,optical}}$ (eV) ^c |
|-----------------------|--------------------|-------------------------------------|-------------------------------------|--|--|--|
| 3 | 8.5 | -5.00 | -3.08 | 1.92 | 604, 558, 519 | 1.94 |
| 4 | 520 | -5.11 | -3.42 | 1.69 | 643, 591, 548 | 1.81 |
| 5 | --- | --- | --- | --- | --- | --- |
| 6 | 750 | -5.07 | -3.26 | 1.81 | 617, 570, 529 | 1.88 |
| 7 | 1140 | -5.17 | -3.36 | 1.81 | 624, 575, 534 | 1.86 |

Table 1.1: Electrochemical and Optical Properties of Pentacene Derivatives.³²

^a HOMO and LUMO energies and electrochemical HOMO-LUMO gaps determined from the onset of the first oxidation and the first reduction waves in cyclic voltammograms.

^b Recorded $E_{1/2}$ values vs. Ag/Ag⁺ in CH₂Cl₂ with TBAPF₆ as supporting electrolyte.

^c Optical HOMO-LUMO gaps determined from the onset of lowest-energy visible absorption band. The onset is defined as the intersection between the baseline and a tangent line that touches the point of inflection.

UV-Vis and electrochemical studies have shown that **6** and **7** are among the most photo-resistant pentacenes (Table 1.1). Therefore, thiosubstituted pentacenes are in general more robust and less susceptible to photodegradation than other functionalized pentacenes. Both **6** and **7** possess the same electrochemical HOMO-LUMO gaps ($E_{\text{g,Echem}}$) and very similar optical HOMO-LUMO gaps ($E_{\text{g,optical}}$). The UV-Vis spectra for **6** and **7** reveal a red-shift in the longest wavelength bands at 617 and 624 nm, respectively, when compared to **3** (Table 1.1). Pentacene **4** shows the greatest red-shift in its longest wavelength band at 643 nm and the lowest electrochemical HOMO-LUMO gap. The reduced HOMO-LUMO gap and red-shifted UV-Vis bands in **6** and **7** can be explained by a combination of electron withdrawing (inductive effect) and resonance effects from the sulfur substituent.³²

1.2.4 Packing Arrangement of Thiosubstituted Pentacenes

The packing arrangements and orientations of molecules in thin films have great impact on the electronic and optical properties of semiconducting materials. It has been shown that the strong intermolecular interactions in a π -stacking arrangement give rise to higher charge mobilities.^{15a} Bare pentacene packs in an edge-to-face fashion, or a herringbone arrangement, with minimal π -stacking.⁴¹ It has been reported that a two-dimensional co-facial π -stacked packing arrangement in acenes leads to greater charge-carrier transport due to overlapping of π -orbitals.^{5,42,43} Kobayashi and co-workers have recently demonstrated that S-S interactions assist co-facial π -stacking in 9,10-bis(methylthio)anthracene.^{44,45} Moreover, they have extended their studies to 6,13-bis(methylthio)pentacene, **13**, to demonstrate a similar pattern of co-facial π -stacking with S-S and S- π interactions.³³ When methylthio groups are substituted at the 6,13 positions, the packing alters to a co-facial π -stacking arrangement (Figure 1.6).³³ Figure 1.6 (a) illustrates the face-to-face pentacene-pentacene distance of 3.39 Å and the interatomic distance of S••C3' to be 3.610 Å. Figure 1.6 (b) highlights the intermolecular S••S' distance between neighboring pentacene columns to be 4.297 Å. These sulfur atoms and neighboring pentacene rings are linked together by the intermolecular S-S interaction between neighboring pentacene columns. The slipped co-facial π -stacking and intermolecular S- π interactions are also demonstrated in Figure 1.6.

To summarize, it is important to note that different substituents functionalized at the 6,13 positions affect the molecular packing of pentacenes. Dependent on the substitution, the solubility and stability of acenes can be altered as well. Therefore, all these factors should be considered when designing organic semiconducting devices.

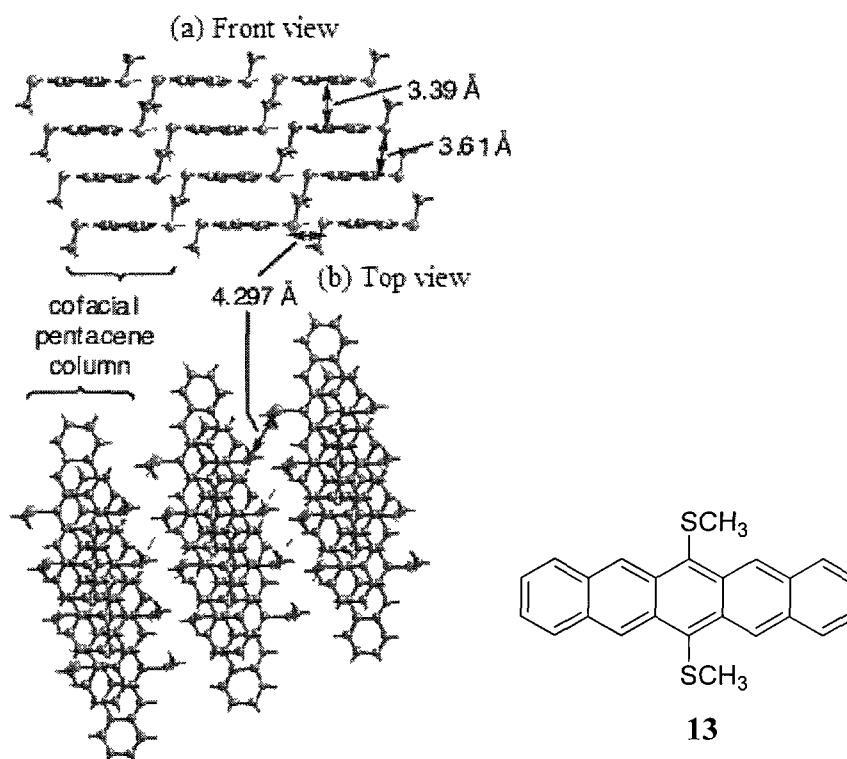


Figure 1.6: 2-D network sheet of 6,13-bis(methylthio)pentacene in the crystal structure: (a) front and (b) top views. Figure taken from reference 33.

1.3 Monosubstituted Pentacenes

While numerous disubstituted pentacenes have been synthesized and characterized, monosubstituted pentacenes have received little attention. From a synthetic perspective, monosubstituted pentacenes are considerably more difficult to prepare than their disubstituted counterparts. Reaction protocols to do so are currently limited. Efforts in this regard are also complicated by the fact that monosubstituted pentacenes are reported to undergo facile oxidative degradation and exhibit generally lower solubilities than their disubstituted counterparts.²³ To date, only three monosubstituted pentacenes have been prepared: 6-hydroxypentacene,⁴⁶ **14**, 6-thien-2'-ylpentacene,²³ **15**, and 6-phenylpentacene,²⁶ **16** (Figure 1.7).

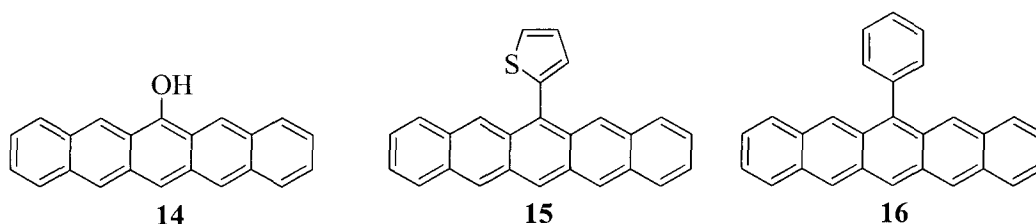
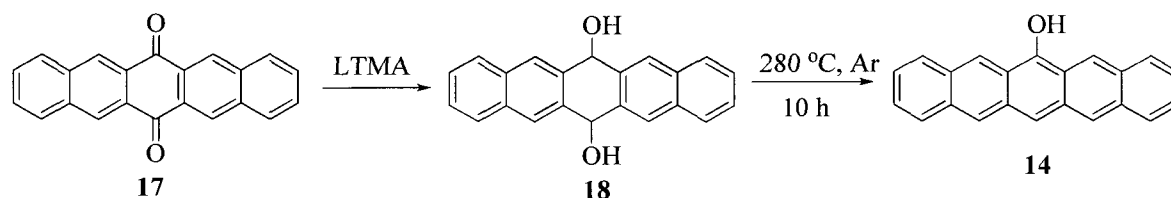
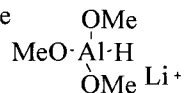


Figure 1.7: Monosubstituted pentacenes derivatives.^{46,23,26}

Monosubstituted pentacene **14** was prepared by Chi using a three step synthesis (Scheme 1.2). Pentacene-6,13-dione, **17**, was first reduced with lithium trimethoxyaluminum hydride (LTMA) to give 6,13-dihydroxy-6,13-dihydropentacene, **18**. Intermediate **18** was then converted to monosubstituted pentacene **14** in either of the following two ways: (1) by heat at 280 °C in an argon atmosphere for about 10 hours or (2) by using a reducing agent such as stannous chloride.



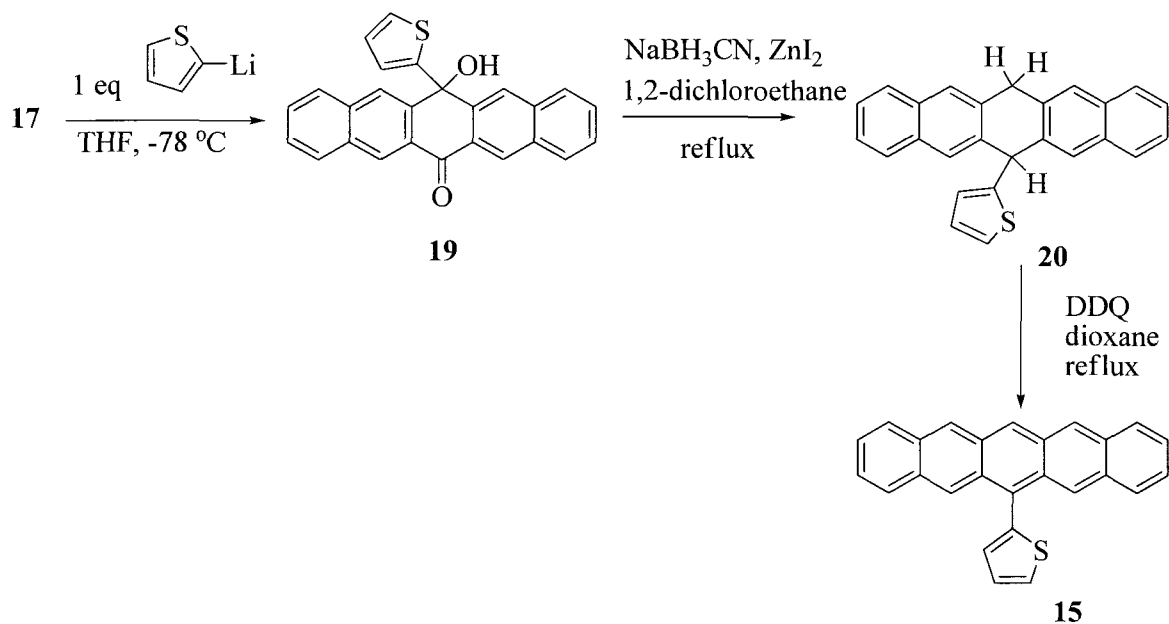
where LTMA = lithium trimethoxyaluminum hydride



Scheme 1.2: Synthesis of 6-hydroxypentacene, **14**.⁴⁶

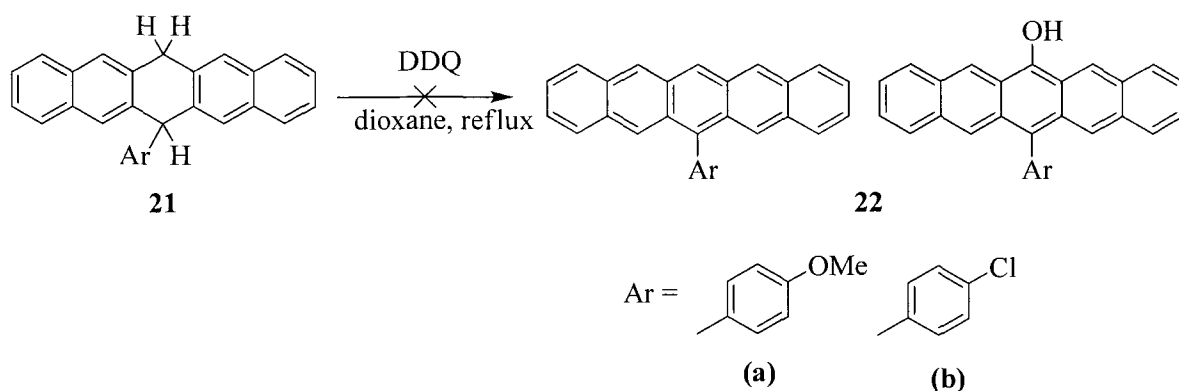
Monosubstituted pentacene **15** was prepared by Vets and co-workers (Scheme 1.3).²³ Attempts were first made to add 2-thienyllithium directly to the carbonyl group of **17** to produce monosubstituted pentacene **15**. Unfortunately, pentacene **15** could not be isolated due to rapid degradation during the workup step.⁴⁷ Thus, another route to synthesize **15** is shown (Scheme 1.3). Addition of the Grignard reagent 2-thienyllithium

to **17** produced 13-hydroxy-13'-thien-2-ylpentacene-6-one, **19**. Reduction of **19** with NaBH_3CN in the presence of ZnI_2 afforded 6,13-dihydro-6'-thien-2-yl-13,13'-dihydropentacene, **20**. Finally, treating **20** with 2,3-dichloro-5,6-dicyanobenzoquinone (DDQ) afforded monosubstituted pentacene **15**.



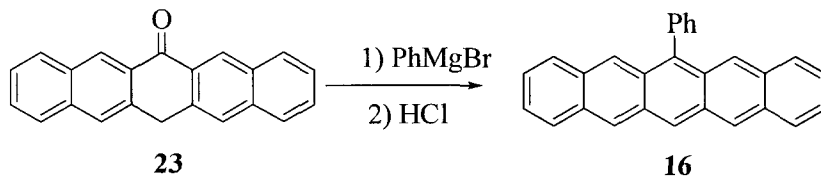
Scheme 1.3: Synthesis of 6-thien-2'-ylpentacene **15**.²³

Vets and coworkers also attempted to synthesize other monoaryl substituted pentacenes, starting with intermediates **21a** and **21b** (Scheme 1.4). However, due to rapid oxidation and instability of these compounds in solution, they degraded during workup and isolation of these monoaryl substituted pentacenes was not possible. Instead side products, **22a** and **22b** were formed.



Scheme 1.4: Attempted synthesis of other monoarylsubstituted pentacenes.²³

Monosubstituted pentacene **16** was prepared by Miao and co-workers (Scheme 1.5).²⁶ Addition of phenyl magnesium bromide to 6-pentaceneone, **23**, followed by a dehydration process using concentrated hydrochloric acid, as illustrated by Clar,⁴⁸ led to the target compound, 6-phenylpentacene, **16**.²⁶



Scheme 1.5: Synthesis of 6-phenylpentacene, **16**.²⁶

1.3.1 Possible Applications of Monosubstituted Pentacenes

Monothiosubstituted pentacenes may hold interesting properties that have yet to be explored. For instance, their ability to assemble differently in thin films from their bithiosubstituted counterparts, may potentially give rise to a set of unique molecular architectures with desirable electron and hole mobilities.^{4,33} Of particular interest is the use of thiol SAMs on gold and their applications as building blocks in fabricating devices

such as biosensors, molecular electronics, transistors, and switches.⁴⁹ Self-assembled monolayers (SAMs) are comprised of small organic subunits that combine spontaneously in a bottom-up fashion to form ordered arrays on solid surfaces or on liquids.^{50,51} SAMs show promise for applications in a wide range of fields, such as in nanotechnology,^{50,52} medicine,⁵³ and device fabrication.⁵⁴

Thiol SAMs on gold were first reported at the beginning of the 1980s by Nuzzo and Allara.⁵⁵ Since then, thiol SAMs have been widely studied due to their easy preparation and the highly ordered arrays they exhibit under ambient conditions.⁵⁶ In particular, conjugated mono and dithiols were found to form highly-ordered robust SAMs on metal surfaces making them of particular interest for use in thin film devices.⁵⁷ Depending on the number of thiol groups attached to gold, charge transport efficiency can be either enhanced or minimized. For instance, alkane dithiols were found to have higher charge transport than alkane monothiols due to stronger coupling through the chemisorption of thiols onto gold surfaces forming Au-S bonds at both ends.⁵⁸ Furthermore, charge transport can be influenced by the differences in dipoles of SAMs formed at the metal-organic layer.⁵⁹ Through chemical modification of SAMs on metal surfaces, these interfacial properties can be fine-tuned to improve metal-organic contacts and performance in organic electronic devices.⁵⁷

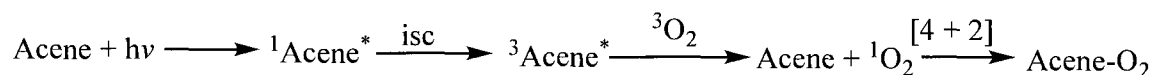
In addition, monosubstituted pentacenes could potentially be used as starting materials for further functionalization.⁴⁶ For example, 6-acetylthiopentacene could be reduced to 6-thiopentacene and then be used to passivate a gold electrode to create a nano-scale thin-film transistor. When thiols are treated onto gold electrodes, the average field-effect mobility measured from these thin-film transistors was $0.022 \text{ cm}^2/\text{Vs}$, which

is approximately two orders of magnitude higher than that of devices without pretreatment.⁶⁰ In addition, the solubility and stability of thiosubstituted pentacenes in a wide range of organic solvents make their application in thin film devices readily accessible.³⁷

1.4 Photodegradation of Acenes

1.4.1 Photooxidation

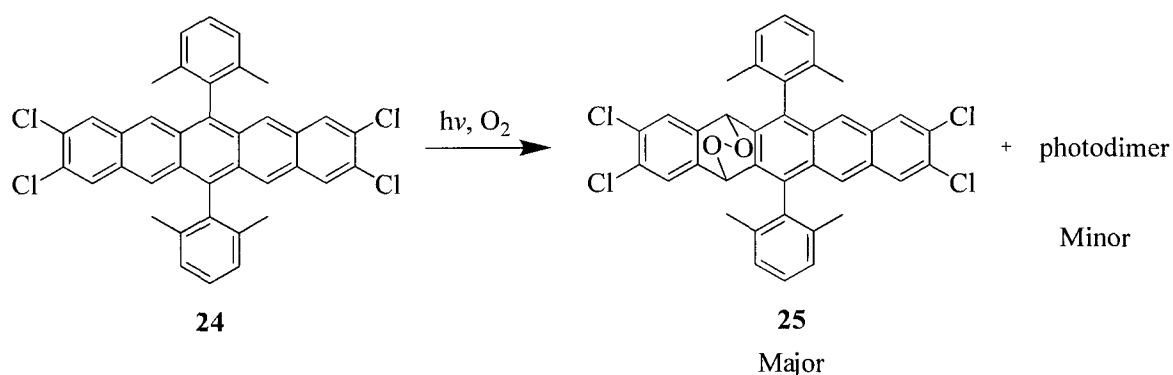
Acenes are unstable under light and air conditions and can easily degrade via two pathways: (1) photooxidation^{24,65} and (2) photodimerization.^{25,64} Of the two pathways, photooxidation is the dominant route of degradation under ambient light and oxygen. Photodimerization, the less common pathway, occurs in the presence of light. Scheme 1.6 shows a potential photooxidation pathway for acenes.⁶¹



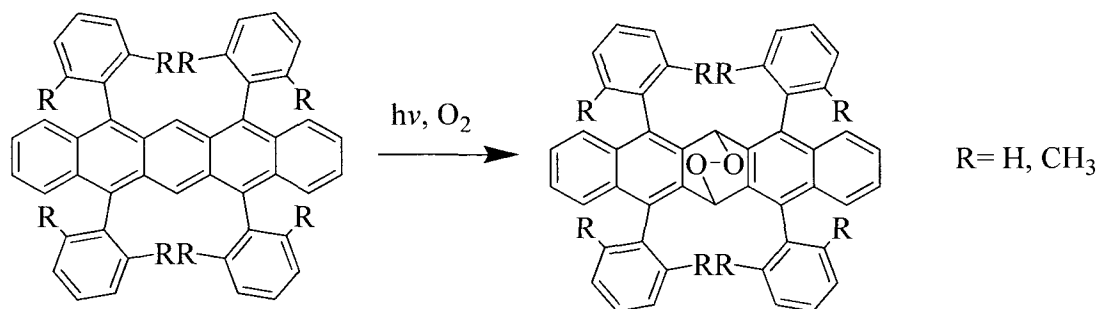
Scheme 1.6: Photooxidation pathway for acenes.⁶¹

First, a photon of light excites the acene from ground state to its lowest excited singlet state. Through intersystem crossing, a non-radiative transition, this singlet excited acene (${}^1\text{Acene}^*$) is promoted to a triplet excited state (${}^3\text{Acene}^*$). The transfer of energy from the acene's triplet excited state to ${}^3\text{O}_2$ results in the formation of singlet oxygen. Oxygen can then add to the acene through a concerted [4 + 2] Diels Alder reaction to form the corresponding endoperoxide adduct (Acene-O_2).⁶¹ In addition, the same endoperoxide can be formed via a biradical path which involves stepwise addition of ${}^1\text{O}_2$ to pentacene.⁶²

Recently, Miller and coworkers studied and characterized the photodegradation products of several substituted pentacenes.⁶³ In particular, when 2,3,9,10-tetrachloro-6,13-bis(2',6'-dimethylphenyl)pentacene, **24**, is exposed to ambient light and air, it decomposes to form the endoperoxide product, **25** (Scheme 1.7). When substituents are present at the central ring, ¹O₂ is added to the 5,14 positions instead. This is because the ortho methyl groups on the phenyl ring provide extra steric hindrance at the 6,13 positions and block oxygen from being added to the center ring (Scheme 1.8)^{32,63} In addition to the formation of the major endoperoxide product, a minor amount of the photodimer product forms under ambient air and light.⁶³ In the case where there is no substitution in the center ring, an endoperoxide product can potentially form at the 6,13 positions of the pentacene via an intermolecular Diels-Alder reaction between ¹O₂ and the 6,13 carbons of the pentacene skeleton (Scheme 1.8).³²



Scheme 1.7: Formation for the endoperoxide of 2,3,9,10-tetrachloro-6,13-bis(2',6'-dimethylphenyl)pentacene on the 5 and 14 position.⁶¹



Scheme 1.8: Formation of endoperoxide at the 6 and 13 position of central ring.³²

1.4.2 Photodimerization

As discussed above, a minor product resulting from photodegradation of pentacenes is the photodimer. Dimerization of pentacene under photochemical conditions was first observed by Birks and co-workers based on an absorption spectrum that showed similar characteristics to that of dianthracene.⁶⁴

Pentacenes dimerization involves an intermolecular [4+4] cycloaddition to form "butterfly" dimers as illustrated in Figure 1.9. Photodimerization can occur in either a symmetric manner with new bonds formed across the 6,13 carbons, or in an unsymmetric manner with new bonds formed at the penultimate rings (5,14 positions or 7,12 positions, see Figure 1.9).^{4,5,65} These photodimers can be synthesized by irradiating a solution of pentacene ($\lambda > 440$ nm) at 120 °C in deoxygenated 1-chloronaphthalene.⁶⁶ For the case of unsubstituted pentacene, the major product is the symmetric photodimer formed at the 6,13 positions and the minor product is the unsymmetric photodimer formed at the 5,14 positions. A recent theoretical study explored the mechanism of photodimerization for many acenes where it was shown that dimerization of pentacenes at the 6,13 carbons occurs via a biradical stepwise mechanism.⁶⁷

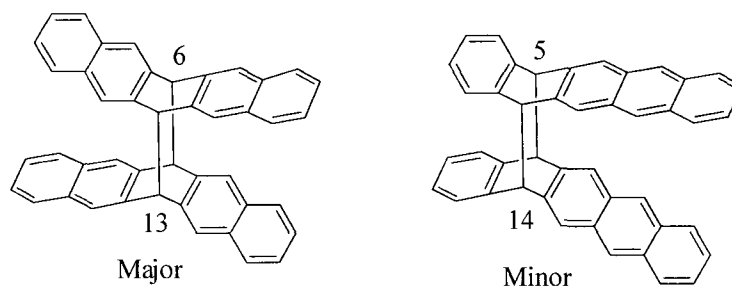
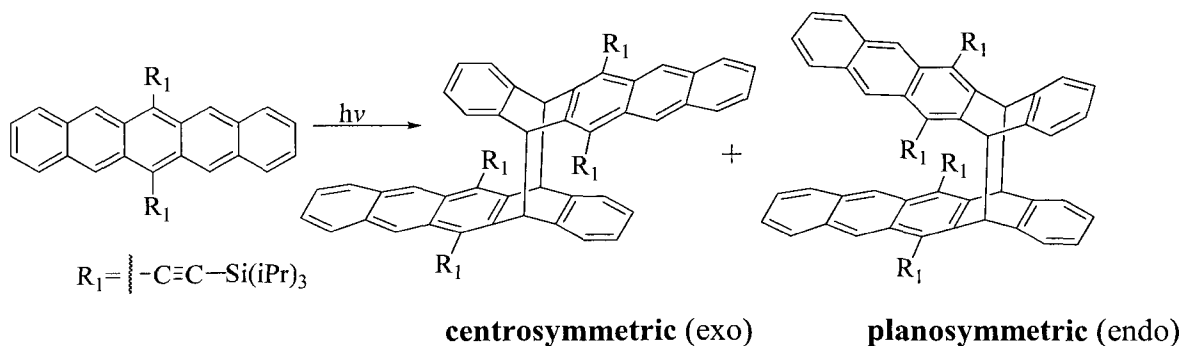


Figure 1.8: "Butterfly" dimers formed at the 6,13 positions (left) and at the 5,14 positions (asymmetric dimer, right).

Under photodegradation conditions, two stereoisomeric products can potentially form, the planosymmetric (endo) or centrosymmetric (exo) photodimers (Scheme 1.9).³⁷ Typically, pentacenes dimerize at the center ring to form a "butterfly" dimer as discussed above (Figure 1.9). However, 6,13 disubstituted pentacenes tend to form photodimers at the 5,14 positions due to steric crowding at the center ring. For instance, when a solution of TIPS pentacene is irradiated with 300 nm UV light, two photocatalysed [4+4] intermolecular cycloadditions selectively form at the 5,14 positions (Scheme 1.9). Photodimerization occurs only at the 5,14 positions for this molecule because of the steric hindrance caused by the TIPS group on the central ring. Following photodimerization, a substituted anthracene core was detected as a chromophore with a corresponding blue-shift in the longest wavelength as analyzed from the UV-Vis spectra.²⁵



Scheme 1.9: Formation of centrosymmetric (exo) and planosymmetric (endo) photodimers from irradiation with UV light.

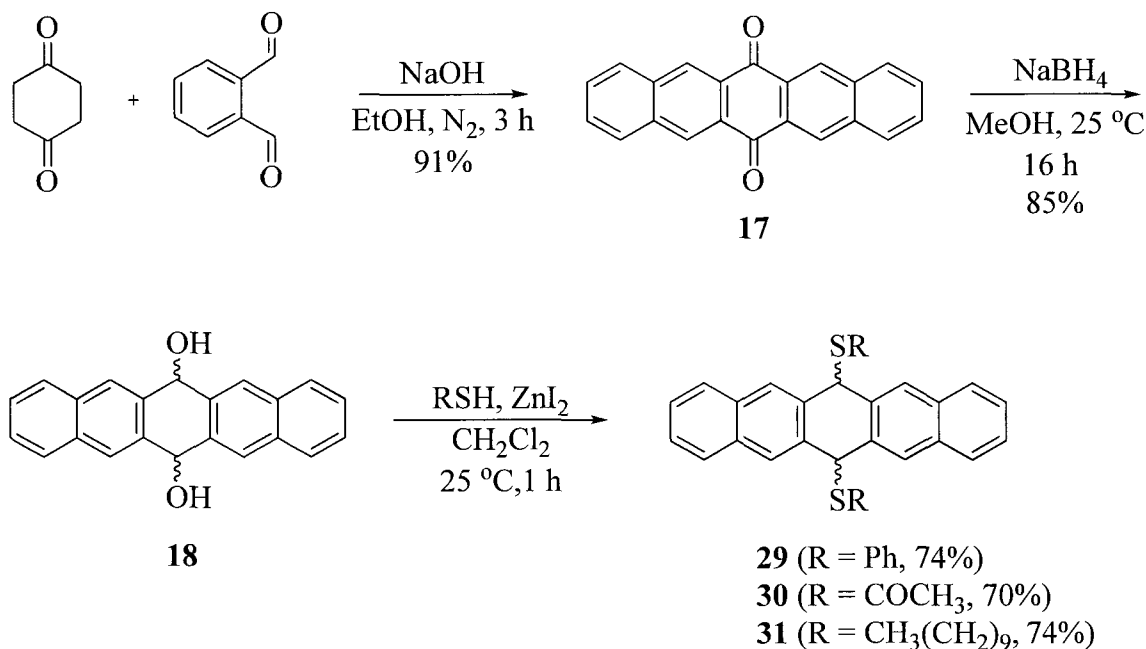
CHAPTER 2: RESULTS AND DISCUSSION

2.1 Synthesis of 6-organothio substituted pentacenes

While many disubstituted pentacenes have been synthesized and characterized, monosubstituted pentacenes have received much less attention. Like pentacene and its disubstituted derivatives, monosubstituted pentacenes are organic semiconductors that may show interesting electronic properties. From a synthetic perspective, however, monosubstituted pentacenes are more difficult to prepare than their disubstituted counterparts due to their reduced symmetry. Furthermore, they are reported to undergo facile oxidative degradation and to exhibit generally lower solubilities than their disubstituted counterparts.²³ Through a combined experimental and theoretical study, Miller and co-workers showed that arylthio and alkylthio substituents provide disubstituted pentacenes with excellent resistance to photooxidation making them ideal candidates for thin film electronic applications.³² Given that 6,13-diorganothio substituted pentacenes show improved solubility and stability over other functionalized pentacenes, we sought to prepare and study novel 6-organothio substituted pentacene derivatives: 6-phenylthiopentacene, **26**, 6-acetylthiopentacene, **27**, and 6-decylthiopentacene, **28**. These three molecules were selected to represent a diverse class of organothio monosubstituted pentacenes.

All three monosubstituted thiopentacenes were synthesized according to the method shown in Schemes 2.1 and 2.2. Pentacene-6,13-dione, **17**, was prepared in 91% yield following the method of Ried²¹ which involves consecutive aldol condensations

between 1,4-cyclohexanedione and *o*-phthalaldehyde (Scheme 2.1). Compound **17**, a yellow solid, was subsequently reduced with sodium borohydride (NaBH_4) at room temperature to afford a mixture of *cis* and *trans*-6,13-dihydroxy-6,13-dihdropentacene, **18**, in 85% yield as an off-white solid. Following Kobayashi's methods,³³ reaction between **18**, the Lewis acid zinc iodide, and thiophenol gave a mixture of *cis* and *trans*-6,13-bis(phenylthio)-6,13-dihdropentacene, **29**, in 74% yield as a light pink solid. Similarly, reaction between **18**, ZnI_2 , and thioacetic acid gave a single diastereomer of 6,13-bis(acetylthio)-6,13-dihdropentacene, **30**, in 70% yield as a light peach-colored solid. Also, reaction between **18**, ZnI_2 , and 1-decanethiol gave a mixture of *cis* and *trans*-6,13-bis(decylthio)-6,13-dihdropentacene, **31**, in 74% yield as a pale pink solid (Scheme 2.1).



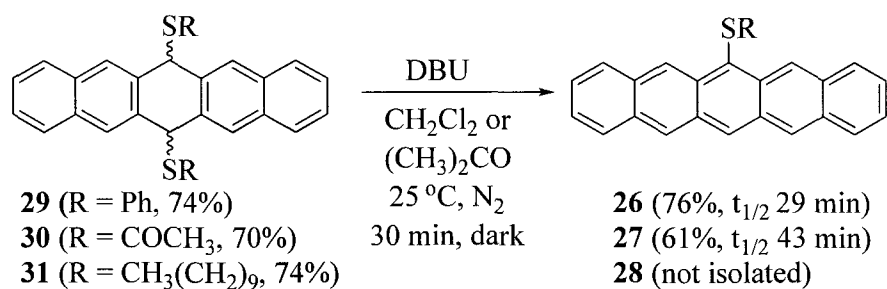
Scheme 2.1: Synthesis of 6,13-bisorganothio-6,13-dihdropentacenes **29**, **30**, **31**.³³

While there are no published procedures to convert molecules like **29**, **30**, and **31** to fully aromatized monosubstituted pentacenes, we found that treating **29** with 1,8-diazabicycloundec-7-ene (DBU) in acetone at room temperature in the dark for 30 minutes under an atmosphere of nitrogen afforded the targeted monoadduct **26** in 76% yield as a dark purple solid. Similarly, treating **30** under the same conditions afforded monoadduct **27** as a dark blue solid in a slightly lower yield of 61% (Scheme 2.2). Treatments of **29** and **30** with DBU in dichloromethane (CH_2Cl_2) resulted in no significant differences in the product formation and yields as compared to reactions run in acetone. The crude products of **26** and **27** were triturated with CH_2Cl_2 /hexanes, washed with excess hexanes, and filtered to afford the corresponding purified products. We found that trituration was only successful when there were minor amounts of oxidation products in the crude reaction. When there were higher amounts of oxidation products present in the crude reaction, it was difficult to obtain a clean NMR spectrum of the corresponding monoadduct. To circumvent this problem, **29** was first dissolved in CH_2Cl_2 and degassed via three freeze-pump-thaw cycles before DBU was added to the reaction mixture. The same procedure was followed for **30**. We found that this degassing step helped to minimize the amount of oxidation products that were formed.

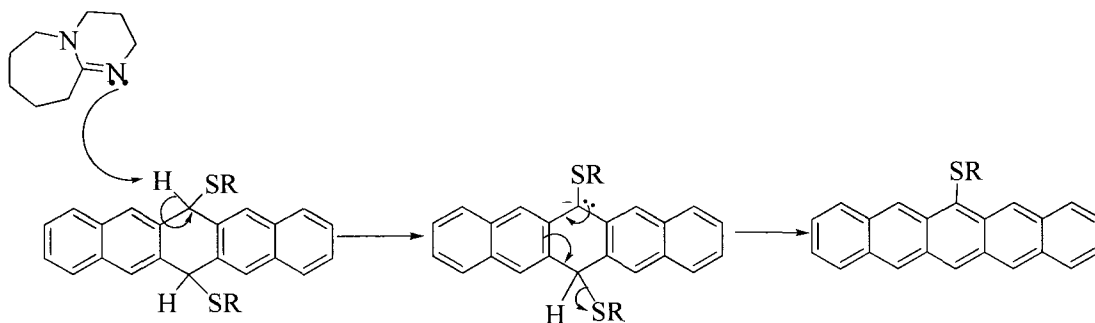
Upon reaction of compound **31** with DBU, the corresponding organothio monosubstituted pentacene, 6-decylthiopentacene, **28**, was detected in the crude reaction mixture. However, conversion of **31** to **28** was low as 1-decanethiol is a poorer leaving group than either the thiophenol or thioacetate groups due to the lack of resonance stabilization. Thus, when compound **31** was reacted under conditions that lead to monoadduct formation from **29** and **30** (DBU, $(\text{CH}_3)_2\text{CO}$ or CHCl_3 , 25°C , N_2 , 30 min) no

reaction was observed. In fact, even after 1.5 hours of reaction time, only starting material **31** was observed by ^1H NMR spectroscopy. After 72 hours of reaction, there is ^1H NMR evidence for formation of monoadduct **28**, but only in low yield and as a mixture with several byproducts including the 6,13-bisadduct and several unknown species. An attempt to isolate small quantities of **28** from this complex reaction mixture was unsuccessful. Scheme 2.3 illustrates a proposed mechanism for the formation of monosubstituted pentacenes **26-28**.

The purified monosubstituted thiopentacenes **26** and **27** were characterized by NMR spectroscopy, UV-Vis spectrophotometry, laser desorption ionization mass spectrometry (LDI-MS) and high-resolution mass spectrometry (HRMS).



Scheme 2.2: Synthesis of pentacene monoadducts **26** and **27**.



Scheme 2.3: Proposed synthesis of monosubstituted pentacenes **26-28** using DBU.

2.2 ^1H NMR spectra of 6-organothio substituted pentacenes

As mentioned in Section 1.3, although three monosubstituted pentacenes have been synthesized,^{23,26,46} there have been no reported NMR characterizations for them. This is most likely due to the fact that monosubstituted pentacenes are less photooxidatively resistant and less soluble than their disubstituted counterparts,²³ hence making NMR characterization more difficult. NMR spectra were obtained for monoadducts **26** and **27** after they were degassed via three freeze-pump-thaw cycles and sealed under vacuum in a Norell J Young sealed NMR tube. Figure 2.1 shows the ^1H NMR spectrum for monoadduct **26**. The typical ^1H NMR spectra for 6-organothio substituted pentacenes show three singlets integrating in a 2:2:1 ratio as indicated in Figure 2.1.

^1H NMR

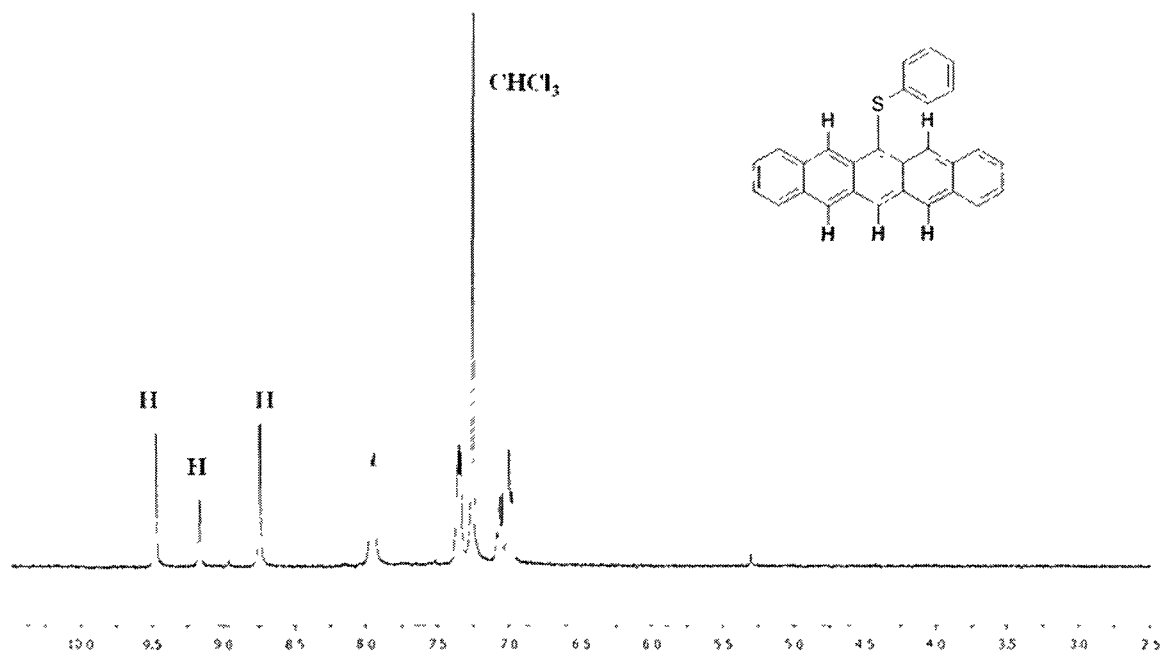


Figure 2.1: ^1H NMR spectrum of 6-phenylthiopentacene, **26** in CDCl_3 .

The assignments of Figure 2.1 are based upon the known ^1H NMR spectrum for bisadduct **27** (Figure 2.2) as well as known ^1H NMR spectra for several other 6,13-bis(organothio) pentacene derivatives. As seen in Figure 2.2, the protons adjacent to S in bisadduct **32** resonate at 9.62 ppm and represent the furthest downfield signal. This is a general trend for organothio substituted pentacenes. Using this information, we similarly assigned the 2 protons (in red) adjacent to the thiophenol group of monoadduct **26** to be the most downfield singlet at 9.48 ppm (Figure 2.1).

^1H NMR

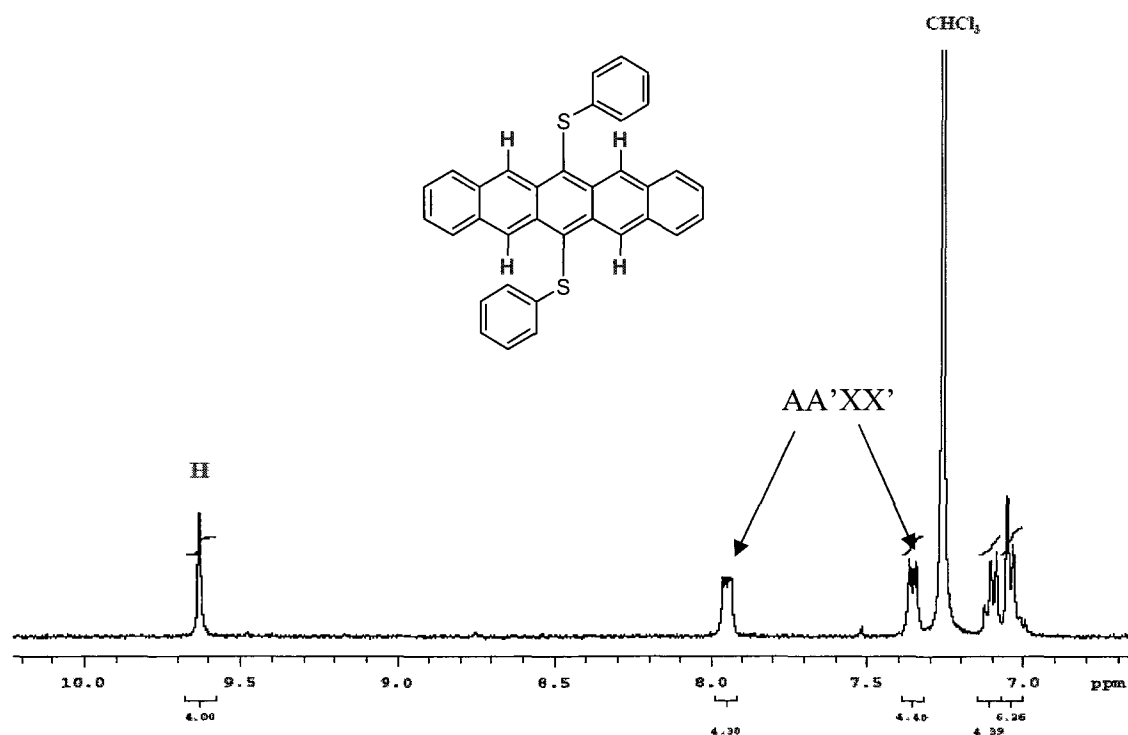


Figure 2.2: ^1H NMR spectrum of 6,13-bis(phenylthio)pentacene, **32** in CDCl_3 .³²

Furthermore, in the case of highly symmetric bisadducts, we typically see an AA'XX' multiplet pattern for the set of protons on the outermost rings of the pentacene (Figure 2.2). Since monoadducts have reduced symmetry compared to bisadducts, an

ABXY multiplet pattern is instead observed for the set of protons on the outermost rings. These two sets of ABXY multiplets corresponding to **26** are found at almost the same region as the AA'XX' multiplets of **32** at 7.94-7.96 ppm and 7.32-7.38 ppm (Figure 2.1).

Similarly, the ^1H NMR spectrum of monoadduct **27** also shows the same characteristic peaks as monoadduct **26**. There are three singlets integrating in a 2:2:1 ratio corresponding to the colored protons of Figure 2.3. These assignments were made by considering the ^1H NMR spectrum of 6,13-bis(acetylthio)pentacene which indicates that the four protons adjacent to the thioacetate group resonate at 9.32 ppm.⁶⁸ Hence, the two protons that are adjacent to the thioacetate group of **27** are assigned the most downfield singlet at 9.48 ppm (Figure 2.3). The ^1H NMR spectrum of monoadduct **27** was also taken in d_6 -DMSO because one multiplet was buried beneath the benzene signal when the ^1H NMR spectrum was recorded in d_6 -benzene.

$^1\text{H NMR}$ in d_6 -DMSO

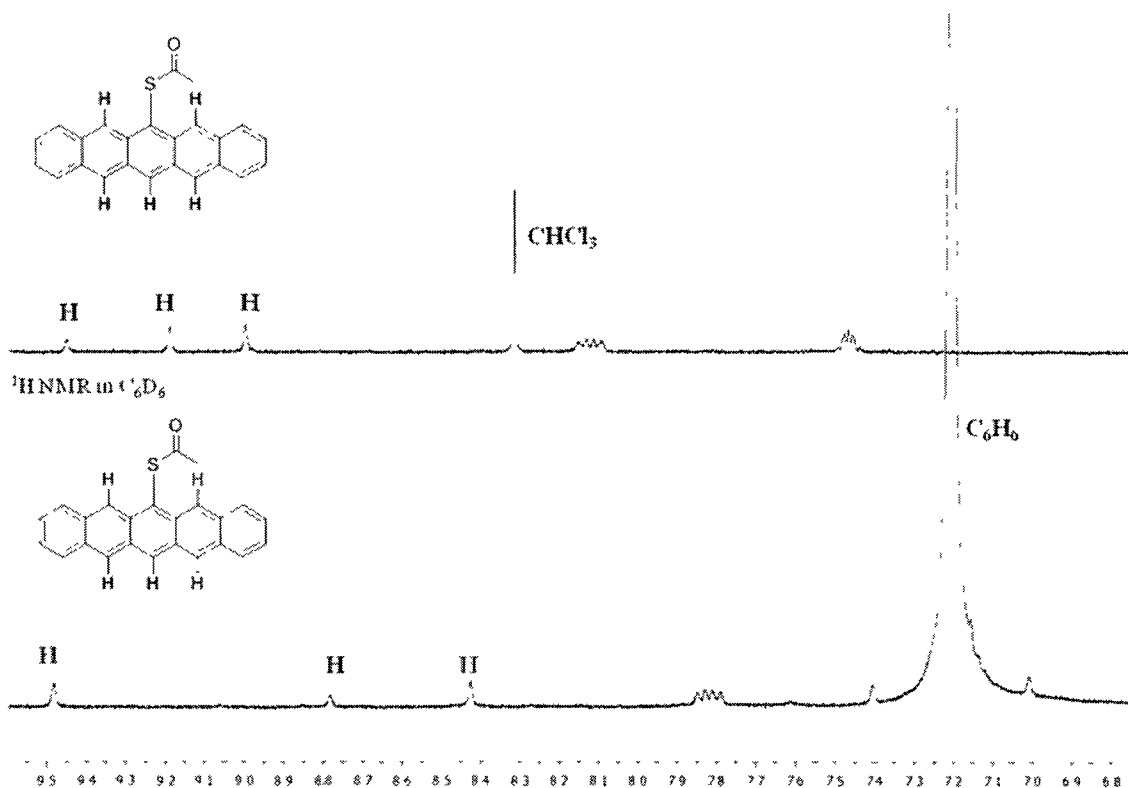


Figure 2.3: Stacked $^1\text{H NMR}$ spectra of 6-acetylthiopentacene, **27**, in d_6 -DMSO and d_6 -benzene.

Monoadducts **26** and **27** show reduced solubility compared to typical 6,13-bis(organothio)substituted pentacenes like **32**. In particular, monoadduct **27** was considerably less soluble in C_6D_6 as compared to monoadduct **26** in CDCl_3 . The solubility of **27** in other solvents such as CDCl_3 and DMSO was similar. Due to its poor solubility, NMR characterization was made more difficult for pentacene **27**.

2.3 Investigations of photodegradation of monoadduct **26** and **27**

2.3.1 Monitoring photodegradation by UV-Vis spectrophotometry

Purified pentacene derivative **26** was dissolved in CH_2Cl_2 to make 2×10^{-4} M solutions and then exposed to ambient light and air at room temperature. UV-Vis spectra

were recorded at regular time intervals until less than 5% of the starting pentacene remained (see Figure 2.4). From Figure 2.4, it is seen that **26** absorbs at 540, 576, and 606 nm. These bands diminished with time while a new set of bands at approximately 363 and 408 nm corresponding to oxidation products increased in magnitude.

UV-Vis spectra recorded after 1.5 hours of exposure to light and air show an unexpected yet surprising blue shift of the shortest wavelength band to 533 nm and an unexpected red shift of the longest wavelength band to 624 nm. This collection of bands, including that at 576 nm, matches those reported for 6,13-bis(phenylthio)pentacene, **32**.³² Thus, when **26** is exposed to air and light, it appears to transform to **32**. This type of reaction has not been reported previously.

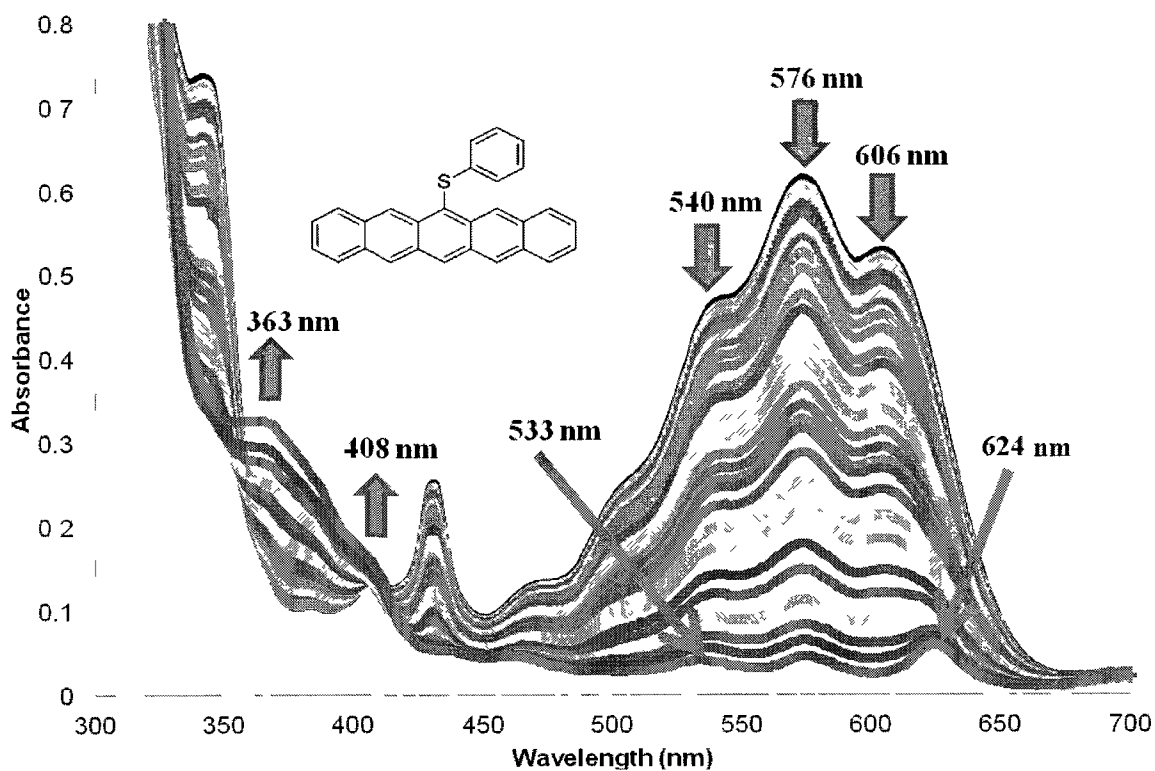


Figure 2.4: UV-Vis study for the photodegradation of 6-phenylthiopentacene, **26**.

Similarly, purified pentacene derivative **27** was dissolved in CH_2Cl_2 to make a saturated solution ($< 2 \times 10^{-4}$ M) and then exposed to ambient light and air at room temperature. From Figure 2.5, it is seen that **27** absorbs at 543, 573, and approximately 606 nm (broad shoulder). These bands diminished with time while a new band at approximately 370 nm corresponding to an oxidation product increased in magnitude. UV-Vis spectra recorded after approximately 2.5 hours of exposure to light and air show no compelling evidence for a transformation reaction as in the case of pentacene **26** (Figure 2.4). A mass spectrum of a solution containing **27** after exposure to light and air did not indicate formation of the corresponding bisadduct.

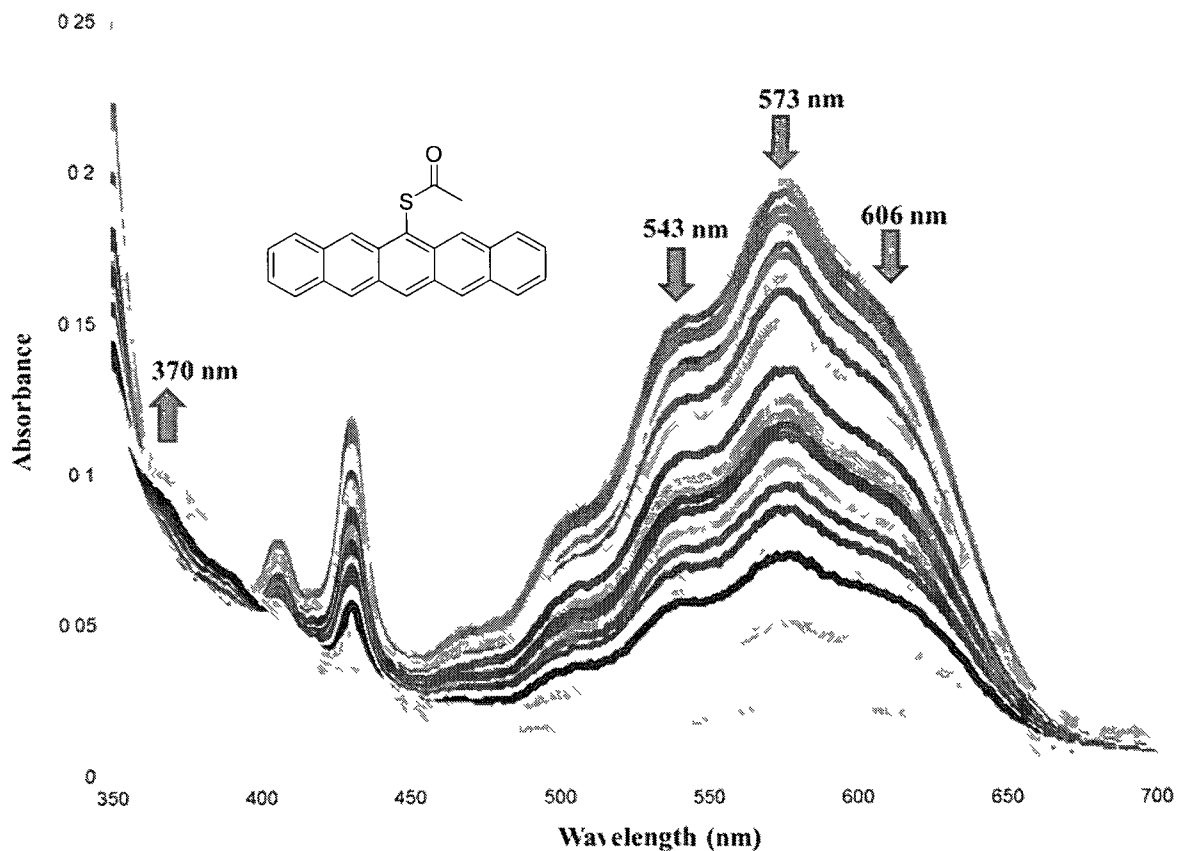


Figure 2.5: UV-Vis study for the photodegradation of 6-acetylthiopyrene, **27**.

The measured half-life of monoadduct **26** was determined under ambient light and air conditions to be 29 minutes (Table 2.1). Monoadduct **26** is shorter lived bisadduct **32**, which has a reported half-life of 1140 minutes under the same conditions.³² This 40 fold reduction in half-life for **26** is surprisingly large and reinforces the need to further study and understand substituent effects in acenes. Monoadduct **27** is moderately longer lived than **26** showing a half-life of 43 minutes, potentially due to the presence of a slightly stronger electron withdrawing group (Table 2.1) which has the effect of lowering HOMO and LUMO energy levels.

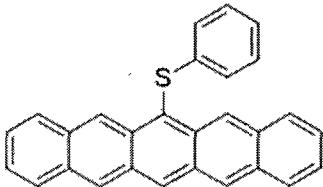
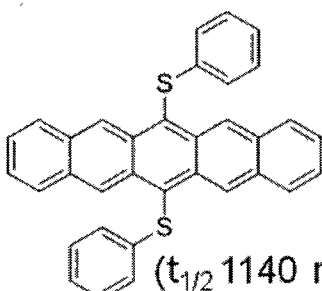
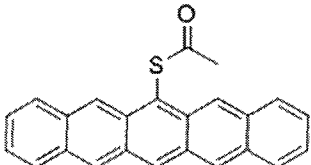
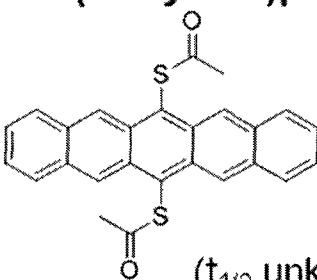
| MONOADDUCT | BISADDUCT |
|---|--|
| <p>6-phenylthiopentacene</p>  <p>($t_{1/2}$ 29 mins)</p> | <p>6,13-bis(phenylthio)pentacene</p>  <p>($t_{1/2}$ 1140 mins)</p> |
| <p>6-acetylthiopentacene</p>  <p>($t_{1/2}$ 43 mins)</p> | <p>6,13-bis(acetylthio)pentacene</p>  <p>($t_{1/2}$ unknown)</p> |

Table 2.1: Half-lives of monoadduct versus bisadduct.

2.3.2 Scaling the photodegradation in a quartz vessel: formation of bisadduct **32** in 20% yield

In Section 2.3.1, the photodegradation of monoadducts **26** and **27** was monitored via UV-Vis spectrophotometry. Figure 2.4 alluded to an unexpected transformation from monoadduct **26** to bisadduct **32**. In order to further investigate this suspected transformation, a large scale reaction was performed. A solution of **26** (13 mg) in CDCl_3 was irradiated with 254 nm UV light for three hours under an argon atmosphere in a quartz round bottom flask (Figure 2.6). A quartz round bottom flask was selected because it absorbs less UV light than Pyrex[®] glassware. The reaction was monitored by color changes and after three hours of irradiation of UV light, the solution color had changed from dark purple (associated with **26**) to blue (associated with **32**). Following work-up,

1.6 mg of bisadduct **32** was isolated (20% yield) and characterized by NMR spectroscopy and LDI mass spectrometry. Hence, this experiment confirms the transformation from monoadduct **26** to bisadduct **32**, as first observed in our UV-Vis spectroscopy study.

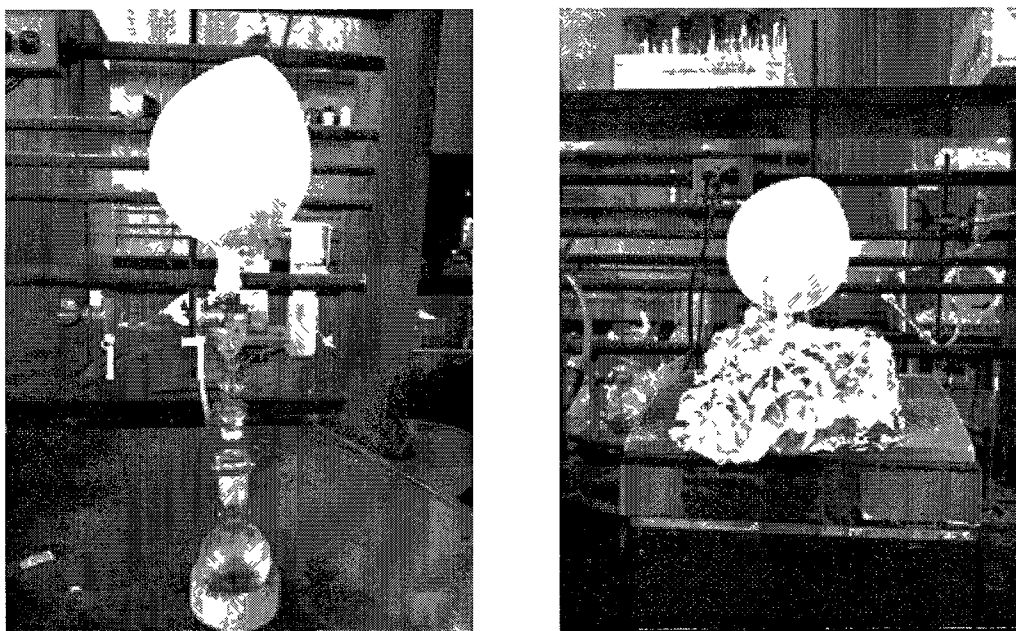


Figure 2.6: Reaction setup for the photodegradation study of **26** dissolved in CDCl_3 in a quartz round bottom flask under an Ar atmosphere (left) and irradiation of a solution of **26** with 254 nm UV light (right).

2.3.3 Monitoring photodegradation of monoadduct **26** by NMR

In order to identify and quantify all photodegradation products formed and their relative concentrations as a function of time, another experiment was performed in a sealed Pyrex® NMR tube with 254 nm UV light irradiation. Pentacene **26** was dissolved in CDCl_3 and the solution was degassed via several freeze-pump-thaw cycles and then sealed under vacuum. Intermittently, the NMR tube was irradiated with 254 nm UV light and product formation monitored by ^1H NMR spectroscopy. The results are summarized in Table 2.2 and Figure 2.7. Formation of bisadduct **32** was confirmed, as was the formation of 6,13-pentacenequinone **17** and endoperoxide product **33**. The formation of

the two oxidation products, **17** and **33**, indicate the presence of oxygen, due either to incomplete removal during degassing or, more likely, a systematic slow leak in the valve NMR tube. The results were reproduced several times and in all trials, the same by-products were identified.

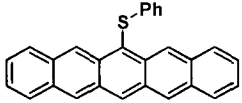
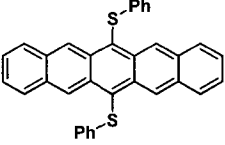
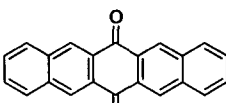
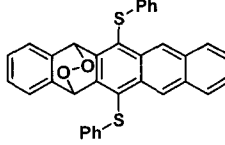
| Irradiation Time (h) | Relative Concentrations (%) | | | |
|----------------------|--|--|---|--|
| |  26 |  32 |  17 |  33 |
| 0 (Day 1) | 99.3 | 0.0 | 0.7 | 0.0 |
| 22 (Day 2) | 98.4 | 0.0 | 1.6 | 0.0 |
| 47 (Day 3) | 92.0 | 2.7 | 2.4 | 2.9 |
| 77 (Day 4) | 80.2 | 6.4 | 3.5 | 10.0 |
| 96 (Day 5) | 69.6 | 8.8 | 4.1 | 17.6 |
| 119 (Day 6) | 49.2 | 13.8 | 5.6 | 31.5 |
| 144 (Day 7) | 19.7 | 19.4 | 8.3 | 52.6 |
| 168 (Day 8) | 9.9 | 18.1 | 9.2 | 62.7 |
| 197 (Day 9) | 3.5 | 13.9 | 10.8 | 71.7 |

Table 2.2: Relative concentrations of **26**, **32**, **17**, and **33** as measured from the crude ^1H NMR spectra over a nine day period with intermittent irradiation of 254 nm UV light.

Figure 2.7 shows the concentration-time profiles using the data from Table 2.2. The graph illustrates the relative concentrations of starting material, bisadduct, and oxidation products based on ^1H NMR analysis. Over the course of nine days, as monoadduct **26** steadily decreased, bisadduct **32** initially increased in concentration reaching a maximum concentration by Day 7 (19.4%) when it was present in approximately equal concentration to **26**. At later times, the concentration of bisadduct **32**

decreased, along with the continued decrease of monoadduct **26**, while ^1H NMR signals corresponding to the oxidation products **17** and **33** grew in intensity. Bisadduct **32** shows a concentration-time profile that is typical for an intermediate while **17** and **33** show typical concentration-time profiles for products.

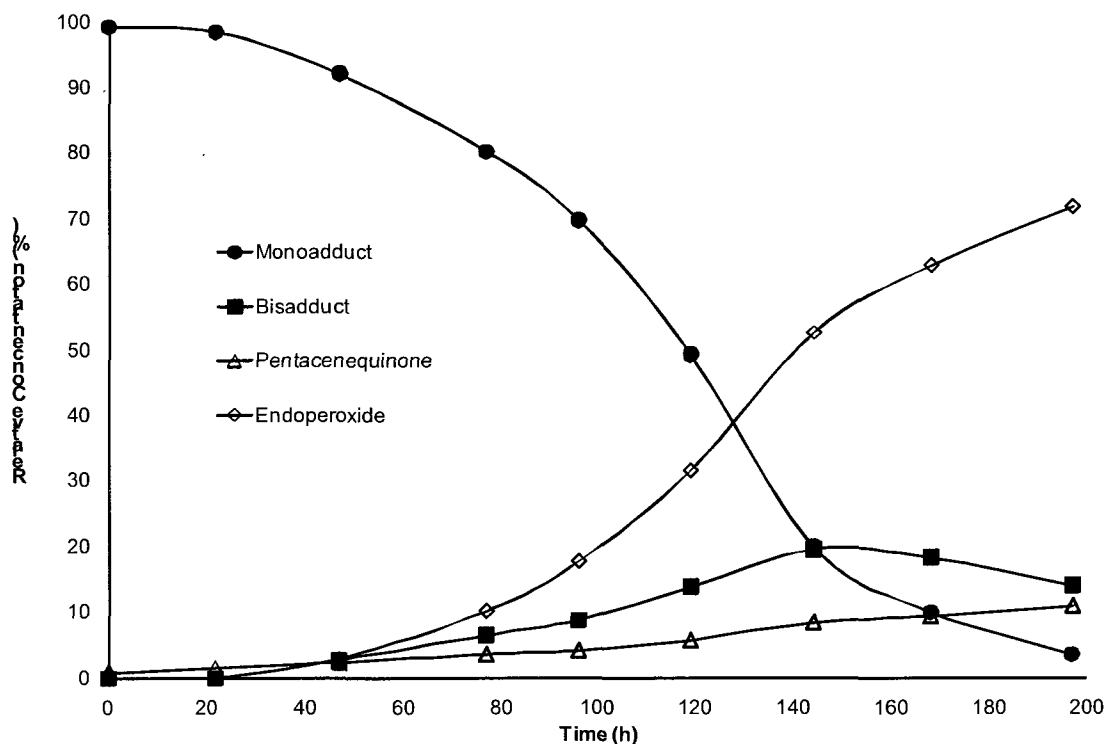


Figure 2.7: Concentration-time profiles of **26**, **32**, **17**, and **33**, observed by ^1H NMR spectroscopy over a nine day period during the photodegradation of **26** in a Pyrex® valve NMR tube. Time refers to the duration of 254 nm light irradiation.

In comparison with the reaction performed in the quartz vessel (Section 2.3.2), the rearrangement from monoadduct **26** to bisadduct **32** is much slower in Pyrex® glass due to its absorption of UV light.

Figure 2.8 shows the ^1H NMR spectra taken over the course of nine days with intermittent irradiation of UV light. Signals corresponding to **17**, **26**, **32**, and **33** are identified.

Based on these experiments, the transformation of **26** to **32** is confirmed. The transformation is initiated by short wavelength UV light and likely does not require oxygen. A control experiment was conducted to test whether light is required to promote the transformation to occur. When a solution of **26** was degassed, sealed under vacuum and kept in the dark for up to four weeks, no transformation to the bisadduct was observed.

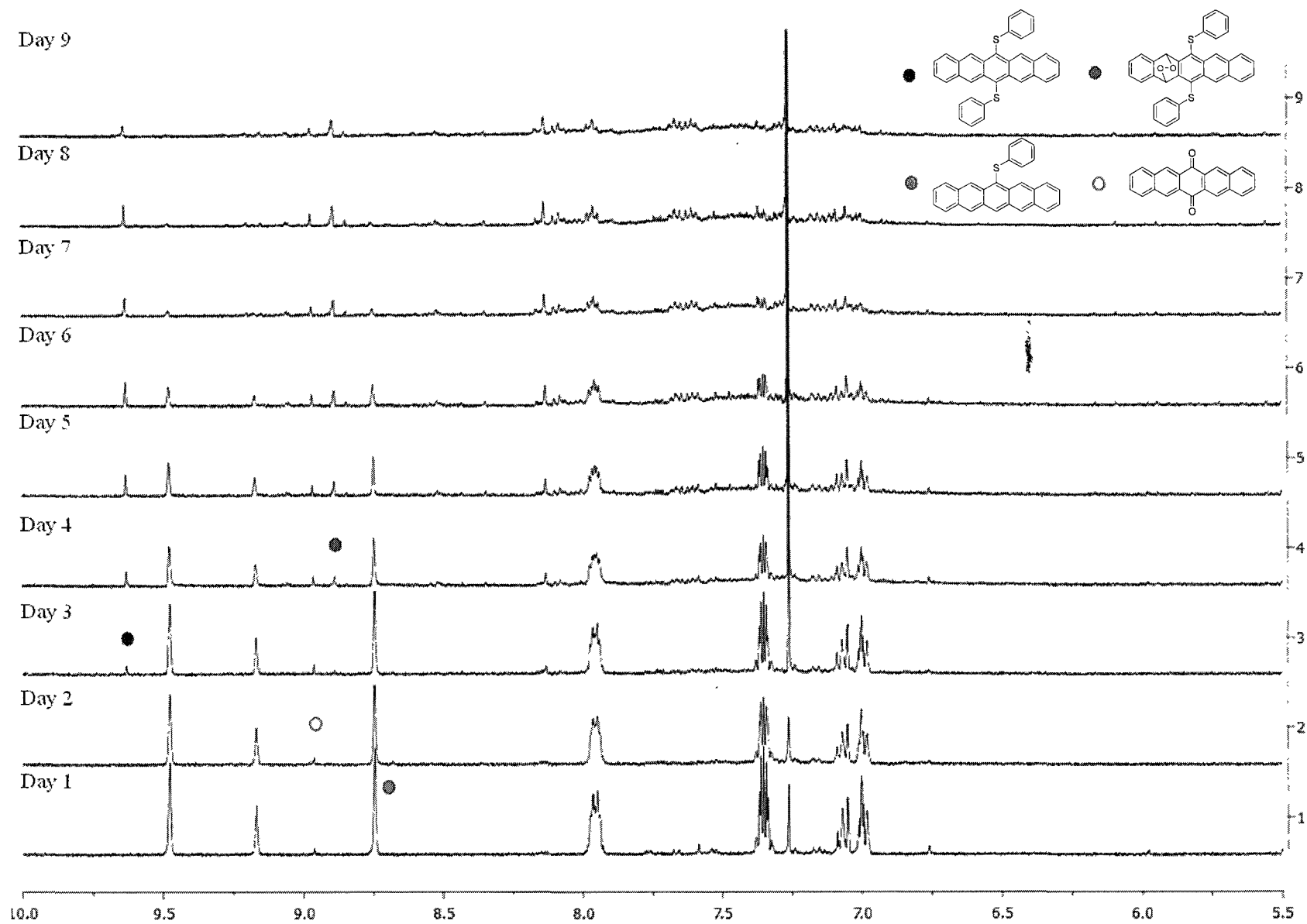


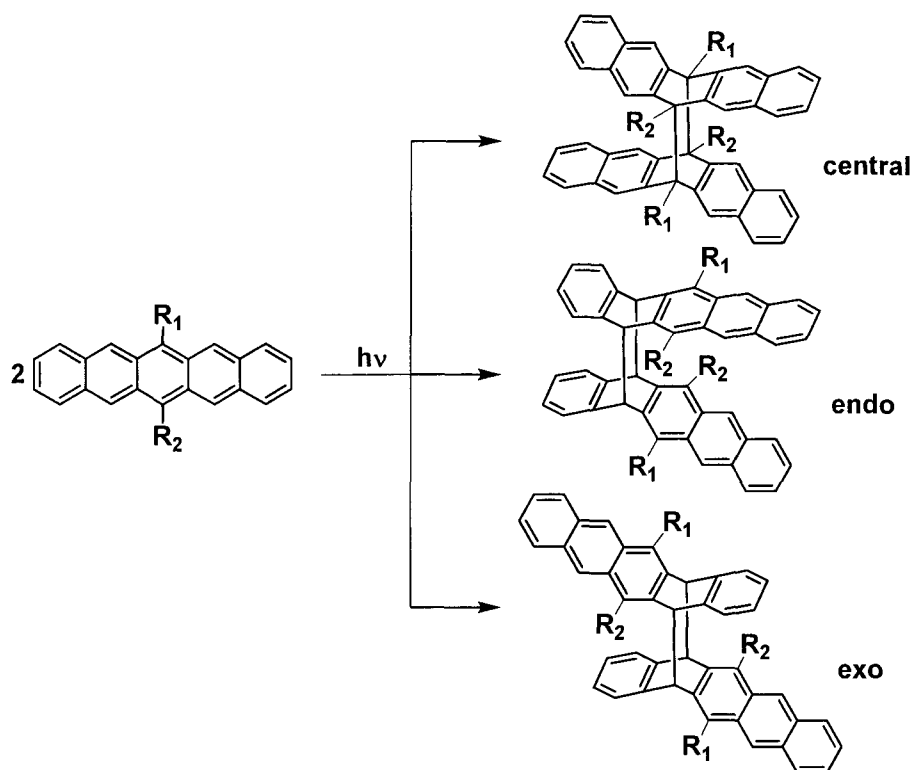
Figure 2.8: ^1H NMR spectra over the course of a nine day period with intermittent irradiation of 254 nm UV light.

2.4 DFT Investigation of Photodimerization

2.4.1 Substitution pattern and effects for dimerization

In order to study the mechanism for the transformation of monoadduct **26** to bisadduct **32**, a DFT computational study was performed. While the project was collaborative in nature, all DFT calculations were performed by Dr. Jennifer Hodgson. We postulated that the transformation from **26** to **32** involves a photodimer of **26** as an intermediate.

Thus, the energies of dimerization of a variety of pentacene derivatives with various substituents at either the 6 or 13 positions or both were studied. Dimerization occurs at either the central 6,13 positions or the penultimate 5,14 positions in either an endo or an exo fashion (Scheme 2.3). The Gibbs free energies of the various dimerizations were calculated using the DFT method M05-2X with a triple-zeta basis set (Table 2.3).⁶⁹ From Table 2.3, it is clear that the energy required for dimerization across the central rings increases dramatically with increased steric bulk at the 6,13 positions. The lowest dimerization energy is seen for pentacene itself, while the 6-substituted pentacenes release much more energy upon dimerization than do the 6,13 disubstituted pentacenes. For example, the Gibbs free energy for central dimerization of 6,13-bis(phenylthio)pentacene, **32**, is 26.4 kcal/mol higher than the same dimerization of 6-phenylthiopentacene, **26**.⁶⁹ For all except pentacene **5**, substituted with the smallest group, central dimerization of 6,13 disubstituted pentacenes is an uphill reaction.



Scheme 2.4: Products of the photodimerization of substituted pentacenes in the absence of oxygen.

| Substituents | ΔG (kcal/mol) | | |
|---|-----------------------|-------|-------|
| | Central | endo | exo |
| $R_1, R_2 = H$ | -22.4 | -13.7 | -13.9 |
| $R_1 = SPh, R_2 = H$ (26) ^a | -14.7 | -15.9 | -15.4 |
| $R_1 = SAc, R_2 = H$ (27) ^a | -12.0 | -14.6 | -15.1 |
| $R_1, R_2 = Cl$ (5) | -0.5 | -18.2 | -20.0 |
| $R_1, R_2 = SPh$ (32) | 11.7 | -17.6 | -20.5 |
| $R_1, R_2 = (tertbutylsilyl)ethyl$ | | | |
| nyl | 17.6 | -4.9 | -11.3 |
| $R_1, R_2 = Ph$ (3) | 42.4 | -5.5 | -14.0 |

^aValues for endo and exo dimerization correspond to endo anti and exo anti diastereomers respectively (see text).

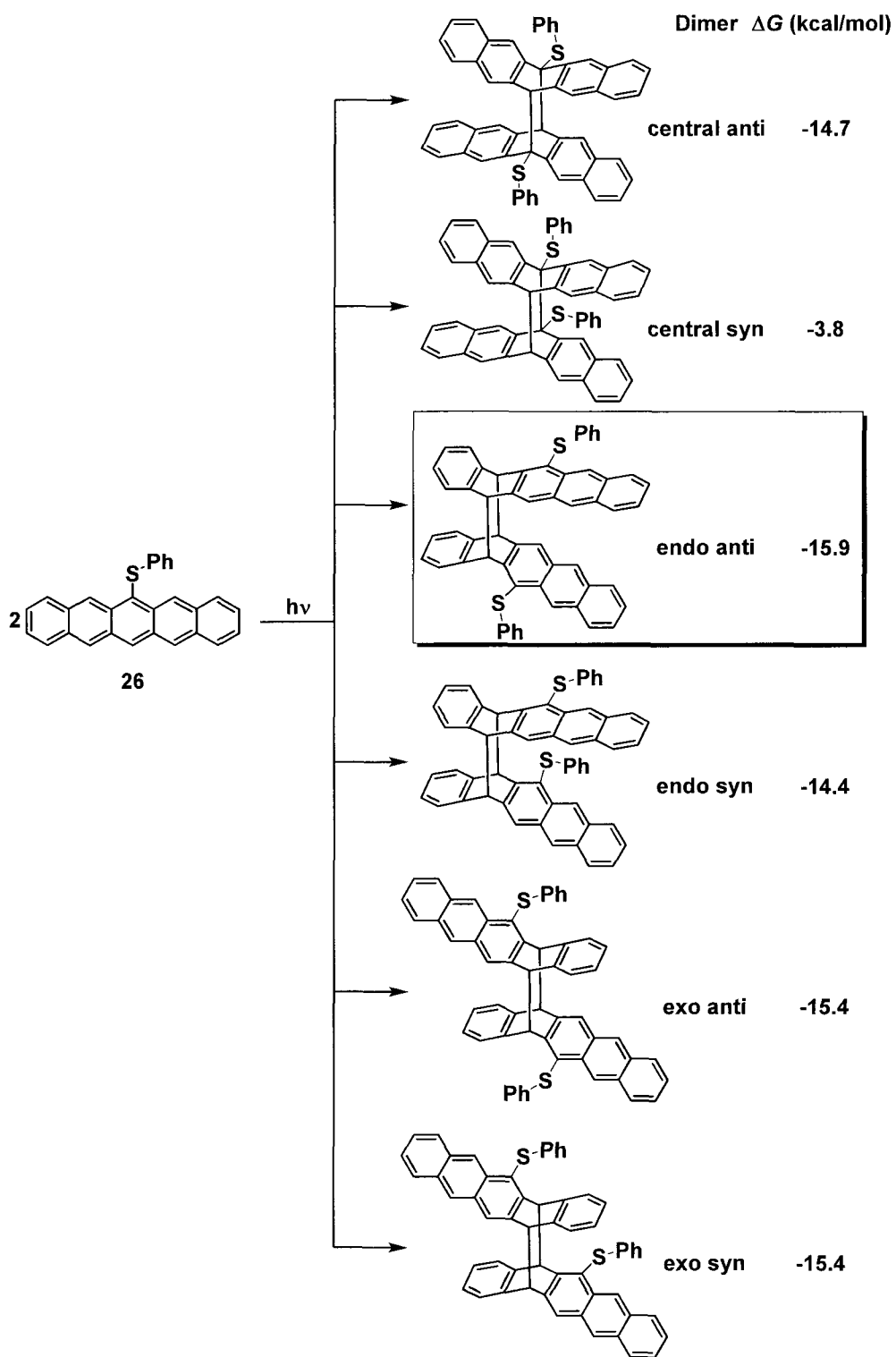
Table 2.3: Gibbs free energies (gas-phase at 298.15 K) for dimerization of substituted pentacenes calculated at the M05-2X/6-311+G(d,p)//B3LYP/6-31G(d) level.⁶⁹

In the past, dimerizations across the 5,14 positions have been observed for pentacenes bearing substituents at the 6 and 13 positions that would otherwise hinder reaction across the central rings.²⁵ Dr. Hodgson's results in Table 2.3 show that central dimerization is unfavorable compared with either endo or exo 5,14 dimerization for all 6,13 disubstituted pentacenes. However, 5,14 dimerizations occurring for pentacenes substituted at only the 6 position show similar energies to central dimerization. The values reported in Table 2.3 refer to the more favorable endo anti and exo anti diastereomers in these cases. Endo and exo 5,14 dimerizations are less favorable for unsubstituted pentacene. The energy differences between endo and exo 5,14 dimerization remain relatively constant for differently substituted pentacenes when smaller substituents are present. In the case of 6,13-bis(*tert*-butylsilylethynyl)pentacene and 6,13-diphenylpentacene, **3**, steric effects from the bulky substituents make endo 5,14 type dimerization less favorable than exo 5,14 type dimerization by 6.4 and 8.5 kcal/mol respectively.⁶⁹

2.4.2 DFT investigation of photodimer products

Dr. Hodgson also studied the mechanism of the transformation of **26** to **32** using the DFT method M05-2X with a triple-zeta basis set.⁶⁹ Scheme 2.5 shows the relative Gibbs free energies of dimerization of the six possible photodimers formed from monoadduct **26** which include central, endo and exo dimers in both anti and syn configurations. From Scheme 2.5, it is seen that all the potential dimers except the central syn dimer have energies within 1.5 kcal/mol of each other. It is therefore postulated that dimerization leads to multiple products, and a complex equilibrium exists between **26** and its various dimers.

Photorearrangement involving phenylthio transfer to form **32** seems highly unlikely for any of the syn diastereomers as well as the exo anti diastereomer. This is because in all of these cases, a highly energetic and/or long distance transfer would be required. Despite exhaustive conformational searching on the central anti dimer, a transition state for the transfer of a phenylthio substituent could not be located. It is thought that the lack of space around the 6,13 sites does not allow for the transfer to occur. Therefore, only one of the dimers, the endo anti dimer of Scheme 2.5, can be reasonably expected to undergo a photorearrangement.



Scheme 2.5: Relative Gibbs free energies (gas-phase at 298.15 K) for the dimerization products of **26** calculated at the M05-2X/6-311+G(d,p)//B3LYP/6-31G(d) level.⁶⁹

2.4.3 Reaction pathways for dimerization and rearrangement of monoadduct **26**

Figures 2.9 and 2.10 show Dr. Hodgson's reaction pathways for the dimerization of **26** (Figure 2.9) and subsequent photorearrangement of the dimer (Figure 2.10). Relative enthalpies, entropies and Gibbs free energies of species along the reaction pathways are shown in Table 2.4. Figure 2.9 and Table 2.4 also illustrate that endo anti dimerization of **26** is similar in both mechanism and energy to the previously reported central-type (6,13 positions) dimerization of unsubstituted pentacene calculated using similar methods.⁶⁷

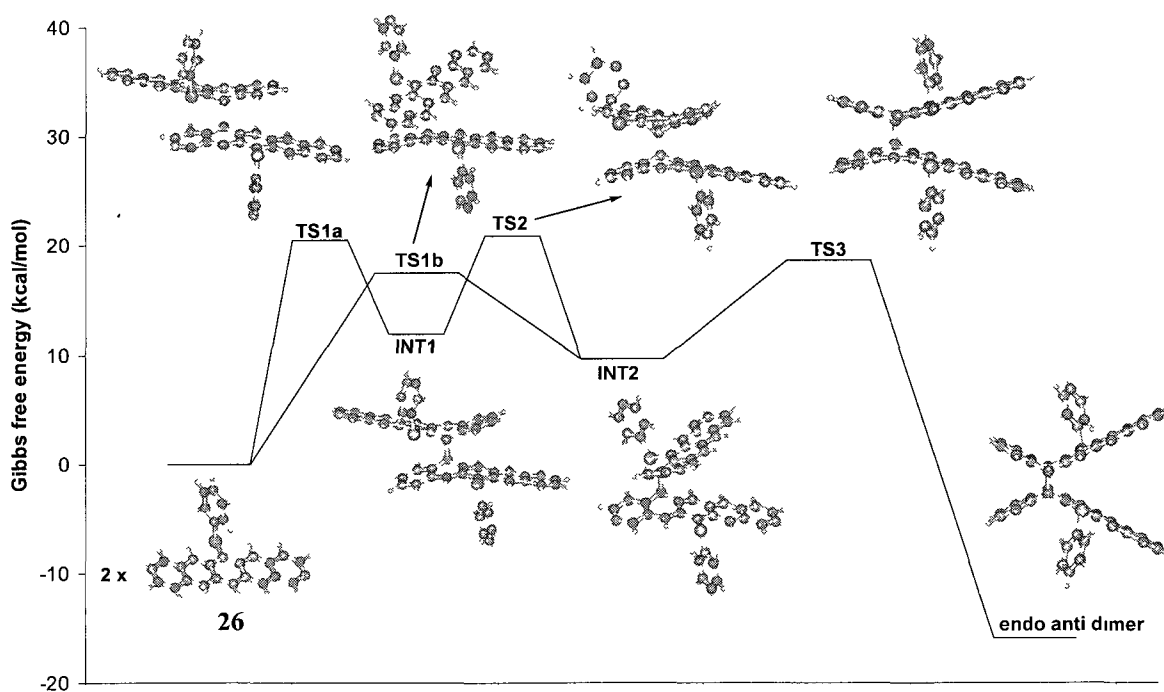


Figure 2.9: Reaction pathway showing Gibbs free energies (298.15 K) for the endo anti dimerization of **26**.⁶⁹

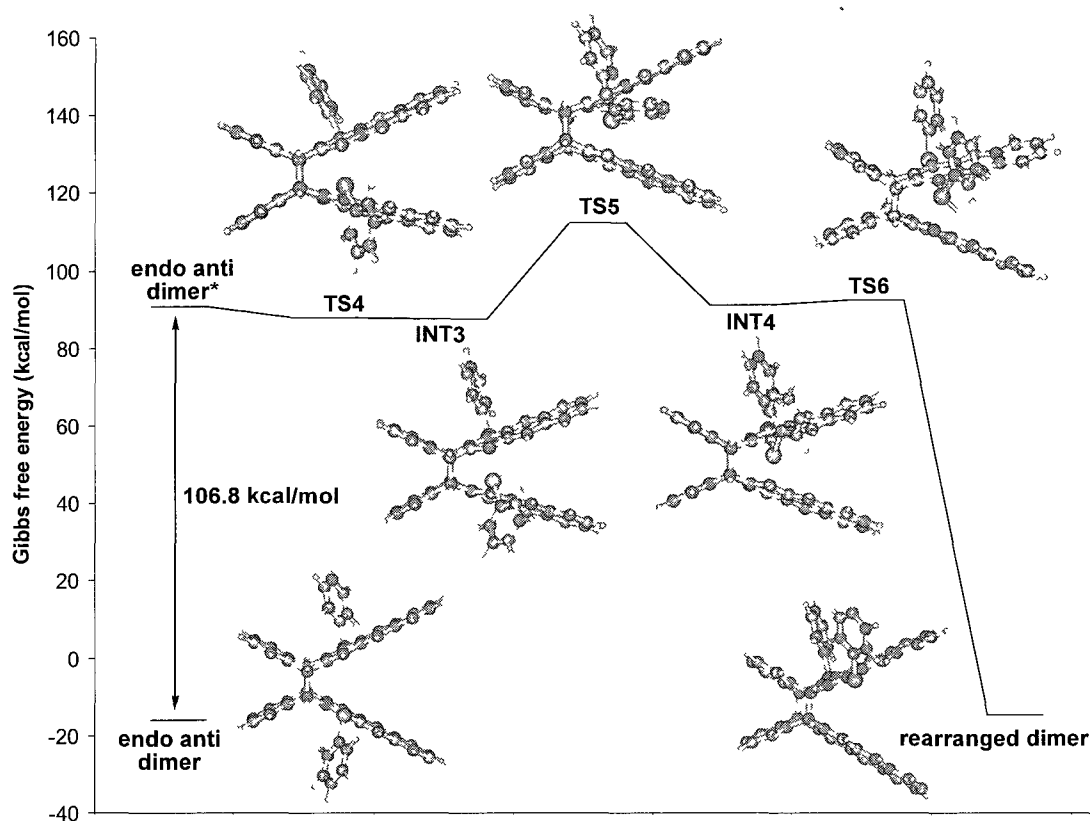


Figure 2.10: Reaction pathway showing Gibbs free energies (298.15 K) for intramolecular substituent transfer on the endo anti photodimer of **26**. Energies are relative to the combined energy of two separate molecules of **26**.⁶⁹

| Species | ΔE (kcal/mol) | ΔS (cal/(molK)) | ΔG (kcal/mol) |
|------------------|-----------------------|-------------------------|-----------------------|
| 26 | 0 | 0 | 0 |
| TS1a | 6.3 | -48.0 | 20.5 ^a |
| TS1b | 3.8 | -46.7 | 17.6 ^a |
| INT1 | -2.1 | -46.8 | 11.8 |
| TS2 | 4.4 | -55.6 | 20.9 ^a |
| INT2 | -3.9 | -45.6 | 9.6 |
| TS3 | 3.1 | -52.4 | 18.7 ^a |
| endo anti dimer | -32.4 | -55.1 | -15.9 |
| TS4 | 70.4 | -58.8 | 87.9 ^a |
| INT3 | 70.1 | -58.7 | 87.6 |
| TS5 | 94.1 | -61.2 | 112.3 ^a |
| INT4 | 73.2 | -60.6 | 91.3 |
| TS6 | 74.9 | -60.1 | 92.5 ^a |
| rearranged dimer | -31.2 | -56.3 | -14.4 |

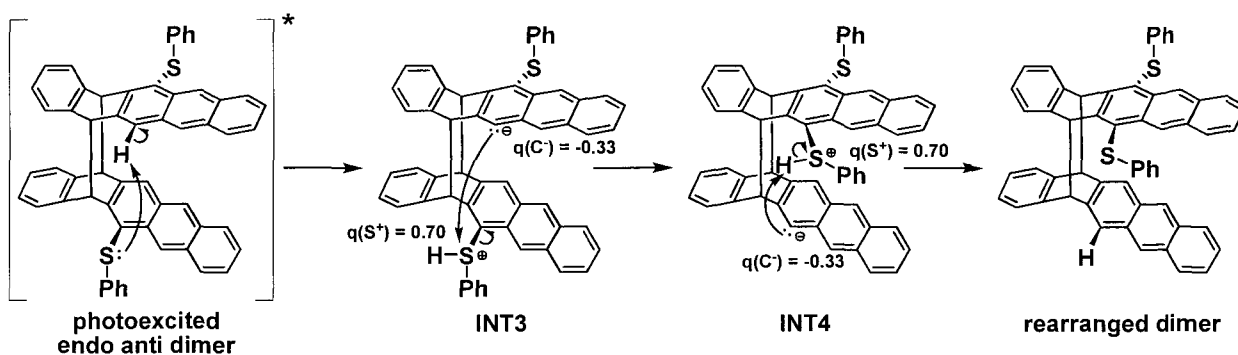
^aTransition state free energies include contributions from the effects of quantum tunneling calculated using the Eckart method.

Table 2.4: Relative enthalpies, entropies and Gibbs free energies (gas-phase at 298.15 K) of species along the reaction pathways of the endo anti dimerization of **26** and subsequent photorearrangement calculated at the M05-2X/6-311+G(d,p)//B3LYP/6-31G(d) level.⁶⁹

Dr. Hodgson's calculations are consistent with dimerization occurring as a multi-step process along one of two possible reaction pathways as illustrated in Figure 2.9. As with pentacene itself, while both reactant **26** and the dimer product are closed-shell species, the various transition states and intermediates show significant biradical character ($\langle S^2 \rangle$ between 0.96 and 1.19). The relative enthalpies and Gibbs free energies of transition states and intermediates are higher in energy than for pentacene dimerization by an average of only 3.6 kcal/mol, likely due to increased steric hindrance in the functionalized pentacene.⁶⁹

2.4.4 Proposed mechanism for the photorearrangement of 6-phenylthiopentacene dimer

Figure 2.10 shows Dr. Hodgson's calculated reaction pathway for intramolecular photorearrangement in the 6-phenylthiopentacene dimer, while Scheme 2.6 shows the arrow-formalism mechanism for this process.⁶⁹ This previously unreported reaction occurs as a multi-step process initiated by photoexcitation of the endo anti dimer. The photoexcited dimer undergoes an intramolecular acid-base reaction involving proton transfer from the 13 position of one pentacene substructure to a sulfur atom attached to C6' on the adjacent pentacene substructure (Scheme 2.6). The resulting intermediate (see INT3 of Figure 2.10 and Scheme 2.5) is a closed-shell zwitterionic species. A charge distribution analysis shows a negative charge of -0.33 at C13 and positive charge of 0.70 at the sulfonium S. INT3 undergoes an intramolecular nucleophilic substitution through the transition state labeled TS5 (Figure 2.10) in which nucleophilic C13 attacks electrophilic sulfur with displacement of anionic C6'. TS5 has some biradical character with $\langle S^2 \rangle = 0.66$. The resulting intermediate, INT4, closely resembles INT3 and is also zwitterionic. The reaction concludes with a second intramolecular proton transfer from the sulfonium group to C6'. Photodimerization of pentacenes is known to be reversible. Our observation of the formation of bisadduct **32** implies dissociation of the rearranged photodimer according to a path analogous to that illustrated in Figure 2.9, in reverse.



Scheme 2.6: Mechanism of the intramolecular photorearrangement of the endo anti photodimer of **26** showing M05-2X/6-311+G(d,p) charges (q) on the zwitterionic intermediates.

In the absence of photoexcitation, the rate determining step of the rearrangement would be the first proton transfer. This reaction has a very high barrier of 103.5 kcal/mol; much too high to be consistent with thermal chemistry (Figure 2.10). Instead, the reaction occurs through a photoexcited pathway in which a photoeximer of the endo anti dimer relaxes to form INT3 (Figure 2.10 and Scheme 2.5) through a very late transition state. A time-dependent DFT calculation at the M05-2X/6-311+G(d,p) level reveals an excited state with a large oscillator strength lying 4.63 eV (106.8 kcal/mol) higher in energy than the ground state dimer (corresponding to a photon at approximately 268 nm) and 3.2 kcal/mol higher in energy than INT3.⁶⁹ It is likely that the reaction proceeds primarily through this excited state (Table 2.5), although a higher energy excited state cannot be excluded. The barriers for the subsequent steps are much lower. The calculated barrier for intramolecular nucleophilic substitution is 24.7 kcal/mol and that for the second proton transfer is only 1.2 kcal/mol.⁶⁹ This last step is highly exergonic releasing 105.7 kcal/mol of energy. Although the photorearrangement is slightly uphill, the overall driving force of the reaction is the release of energy from the photoexcited endo anti dimer.


| Molecule | Excited state | Excitation energy (eV) | Wavelength (nm) | Oscillator strength (f-value) |
|--|---------------|------------------------|-----------------|-------------------------------|
|  Endo anti dimer | 1 | 3.42 | 362 | 0.00 |
| | 2 | 3.51 | 354 | 0.17 |
| | 3 | 3.94 | 315 | 0.02 |
| | 4 | 3.98 | 312 | 0.01 |
| | 5 | 4.09 | 304 | 0.00 |
| | 6 | 4.09 | 303 | 0.02 |
| | 7 | 4.18 | 297 | 0.00 |
| | 8 | 4.23 | 293 | 0.00 |
| | 9 | 4.63 | 268 | 0.63 |
| | 10 | 4.94 | 251 | 0.03 |

Table 2.5: Excited states calculated at the TD-M05-2X/6-311+G(d,p)//B3LYP/6-31G(d) level for the endo anti photodimer of 6-phenylthiopentacene.

CHAPTER 3: CONCLUSIONS

In conclusion, two new organothio substituted pentacene derivatives, 6-phenylthiopentacene, **26**, and 6-acetylthiopentacene, **27**, have been prepared through a novel dehydrogenative aromatization and elimination reaction using DBU as reagent. Monoadduct **26** was shown to undergo a transformation reaction to 6,13-bis(phenylthio)pentacene, **32**, under short wavelength (254 nm) UV conditions irrespective of the presence or absence of O₂. Through a computational study using the density function theoretical method M05-2X, we identified this photorearrangement as a multi-step intramolecular process initiated by the photoexcitation of the endo anti dimer of **26**. The photoexcited dimer undergoes an intramolecular acid-base reaction involving proton transfer from the 13 position of one pentacene substructure to a sulfur atom attached to C6' on the adjacent pentacene substructure, forming a closed-shell zwitterionic species. This species undergoes an intramolecular nucleophilic substitution, in which the nucleophilic C13 attacks electrophilic sulfur with displacement of anionic C6' to form a second zwitterionic species. The reaction concludes with a second intramolecular proton transfer from the sulfonium group to C6'. Bisadduct **32** is then formed by dissociation of the rearranged photodimer.

While **26** undergoes a transformation reaction to form **32**, there is no experimental evidence to support a similar transformation reaction of 6-acetylthiopentacene, **27**, to the corresponding bisadduct.

CHAPTER 4: EXPERIMENTALS

4.1 General Methods

¹H NMR Spectra:

¹H NMR spectra were obtained either on a Varian Mercury Plus 400 FT-NMR operating at 399.768 MHz or a Varian INOVA 500 FT-NMR operating at 499.763 MHz. All chemical shift (δ_{H}) values were reported in parts per million (ppm) relative to (CH₃)₄Si (TMS) unless otherwise noted.

¹³C NMR Spectra:

¹³C NMR spectra were obtained either on a Varian Mercury Plus 400 FT-NMR operating at 100.522 MHz or a Varian INOVA 500 FT-NMR operating at 125.666 MHz. All chemical shift (δ_{H}) values were reported in parts per million (ppm) relative to (CH₃)₄Si (TMS) unless otherwise noted.

Mass Spectrometry:

Mass spectra were obtained on a LDI-TOF-MS (Shimadzu-Kratos Axima) mass spectrometer. High-resolution mass spectra were recorded at the Notre Dame mass spectrometry facility.

UV-Vis Spectrophotometry:

UV-visible spectra were obtained on a Nikolet Evolution 300 spectrophotometer using a 1 cm quartz cell. Dilute solutions were prepared (2×10^{-4} M) and monoadducts **21** and **22**

were dissolved with DCM. Before the experiment began, the cells were protected from light at which the initial spectrum was taken. Each cell was then exposed to ambient light and air at room temperature for a certain amount of time by loosening the cap to allow for oxygen exchange to take place and then the cap was placed back on and placed back in the spectrophotometer. UV-Vis spectra were recorded at regular time intervals until less than 5% of the starting pentacene remained.

Norell J Young Sealed Tube Reactions:

Pentacene derivatives were dissolved in either CDCl_3 or C_6D_6 in a Norell J Young sealed NMR tube and degassed using three cycles of freeze-pump-thaw. The sealed NMR tube was then sealed under argon and irradiated with short UV (254 nm) light. ^1H NMR was used to characterize and monitor the concentrations of the photodegraded products corresponding from the starting pentacene derivative.

Theoretical methods: Calculations in this work were carried out using Gaussian 03. Geometries of all species were fully optimized at the B3LYP/6-31G(d) level of theory and frequencies were also calculated at this level and scaled by appropriate scale factors.⁷⁰ When the restricted wavefunction was unstable, calculations were performed using unrestricted DFT methods. Transition state structures were verified by their (single) imaginary frequencies and by IRC calculations in the forward and reverse directions along the reaction paths. For all species, full systematic conformational searches (at a resolution of 120°) were carried out to ensure that global rather than merely local minima were located. Improved energies for all reaction species were calculated at the M05-

2X/6-311+G(d,p) level.⁷¹ This method has previously been shown to compare well with experimental values for the reaction energies of acene dimerizations,⁷² giving similar results to the M06-2X level recently implemented in an in-depth mechanistic study of acene dimerization.⁶⁷ Gibbs free energies (ΔG) and free energies of activation (ΔG^\ddagger) were calculated at 298.15 K and 1 atm using standard textbook formulae for the statistical thermodynamics of an ideal gas under the harmonic oscillator rigid rotor approximation in conjunction with the optimized geometries and scaled frequencies.⁷³ For transition state calculations, the level of quantum-mechanical tunneling was calculated using the Eckart method,⁷⁴ applied using M05-2X/6-311+G(d,p) barriers and enthalpies and B3LYP/6-31G(d) imaginary frequencies. The effective free energy barrier including tunneling, $\Delta G_{\text{eff}}^\ddagger$, was found from the equation $Q\exp(-\Delta G^\ddagger/RT) = \exp(-\Delta G_{\text{eff}}^\ddagger/RT)$, where Q is the Eckart tunneling coefficient. Charge distributions were calculated using an NBO population analysis performed in GAUSSIAN at the M05-2X/6-311+G(d,p) level of theory

4.2 Column Chromatography

Sand was obtained from Fisher Scientific Co.

Silica Gel (40 μm Flash Chromatography Packing) was obtained from J. T. Baker Chemical Co. Silica gel (38-75 μm Flash Chromatography Packing) was obtained from Natland International Co.

4.3 Solvents

Note: All solvents were used without further purification unless otherwise noted.

Acetone (reagent grade) was obtained from Pharmco.

Chloroform (CHCl_3) was obtained from Fisher Scientific Co.

Deuterated NMR solvents were obtained from Cambridge Isotope Laboratories.

Dichloromethane (CH_2Cl_2) was obtained from Fisher Scientific Co.

Dimethylsulfoxide (DMSO) (anhydrous) was obtained from Alfa Aesar Chemical Co.

Ethanol (anhydrous) was obtained from Pharmco.

Ethanol (95%) was obtained from Pharmco.

Hexanes were obtained from Fisher Scientific Co.

Methanol (CH_3OH) was obtained from Pharmco.

4.4 Reagents

Note: All solvents were used without further purification unless otherwise noted.

Aluminum foil (Al^0) was obtained from Reynolds.

Calcium chloride (CaCl_2) was obtained from Fisher Scientific Co.

Chloranil ($\text{C}_6\text{Cl}_4\text{O}_2$) was obtained from Aldrich Chemical Co.

1,4-Cyclohexanedione ($\text{C}_6\text{H}_8\text{O}_2$) was obtained from Alfa Aesar Chemical Co.

1-Decanethiol ($\text{C}_{10}\text{H}_{22}\text{S}$) was obtained from Alfa Aesar Chemical Co.

1,8-Diazabicycloundec-7-ene ($\text{C}_9\text{H}_{16}\text{N}_2$) was obtained from Aldrich Chemical Co.

2, 3-Dichloro-5,6-dicyano-1,4-benzoquinone (DDQ) was obtained from Aldrich Chemical Co.

o-phthalaldehyde ($\text{C}_8\text{H}_6\text{O}_2$) was obtained from Aldrich Chemical Co.

Palladium on activated carbon (10% Pd/C) was obtained from Aldrich Chemical Co.

Potassium carbonate (K_2CO_3) was obtained from Fisher Scientific Co.

Sodium bisulfite ($NaHSO_3$) was obtained from EM Science.

Sodium borohydride ($NaBH_4$) was obtained from Aldrich Chemical Co.

Sodium chloride ($NaCl$) was obtained from J.T. Baker Chemical Co.

Sodium hydroxide ($NaOH$) was obtained from EM Science.

Sodium Sulfate (Na_2SO_4) was obtained from J.T. Baker Chemical Co.

Sodium thiosulfate (NaS_2O_3) was obtained from J.T. Baker Chemical Co.

Sulfuric Acid (H_2SO_4) was obtained from J.T. Baker, ACS reagent grade.

Thioacetic acid (CH_3COSH) was obtained from Acros Chemical Co.

Thiophenol (C_6H_6S) was obtained from Aldrich Chemical Co.

Zinc bromide ($ZnBr_2$) was obtained from Acros Organic Co.

Zinc iodide (ZnI_2) was obtained from Acros Organic Co.

4.5 Syntheses

6,13-pentacenequinone (17). *O*-phthalaldehyde (5 g, 37.3 mmol) and 1,4-cyclohexanedione (2 g, 17.8 mmol) were dissolved in 300 mL of ethanol and stirred under nitrogen in a 500 mL round bottom flask. To this mixture, a 10% NaOH aqueous solution (3 g, 75.0 mmol) was slowly added via a syringe. The reaction turned from yellow to orange to brown and upon stirring for three hours, the reaction finally turned yellow again. The crude reaction mixture was quenched with water and washed with ethanol and water. The purified product was dried under vacuum overnight to yield a

bright yellow solid (4.99 g, 91%). ^1H NMR (400 MHz, CDCl_3): δ (ppm) 8.96 (s, 4H), 8.13- 8.16 (m, 4H), 7.71-7.74 (m, 4H).

Mixture of *cis* and *trans*-6,13-dihydroxy-6,13-dihdropentacene (18). Pentacene-6,13-dione, **17** (1.0 g, 3.3 mmol) was dissolved in methanol (50 mL) in a round bottom flask. NaBH_4 (1.24 g, 33 mmol) was added in small portions to the flask while kept in an ice bath. The reaction mixture lightens upon reduction. After stirring for 16 h under N_2 , the reaction mixture was quenched with water (15 mL), filtered, and washed with additional water (2 x 10 mL) and small amounts of cold methanol to yield an off-white solid as a mixture of diastereomers (0.86 g, 85 %). Major isomer: ^1H NMR (400 MHz, CDCl_3): δ (ppm) 8.07 (s, 4H), 7.89-7.92 (m, 4H), 7.51-7.53 (m, 4H), 5.88-5.89 (d, 2H, $J = 5.6$ Hz), 3.29-3.31 (d, 2H, $J = 5.6$ Hz); Minor isomer: ^1H NMR (400 MHz, CDCl_3) δ (ppm) 8.14 (s, 4H), 6.20-6.22 (d, 2H, $J = 5.6$ Hz), 3.49-3.51 (d, 2H, $J = 5.6$ Hz)

6-(phenylthio)pentacene (26). A mixture of *cis* and *trans*-**29** (0.071 g, 0.14 mmol) was dissolved in dichloromethane (5 mL) and the resulting mixture was degassed using three freeze-pump-thaw cycles. The resulting solution was warmed to room temperature with protection from light and air. DBU (0.040 mL, 0.27 mmol) was added directly into the reaction mixture in one portion. Immediately, the solution mixture turned dark blue, an indication of pentacene formation. The reaction mixture was stirred for 30 minutes under N_2 . The organic layer was washed with water (2 x 10 mL) and with brine (2 x 10 mL). The organic layer was dried with anhydrous Na_2SO_4 and concentrated to afford a blue crude material. The crude product was triturated with CH_2Cl_2 /hexanes, washed with excess hexanes, and filtered to afford a dark purple solid (0.042 g, 76 %). In solution, the product is unstable to light and air. However, if stored in the dark, the solid is stable for

months. ^1H NMR (400 MHz, CDCl_3): δ (ppm) 9.48 (s, 2H), 9.17 (s, 1H), 8.74 (s, 2H), 7.94-7.96 (m, 4H), 7.32-7.38 (m, 4H), 6.98-7.09 (m, 5H); $^{13}\text{C}\{^1\text{H}\}$ NMR (125 MHz, CDCl_3): δ (ppm) 133.3, 133.0, 131.7, 131.1, 130.4, 129.3, 129.1, 128.2, 127.7, 126.6, 126.0, 125.8, 125.6, 125.1; LDI-MS m/z : 386 [M^+]; HRMS (ESI) calcd for $\text{C}_{28}\text{H}_{18}\text{S}$ (M^+) 386.1124; found, 386.1117; UV-Vis (CH_2Cl_2 , λ_{max}): 540 nm, 576 nm, 606 nm.

6-acetylthiopentacene (27). Following a similar procedure as above, compound **30** (0.080 g, 0.19 mmol) was dissolved in dichloromethane (5 mL) and the resulting mixture was degassed using three freeze-pump-thaw cycles. The resulting solution was warmed to room temperature with protection from light and air. DBU (0.055 mL, 0.37 mmol) was added directly into the reaction mixture in one portion. Immediately, the mixture turned dark blue/purple, an indication of pentacene formation. The reaction mixture was stirred for 30 minutes under N_2 . The organic layer was washed with water (2 x 10 mL) and with brine (2 x 10 mL). The organic layer was dried with anhydrous Na_2SO_4 and concentrated to afford a crude blue solid. The crude product was triturated with CH_2Cl_2 /hexanes, washed with excess hexanes, and filtered to afford a blue solid as product (0.040 g, 61 %). ^1H NMR (400 MHz, C_6D_6): δ (ppm) 9.48 (s, 2H), 8.79 (s, 1H), 8.43 (s, 2H), 7.77-7.85 (m, 4H), 2.01 (s, 3H). LDI-MS m/z : 352 (M^+); HRMS (ESI) calcd for $\text{C}_{24}\text{H}_{17}\text{OS}$ ($\text{M} + \text{H}$) 353.0995; found, 353.0982; UV-Vis (CH_2Cl_2 , λ_{max}): 543 nm, 573 nm, 606 nm (shoulder).

6,13-bis(phenylthio)-6,13-dihydropentacene (29). To a dry round bottom flask was added anhydrous ZnI_2 (0.50 g, 1.6 mmol), compound **18** (0.50 g, 1.6 mmol), and 50 mL of CH_2Cl_2 . To the resulting mixture, thiophenol (0.36 mL, 3.5 mmol) was added. The

reaction was stirred under N₂ for 1 h and reaction progress was monitored by thin layer chromatography (TLC). After the reaction was completed, it was quenched with water (25 mL) and excess ZnI₂ was filtered off. The mixture was extracted with CH₂Cl₂ (2 x 20 mL) and the combined organic layers were washed with water (2 x 10 mL), saturated sodium bisulfite (2 x 10 mL) and brine (2 x 10 mL). The resulting solution was dried over anhydrous Na₂SO₄ and concentrated to afford a light pink solid consisting of two isomers (0.59 g, 74 %). Major isomer: ¹H NMR (400 MHz, CDCl₃): δ (ppm) 7.64-7.67 (m, 4H), 7.49-7.51 (m, 4H), 7.46 (s, 4H), 7.41-7.44 (m, 4H), 7.38-7.40 (m, 2H), 7.30-7.34 (m, 4H), 5.70 (s, 2H); Minor isomer: ¹H NMR (400 MHz, CDCl₃): δ (ppm) 8.00 (s, 4H), 7.75-7.77 (m, 4H), 7.17-7.19 (m, 4H), 6.01 (s, 2H); MALDI-MS (S₈ matrix) *m/z*: 496 (M⁺). A small portion of the product mixture was resolved by silica gel column chromatography using hexanes/CH₂Cl₂ (10:1) as eluent. ¹³C{¹H} NMR of isolated major isomer (125 MHz, CDCl₃) δ (ppm) 136.4, 135.5, 133.9, 132.4, 128.9, 128.8, 127.8, 127.5, 126.1, 54.6.

6,13-bis(acetylthio)-6,13-dihydropentacene (30). To a dry round bottom flask was added anhydrous ZnI₂ (1.06 g, 3.32 mmol), compound **18** (0.52 g, 1.67 mmol), and 50 mL of CH₂Cl₂. To the resulting mixture, thioacetic acid (0.25 mL, 3.54 mmol) was added. The reaction was stirred under N₂ for 1 h and monitored by TLC. After reaction was completed, it was quenched with water (25 mL) and excess ZnI₂ was filtered out. The mixture was extracted with CH₂Cl₂ (2 x 10 mL) and the combined organic layers were washed with water (2 x 10 mL), saturated sodium bisulfite solution (2 x 10 mL), and brine (2 x 10 mL). The resulting solution was dried over anhydrous Na₂SO₄ and concentrated to afford a light peach-colored solid as a single isomer (0.50 g, 70 %). No

purification was required. ^1H NMR (400 MHz, CDCl_3): δ (ppm) 8.06 (s, 4H), 7.81-7.84 (m, 4H), 7.45-7.48 (m, 4H), 6.57 (s, 2H); 2.40 (s, 6H); $^{13}\text{C}\{^1\text{H}\}$ NMR (125 MHz, CDCl_3): δ (ppm) 194.3, 135.2, 133.0, 127.8, 127.5, 126.6, 46.2, 30.4; HRMS (ESI) calcd for $\text{C}_{26}\text{H}_{20}\text{NaO}_2\text{S}_2$ ($\text{M} + \text{Na}$) 451.0797; found, 451.0821.

6,13-bis(decylthio)-6,13-dihydropentacene (31)

To a dry round bottom flask was added anhydrous ZnI_2 (1.06 g, 3.32 mmol), compound **18** (0.54 g, 1.73 mmol), and 50 mL of CH_2Cl_2 . To the resulting mixture, 1-decanethiol (0.25 mL, 1.18 mmol) was added. The reaction was stirred under N_2 for 1 h and monitored by TLC. After reaction was completed, it was quenched with water (25 mL) and excess ZnI_2 was filtered out. The mixture was extracted with CH_2Cl_2 (2 x 10 mL) and the combined organic layers were washed with water (2 x 10 mL), saturated sodium bisulfite solution (2 x 10 mL), and brine (2 x 10 mL). The resulting solution was dried over anhydrous Na_2SO_4 and concentrated to afford a light peach-colored solid as a single isomer (0.80 g, 74 %). No purification was required. ^1H NMR (400 MHz, CDCl_3): δ (ppm) 7.83-7.84 (m, 4H); 7.83 (s, 4H); 7.46-7.48 (m, 4H); 5.41 (s, 2H); 2.71 (t, 4H, $J = 6.0$ Hz); 1.71 (m, 4H); 1.42 (m, 4H); 1.26 (m, 24H); 0.89 (t, 6H, $J = 5.6$ Hz); $^{13}\text{C}\{^1\text{H}\}$ NMR (125 MHz, CDCl_3): δ (ppm) 135.3, 132.6, 127.6, 127.4, 126.1, 48.1, 39.3, 33.9, 31.9, 29.6, 29.59, 29.4, 29.3, 29.2, 22.7, 14.2; LDI-MS m/z : 623 (M^+).

References

- ¹ Harvey, R. G. *Polycyclic Aromatic Hydrocarbons*. Wiley-VCH: New York, 1997.
- ² Mondal, R.; Tonshoff, C.; Khon, D.; Neckers, D.; Bettinger, H. *J. Am. Chem. Soc.* **2009**, *131*, 14281.
- ³ Clar, E. *Ber. dtsh. Chem. Ges.* **1939**, *72*, 2137.
- ⁴ Anthony, J. E. *Angew. Chem. Int. Ed* **2008**, *47*, 452.
- ⁵ Bendikov, M.; Wudl, F.; Perepichka, D. *Chem. Rev.* **2004**, *104*, 4891.
- ⁶ Biermann, D.; Schmidt, W. *J. Am. Chem. Soc.* **1980**, *102*, 3163.
- ⁷ Tonshoff, C.; Bettinger, H. *Angew. Chem. Int. Ed.* **2010**, *49*, 4125.
- ⁸ a) Yamada, H.; Yamashita, M.; Kikuchi, M.; Watanabe, H.; Okujima, T.; Uno, H.; Ogawa, T.; Ohara, K.; Ono, N. *Chem. Eur. J.* **2005**, *11*, 6212. b) Uno, H.; Yamashita, Y.; Kikuchi, M.; Watanabe, H.; Yamada, H.; Okujima, T.; Ogawa, T.; Ono, N. *Tetrahedron Lett.* **2005**, *46*, 1981. c) Yamada, H.; Kawamura, E.; Sakamoto, S.; Yamashita, Y.; Okujima, T.; Uno, H.; Ono, N. *Tetrahedron Lett.* **2006**, *47*, 7501. d) Masumoto, A.; Yamashita, Y.; Go, S.; Kikuchi, T.; Yamada, H.; Okujima, T.; Ono, N.; Uno, H. *Jpn. J. Appl. Phys.* **2009**, *48*, 051505. e) Katsuta, S.; Yamada, H.; Okujima, T.; Uno, H. *Tetrahedron Lett.* **2010**, *51*, 1397.
- ⁹ (a) Clar, E.; John, Fr. *Ber. Dtsch. Chem.* **1929**, *62*, 3027. (b) Clar, E.; John, Fr.; *Ber. Dtsch. Chem.* **1931**, *64*, 981.
- ¹⁰ The number of papers related to the concept pentacene was obtained by searching with the word “pentacene” on SciFinder® Scholar Chemistry Database.
- ¹¹ Hawley-Fedder, R. A.; Parsons, M. L.; Karasek, F.W. *J. Chromat.* **1987**, *387*, 207.
- ¹² De Vries, M. S.; Reihls, K.; Wendt, H. R.; Golden, W. G.; Hunziker, H. E.; Fleming, R.; Peterson, E.; Chang, S. *Geochim. Cosmochim. Acta.* **1993**, *57*, 933.
- ¹³ Kitamura, M.; Arakawa, Y. *J. Phys.* **2008**, *20*, 184011.
- ¹⁴ Laquindanum, J.; Katz, H.; Lovinger, A. *J. Am. Chem. Soc.* **1998**, *120*, 664.
- ¹⁵ (a) Janzen, D.; Burand, M.; Ewbank, P.; Pappenfus, T.; Higuchi, H.; da Silva Filho, D.; Young, V.; Bredas, J.; Mann, K. *J. Am. Chem. Soc.* **2004**, *126*, 15295. (b) Xiao, K.; Liu, Y.; Qi, T.; Zhang, W.; Wang, F.; Gao, J.; Qiu, W.; Ma, Y.; Cui, G.; Chen, S.; Zhan, X.; Yu, G.; Qin, J.; Hu, W.; Zhu, D. *J. Am. Chem. Soc.* **2005**, *127*, 13281.

-
- ¹⁶ Facchetti, A.; Letizia, J.; Yoon, M.; Mushrush, M.; Katz, H.; Marks, T. *Chem.Mater.* **2004**, *16*, 4715.
- ¹⁷ Anthony, J. E. *Chem. Rev.* **2006**, *106*, 5028.
- ¹⁸ (a) Klauk, H.; Halik, M.; Zschieschang, U.; Schmid, G.; Radlik, W.; Weber, W. *J. Appl. Phys.* **2002**, *92*, 5259. (b) Stadlober, B.; Zirkl, M.; Beutl, M.; Leising, G.; Gogonea, S. B.; Bauer, S. *Appl. Phys. Lett.* **2005**, *86*, 242902. (c) Hwang, D.K.; Lee, K.; Kim, J.H.; Im, S.; Kim, C.S.; Baik, H.K.; Park, J.H.; Kim, E. *Appl. Phys. Lett.* **2005**, *88*, 243513.
- ¹⁹ Lee, S.; Koo, B.; Shin, J.; Lee, E.; Park, H.; Kim, H. *Appl. Phys. Lett.* **2006**, *88*, 162109.
- ²⁰ Jang, B. B.; Lee, S. H.; Kafafi, Z. H. *Chem.Mater.* **2006**, *18*, 449.
- ²¹ Ried, W.; Anthöfer, F. *Angew. Chem.* **1953**, *65*, 601.
- ²² Cava, M. P.; Deana, A. A.; Muth, K. *J. Am. Chem. Soc.* **1959**, *81*, 6458.
- ²³ Vets, N.; Smet, M.; Dehaen, W. *Synlett.* **2005**, 217.
- ²⁴ (a) Ono, K.; Totani, H.; Hiei, T.; Yoshino, A.; Saito, K.; Eguchi, K.; Tomura, M.; Nishida, J.; Yamashita, Y. *Tetrahedron.* **2007**, *63*, 9699. (b) Etienne, A.; Beauvois, C. *Compt. Rend.* **1954**, *239*, 64.
- ²⁵ Coppo, P.; Yeates, S. *Adv.Mater.* **2005**, *17*, 3001.
- ²⁶ Miao, Q.; Chi, X.; Xiao, S.; Zeis, R.; Lefenfeld, M.; Siegrist, T.; Steigerwald, M.; Nuckolls, C. *J. Am. Chem. Soc.* **2005**, *128*, 1340.
- ²⁷ Huang, Z.; Jiang, Y.; Yang, X.; Fu, Y.; Cao, W.; Zhang, J. *Synth. Metals.* **2009**, *159*, 1552-1556.
- ²⁸ Miller, G. P.; Mack, J.; Briggs, J. *Org. Lett.* **2000**, *2*, 3983.
- ²⁹ (a) Trosi, A.; Orlandi, G.; Anthony, J. E. *Chem. Mater.* **2005**, *17*, 5024. (b) Benard, C. P.; Geng, Z.; Heuft, M. A.; VanCrey, K.; Fallis, A. G. *J. Org. Chem.* **2007**, *72*, 7229. (c) Jiang, J.; Kaafarani, B. R.; Neckers, D. C. *J. Org. Chem.* **2006**, *71*, 2155.
- ³⁰ Anthony, J. E.; Brooks, J. S.; Eaton, D. L.; Parkin, S. R. *J. Am. Chem. Soc.* **2001**, *123*, 9482.
- ³¹ (a) Okamoto, T.; Senatore, M. L.; Ling, M.; Mallik, A. B.; Tang, M. L.; Bao, Z. *Adv. Mater.* **2007**, *19*, 3381. (b) Swartz, C. R.; Parkin, S. R.; Bullock, J. E.; Anthony, J. E.; Mayer, A.C.; Malliaras, G. G. *Org. Lett.* **2005**, *7*, 3163.
- ³² Kaur, I.; Jia, W.; Kopreski, R.; Selvarasah, S.; Dokmeci, M.; Pramanik, C.; McGruer, N.; Miller, G. *J. Am. Chem. Soc.* **2008**, *130*, 16274.

-
- ³³ Kobayashi, K.; Shimaoka, R.; Kawahata, M.; Yamanaka, M.; Yamaguchi, K. *Org. Lett.* **2006**, *8*, 2385.
- ³⁴ Ito, K.; Suzuki, T.; Sakamoto, Y.; Kubota, D.; Inoue, Y.; Sato, F.; Tokito, S. *Angew. Chem.* **2003**, *42*, 1159.
- ³⁵ Odom, S. A.; Parkin, S. R.; Anthony, J. E. *Org. Lett.* **2003**, *5*, 4245.
- ³⁶ a) Tang, C. W. *App. Phys. Lett.* **1986**, *48*, 183. b) Hoppe, H.; Sariciftci, N. S. *J. Mat. Res.* **2004**, *19*, 1924.
- ³⁷ Reichwagen, J.; Hopf, H.; Del Guerso, A.; Desvergne, J.; Bouas-Laurent, H. *Org. Lett.* **2004**, *6*, 1899.
- ³⁸ Li, Y.; Wu, Y.; Liu, P.; Prostran, Z.; Gardner, S.; Ong, B. *Chem. Mater.* **2007**, *19*, 418.
- ³⁹ (a) Wolak, M. A.; Jang, B. B.; Palilis, L. C.; Kafafi, Z. H. *J. Phys. Chem. B.* **2004**, *108*, 5492. (b) Maliakal, A.; Raghavachari, K.; Katz, H.; Chandross, E.; Siegrist, T. *Chem. Mater.* **2004**, *16*, 4980.
- ⁴⁰ Payne, M. M.; Parkin, S. R.; Anthony, J. E.; Kuo, C. C.; Jackson, T. N. *J. Am. Chem. Soc.* **2005**, *127*, 4986.
- ⁴¹ (a) Cornil, J.; Calbert, J. P.; Bredas, J. L. *J. Am. Chem. Soc.* **2001**, *123*, 1250. (b) Fritz, S.E.; Martin, S. M.; Frisbie, C. D.; Ward, M. D.; Toney, M. F. *J. Am. Chem. Soc.* **2004**, *126*, 4084.
- ⁴² Reichmanis, E.; Katz, H.; Kloc, C.; Maliakal, A. *Bell Lab. Tech. J.* **2005**, *10*, 87.
- ⁴³ (a) Curtis, M. D.; Cao, J.; Kampf, J. W. *J. Am. Chem. Soc.* **2004**, *124*, 4318. (b) Bredas, J. L.; Beljonne, D.; Coropceanu, V.; Cornil, J. *Chem. Rev.* **2004**, *104*, 4971.
- ⁴⁴ Kobayashi, K.; Masu, H.; Shuto, A.; Yamaguchi, K. *Chem. Mater.* **2005**, *17*, 6666.
- ⁴⁵ (a) Werz, D. B.; Gleiter, R.; Rominger, F. *J. Am. Chem. Soc.* **2002**, *124*, 10638. (b) Gleiter, R.; Werz, D. B. *Chem. Lett.* **2005**, *34*, 126.
- ⁴⁶ Chi, X. (Lucent Technologies Inc., USA). Synthesis of Acenes and Hydroxyacenes. US Patent 2010/0144086A1, June 10, 2010.
- ⁴⁷ Vets, N.; Doctoral Dissertation, Katholieke University, Leuven, Belgium, **2006**.
- ⁴⁸ Clar, E. *Polycyclic Hydrocarbons. Volumes 1 and 2*. Academic Press, Inc.: London, 1964.

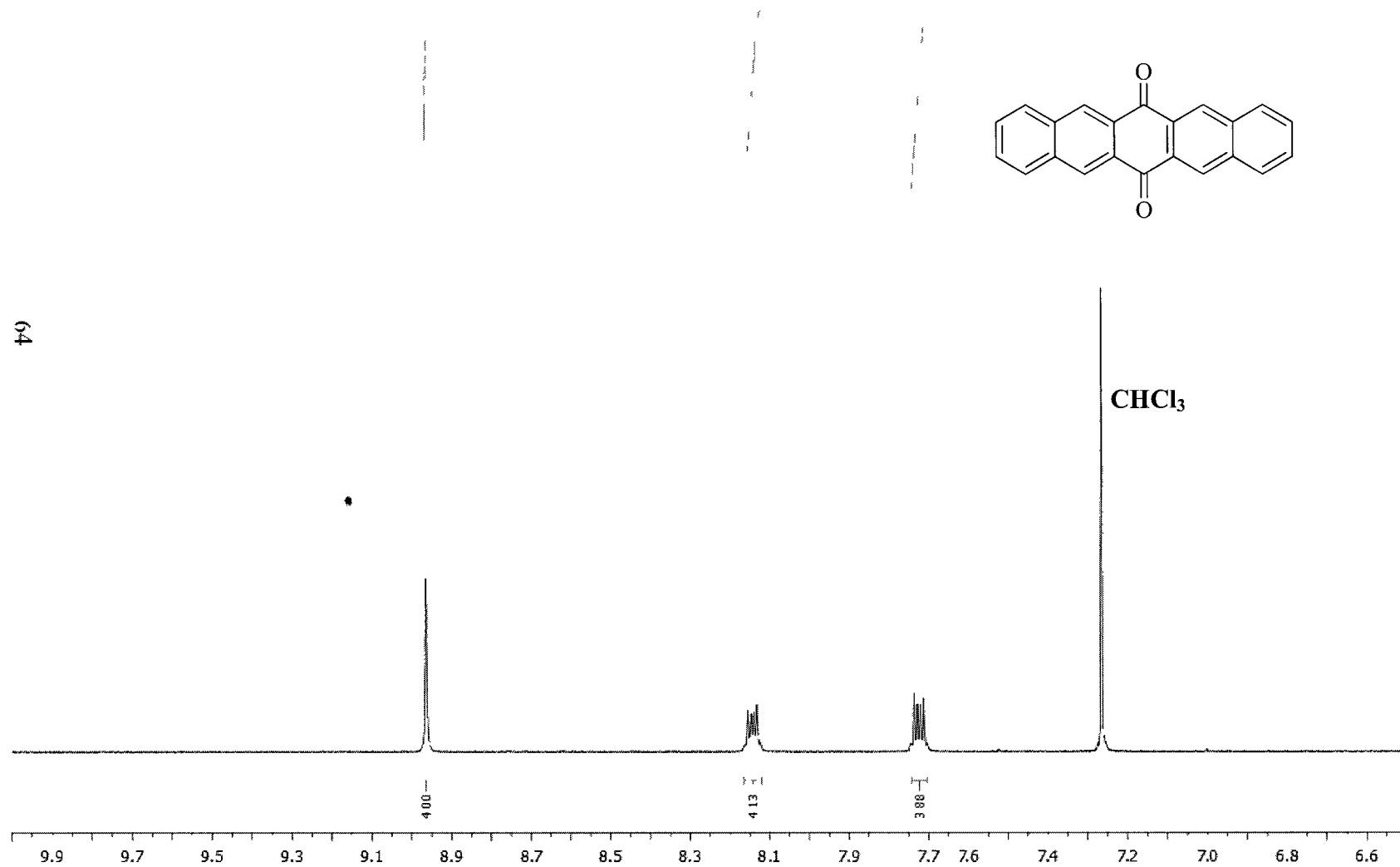
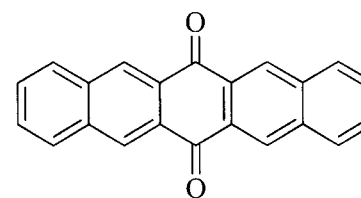
-
- ⁴⁹ (a) Wang, Y.; Zhou, Y.; Sokolov, J.; Rigas, B.; Levon, K.; Rafailovich, M. *Biosens. Bioelectron.* **2008**, *24*, 162. (b) Chen, H.; Heng, C. K.; Pui, P. D.; Zhou, X. D.; Lee, A. C.; Lim, T. M.; Tan, S. N. *Anal. Chim. Acta.* ,**2005**, *554*, 52. (c) Huang, T. J.; Brough, B.; Ho, C. M.; Liu, Y.; Flood, A. H.; Bonvallet, P. A.; Tseng, H. R. Stoddart, J. F.; Baller, M.; Magonov, S. *Appl. Phys. Lett.* **2004**, *85*, 5391.
- ⁵⁰ Love, J. C.; Estroff, L. A.; Kriebel, J. K. Nuzzo, R. G.; Whitesides, G. M. *Chem. Rev.* **2005**, *105*, 1103.
- ⁵¹ Wang, J.; Kaur, I.; Diaconescu, B.; Tang, J.; Miller, G.; Pohl, K. *ACS Nano.* **2011**, *5*, 1792.
- ⁵² (a) Drechsler, U.; Erdogan, B.; Rotello, V.M. *Chem. Eur. J.* **2004**, *16*, 5570. (b) Daniel, M. C.; Astruc, D. *Chem. Rev.* **2004**, *104*, 293.
- ⁵³ Takeuchi, S.; DiLuzio, W. R.; Weibel, D. B.; Whitesides, G. M. *Nano Lett.* **2005**, *5*, 1819.
- ⁵⁴ Campbell, I. H.; Kress, J. D.; Martin, R. L.; Smith D. L. *Appl. Phys. Lett.* **1997**, *71*, 3528.
- ⁵⁵ Nuzzo, R. G.; Allara, D. L. *Langmuir.* **1985**, *1*, 45.
- ⁵⁶ Vericat, C.; Vela, M. E.; Benitez, G.; Carro, P.; Salvarezza, R. C. *Chem. Soc. Rev.* **2010**,*39*, 1805.
- ⁵⁷ de Boer, B.; Hadipour, A.; Mandoc, M.; van Woudenberg, T.; Blom. P. *Adv. Mater.* **2005**, *17*, 621.
- ⁵⁸ Engelkes, V.; Beebe, J.; Frisbie, C. *J. Am. Chem. Soc.* **2004**, *126*,14287.
- ⁵⁹ Kobayashi, S.; Nishikawa, T.; Takenobu, T.; Mori, S.; Shimoda, T.; Mitani, T.; Shimotani, H.; Yoshimoto, N.; Ogawa, Y.; Iwasa, Y. *Nat. Mater.* **2004**,*3*, 317.
- ⁶⁰ Tulevski, G.; Miao, Q.; Afzali, A.; Graham, T.; Kagan, C.; Nuckolls, C. *J. Am. Chem. Soc.* **2006**, *128*, 1788.
- ⁶¹ Foote, C. S. *Photochem. Photobiol.* **1991**, *54*, 659.
- ⁶² Reddy, A. R.; Bendikov, M. *Chem. Commun.* **2006**, 1179.
- ⁶³ Prusevich, P.; B. S. Thesis, University of New Hampshire, Durham, NH, 2010.
- ⁶⁴ Birks, J. B.; Appleyard, J. H.; Pope, R. *Photochem. Photobiol.* **1963**, *2*, 493.
- ⁶⁵ Zhao, Y.; Cai, X.; Danilov, E.; Li, G.; Neckers, D. *Photochem. Photobiol. Sci.* **2009**, *8*, 34.

-
- ⁶⁶ Berg, O.; Chronister, E. L.; Yamashita, T.; Scott, G. W.; Sweet, R. M.; Calabrese, J. *J. Phys. Chem. A*, **1999**, *103*, 2451.
- ⁶⁷ Zade, S. S.; Zamoshcik, N.; Reddy, A. R.; Fridman-Marueli, G.; Sheberla, D.; Bendikov, M. *J. Am. Chem. Soc.* **2011**, *133*, 10803.
- ⁶⁸ Pramanik, C.; Doctoral Dissertation, University of New Hampshire, Durham, NH, **2011**.
- ⁶⁹ Chan, J.; Hodgson, J.; Lin, W.; Miller, G. *Synthesis, characterization and photorearrangements of 6-phenylthiopentacene*. Manuscript in preparation.
- ⁷⁰ Scott, A. P.; Radom, L. *J. Phys. Chem.* **1996**, *100*, 16502.
- ⁷¹ Zhao, Y.; Schultz, N. E.; Truhlar, D. G. *J. Chem. Theory Comput.* **2006**, *2*, 364.
- ⁷² Zhao, Y.; Truhlar, D. G. *Acc. Chem. Res.* **2008**, *41*, 157.
- ⁷³ See for example Steinfeld, J. I.; Francisco, J. S.; Hase, W. L. *Chemical Kinetics and Dynamics*; Prentice Hall: Englewood Cliffs, NJ, 1989.
- ⁷⁴ Eckart, C. *Phys. Rev.* **1930**, *35*, 1303.

APPENDICES

^1H NMR

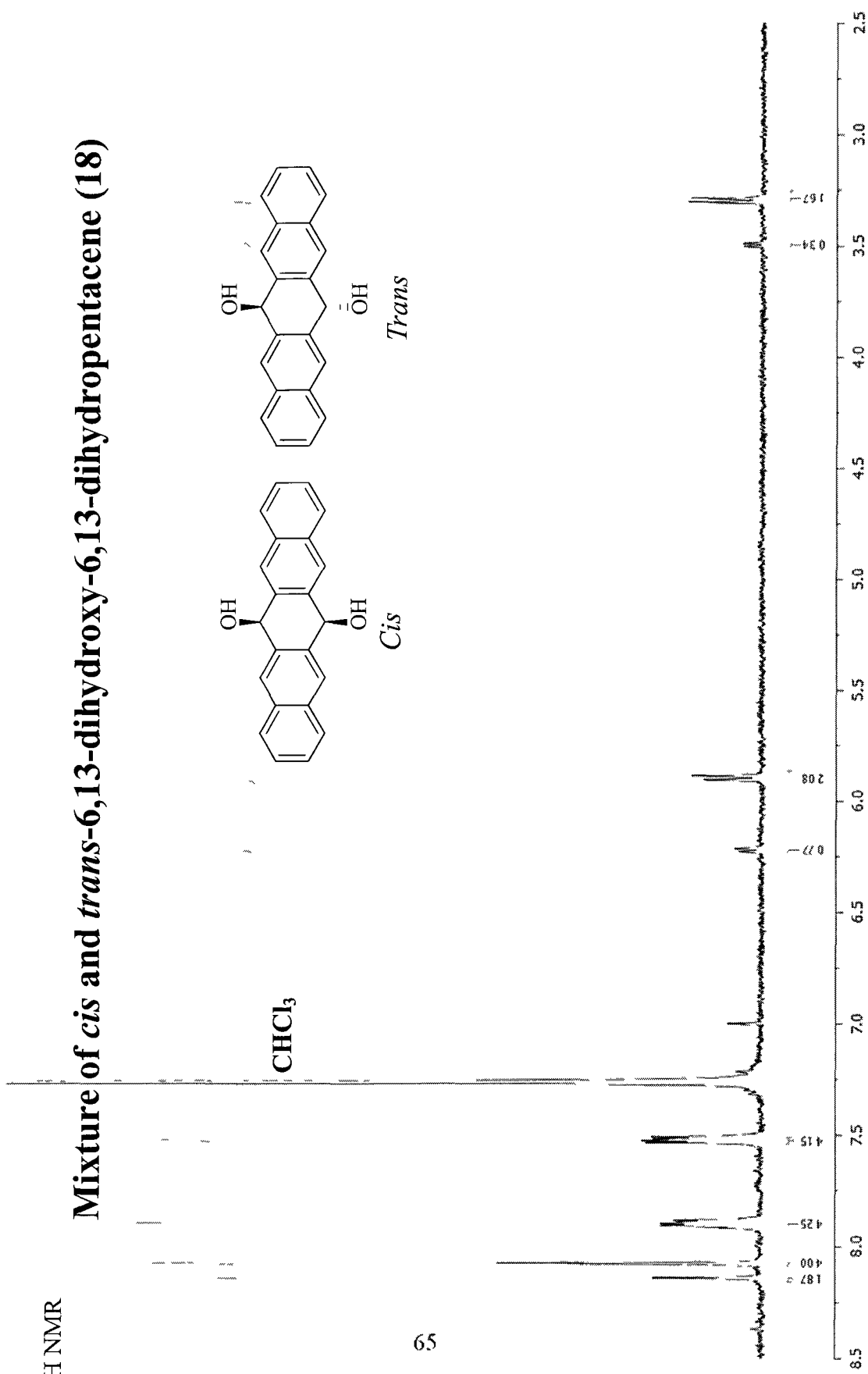
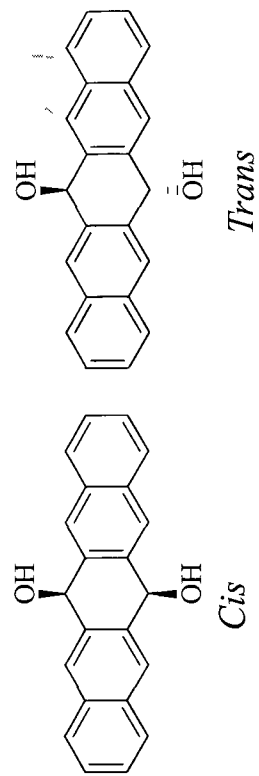
6,13-Pentacenequinone (17)



64

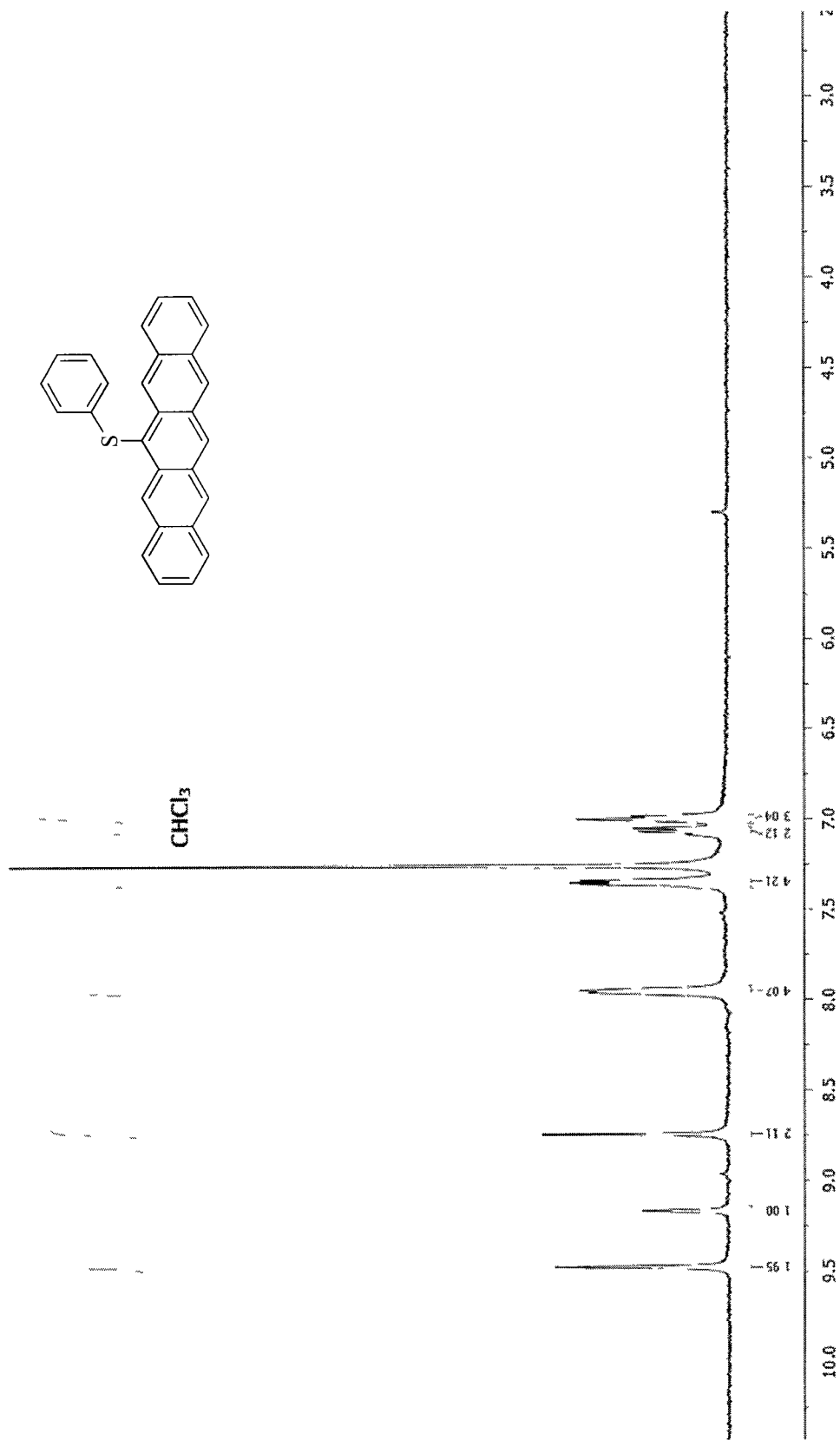
¹H NMR

Mixture of *cis* and *trans*-6,13-dihydroxy-6,13-dihydropentacene (18)



$^1\text{H NMR}$

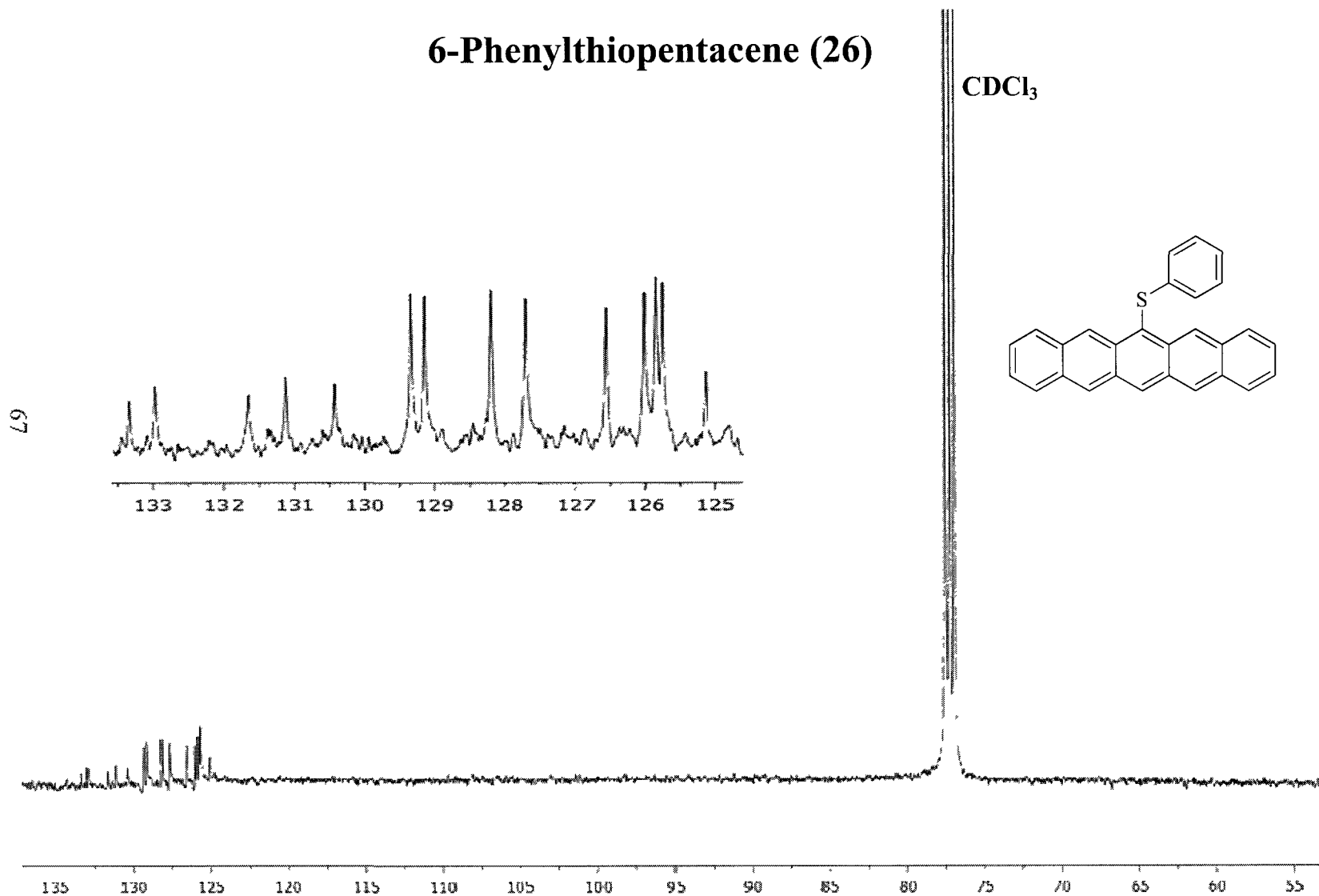
6-Phenylthiophentacene (26)



^{13}C NMR

6-Phenylthiopentacene (26)

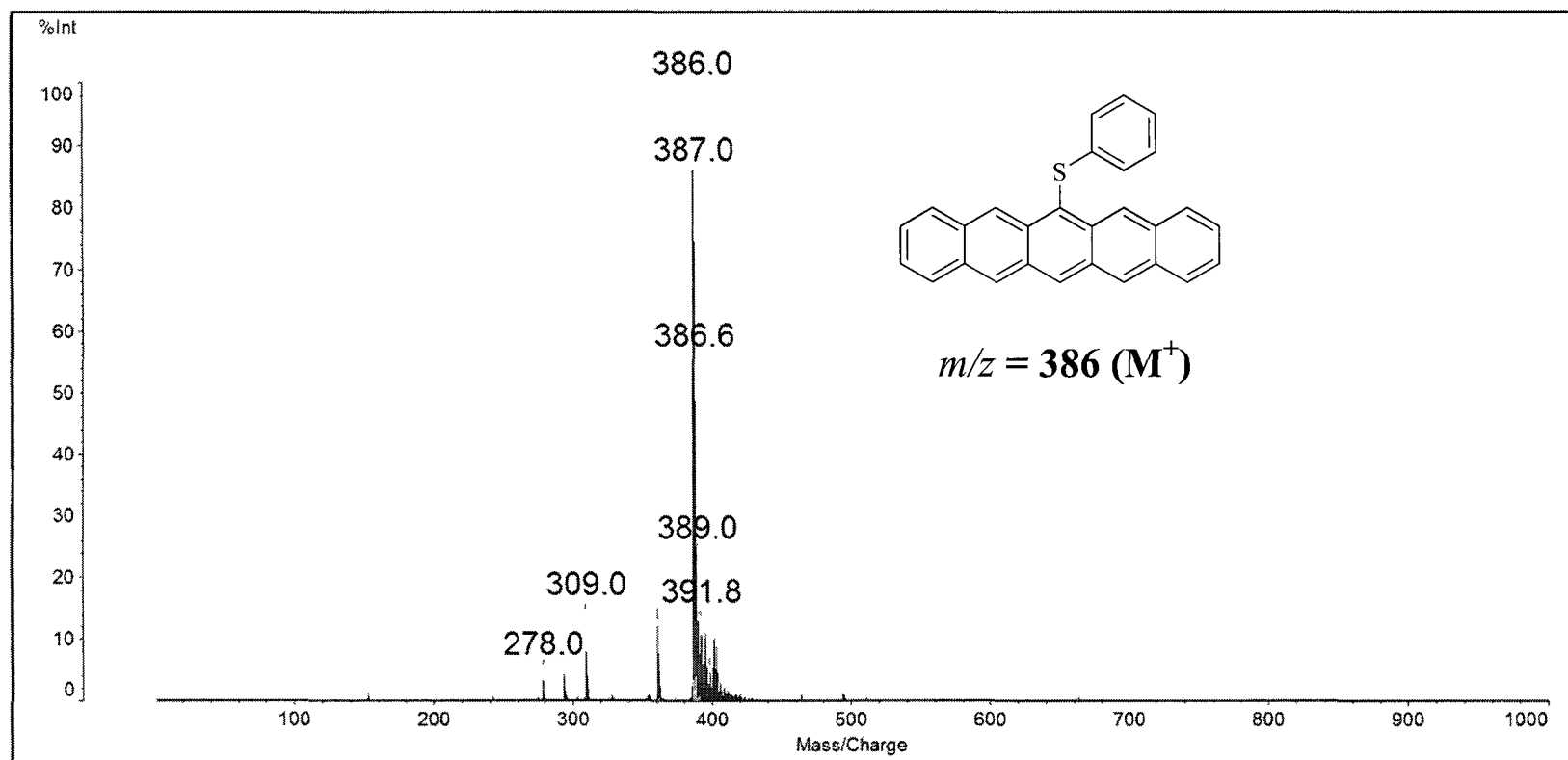
CDCl_3



LDI-MS

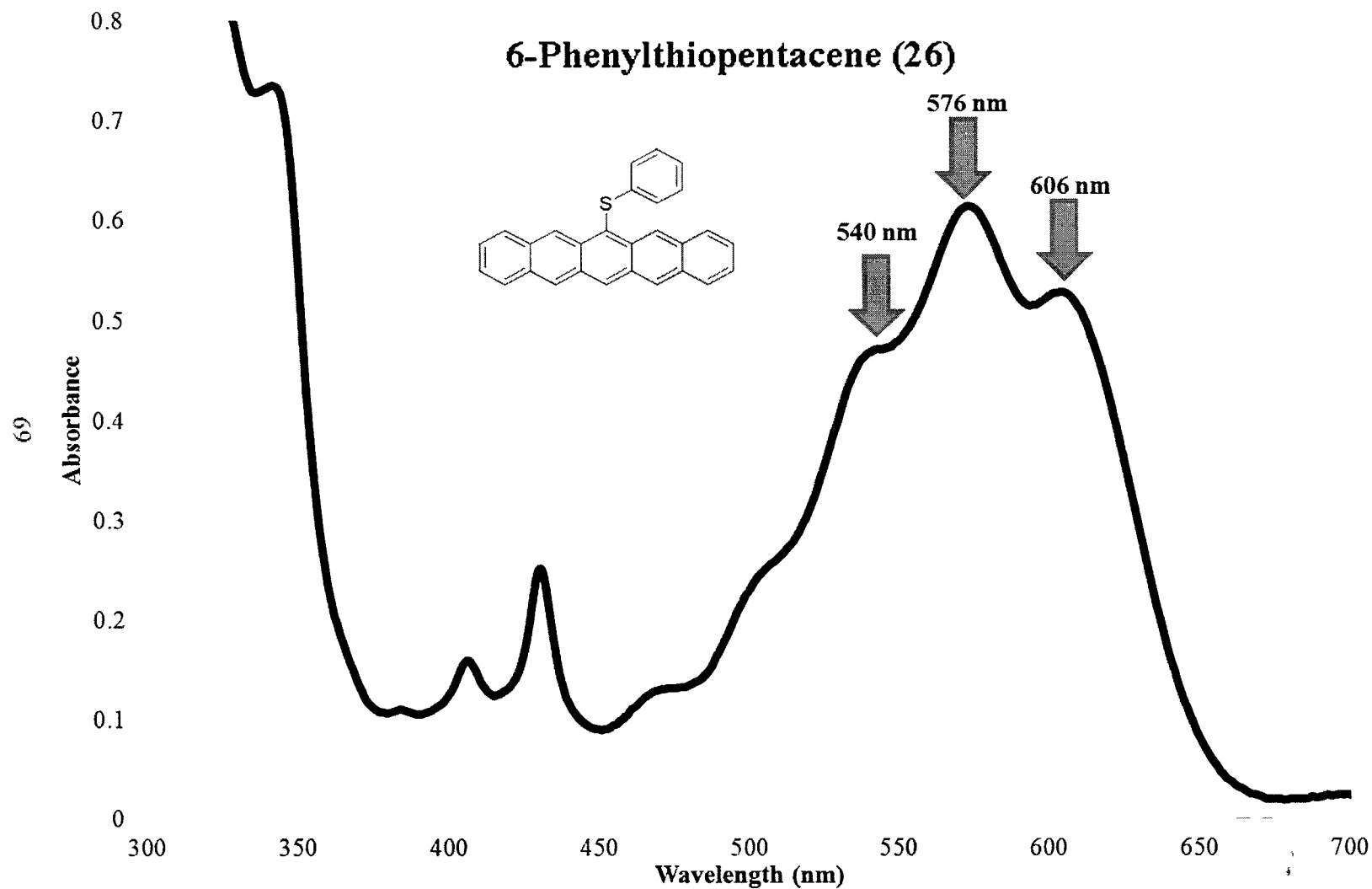
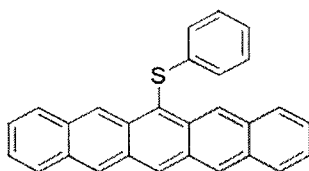
6-Phenylthiopentacene (26)

89



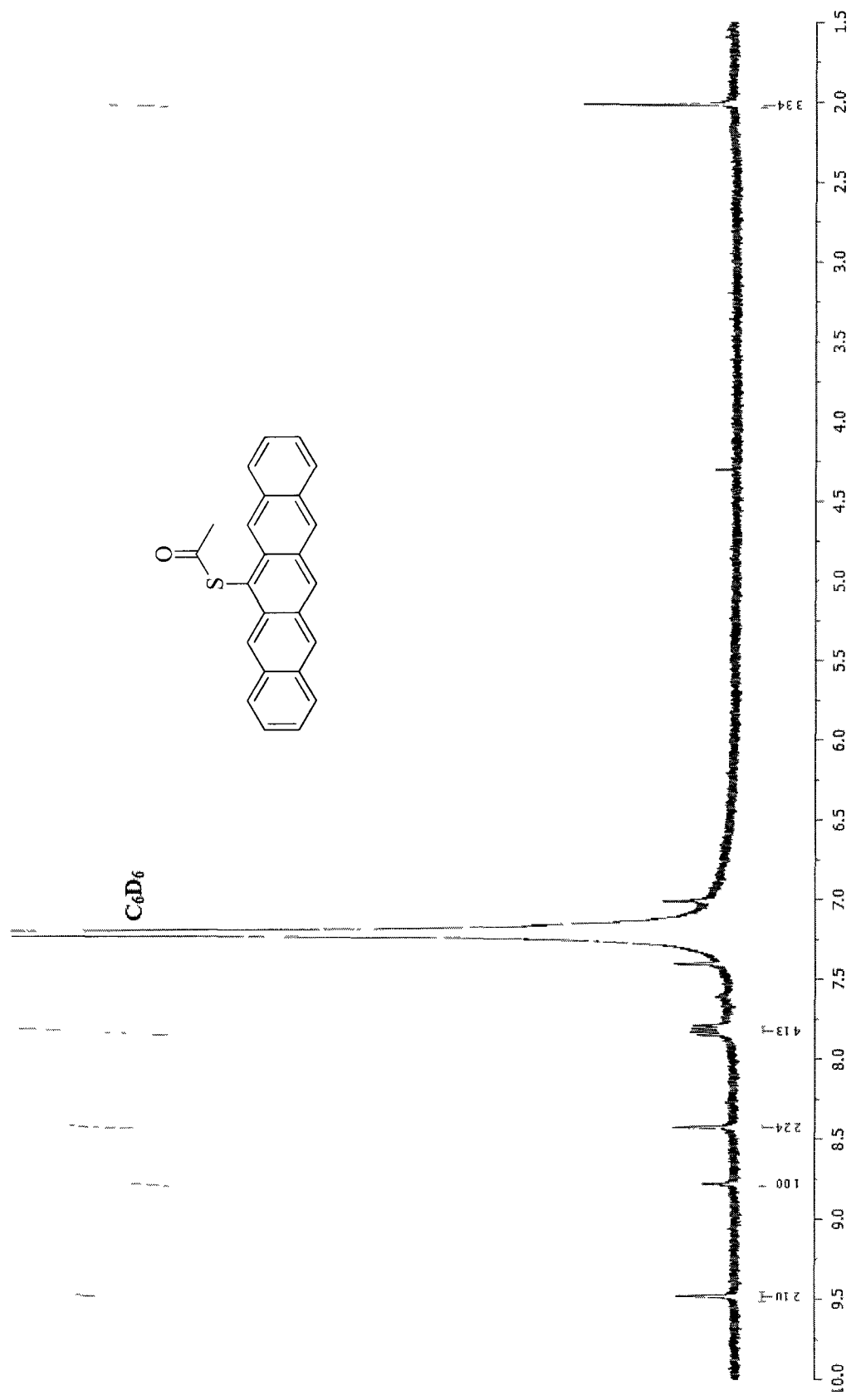
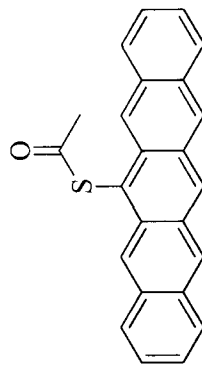
UV-Vis

6-Phenylthiopentacene (26)



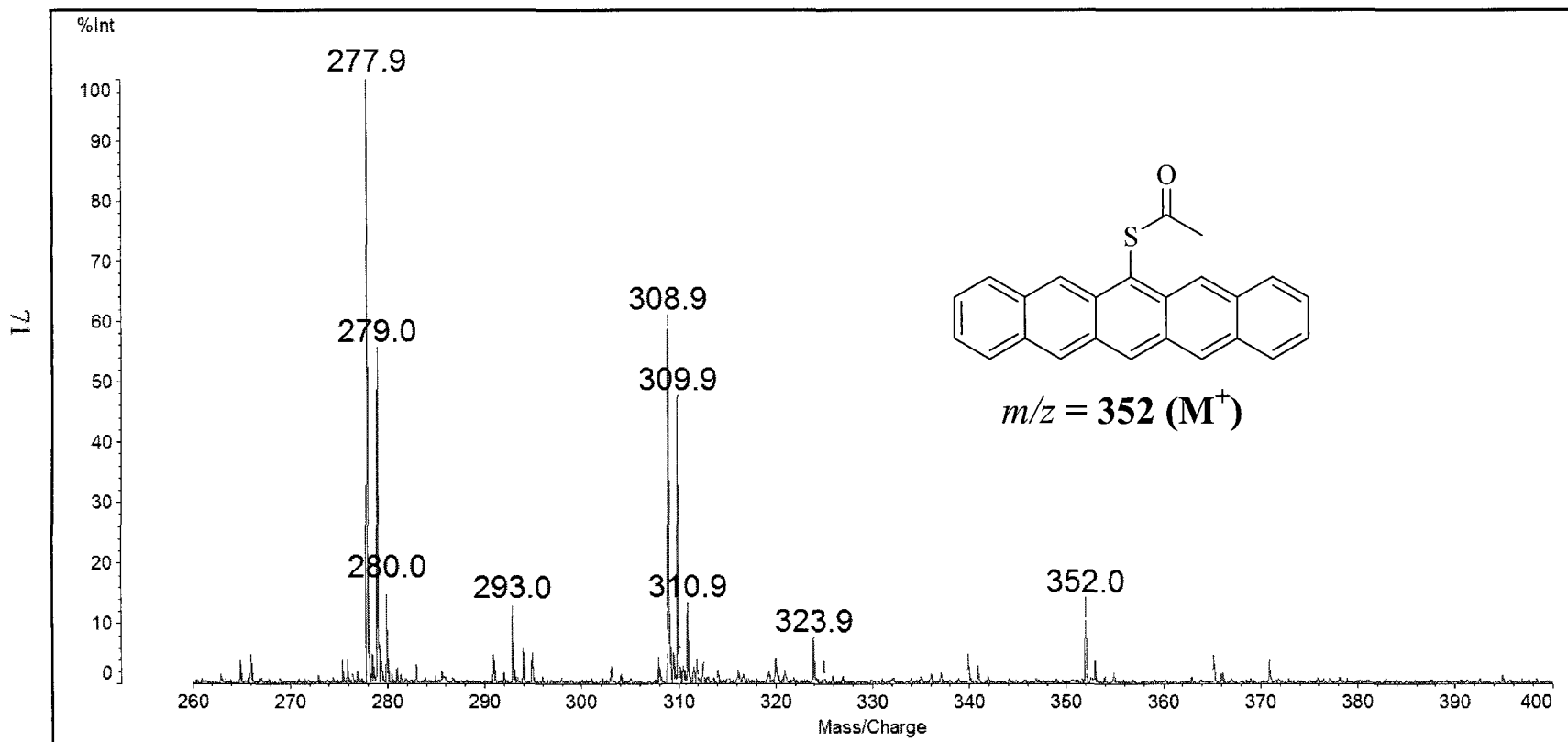
¹H NMR

6-Acetylthiophentacene (27)



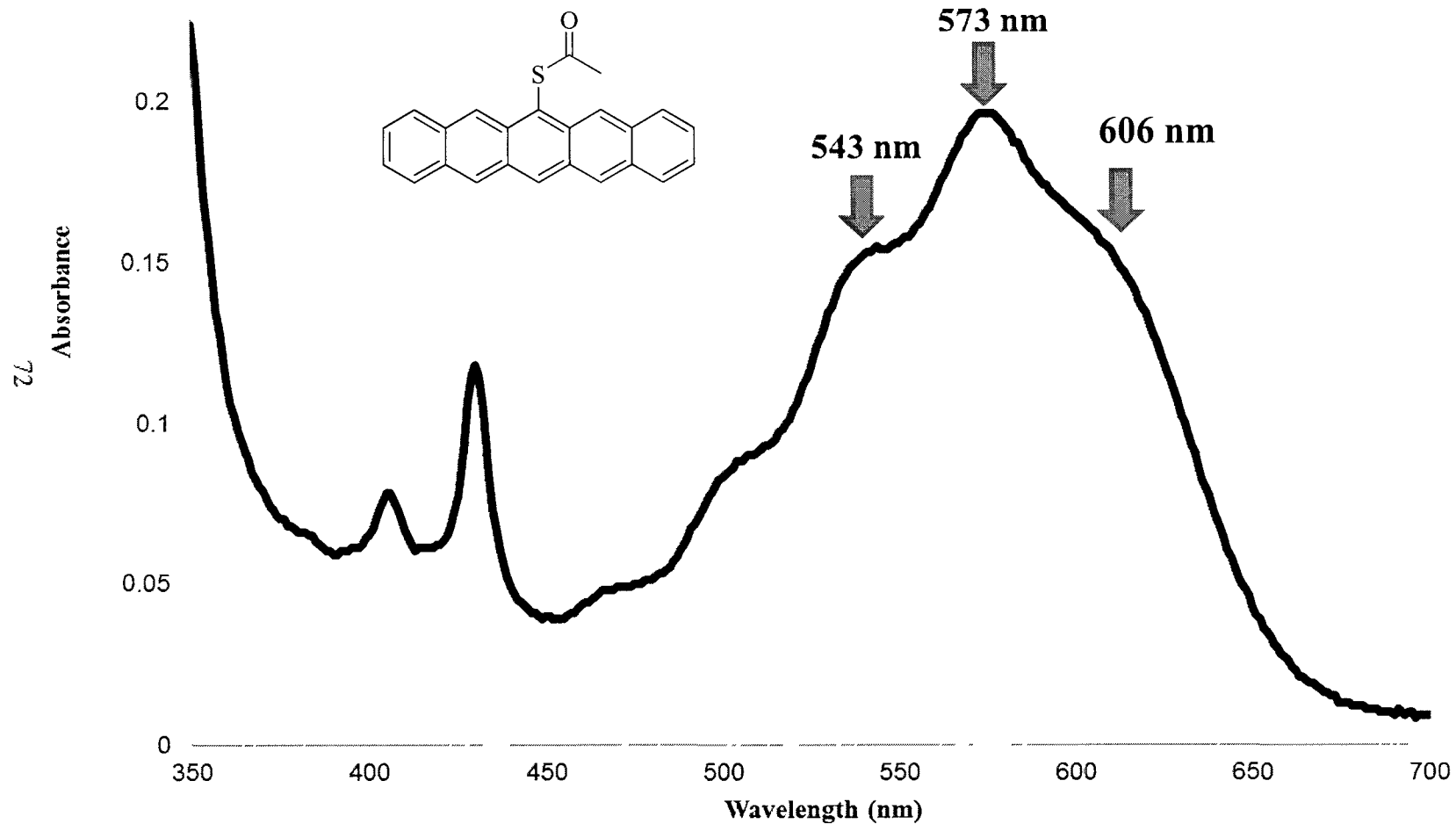
LDI-MS

6-Acetylthiopentacene (27)



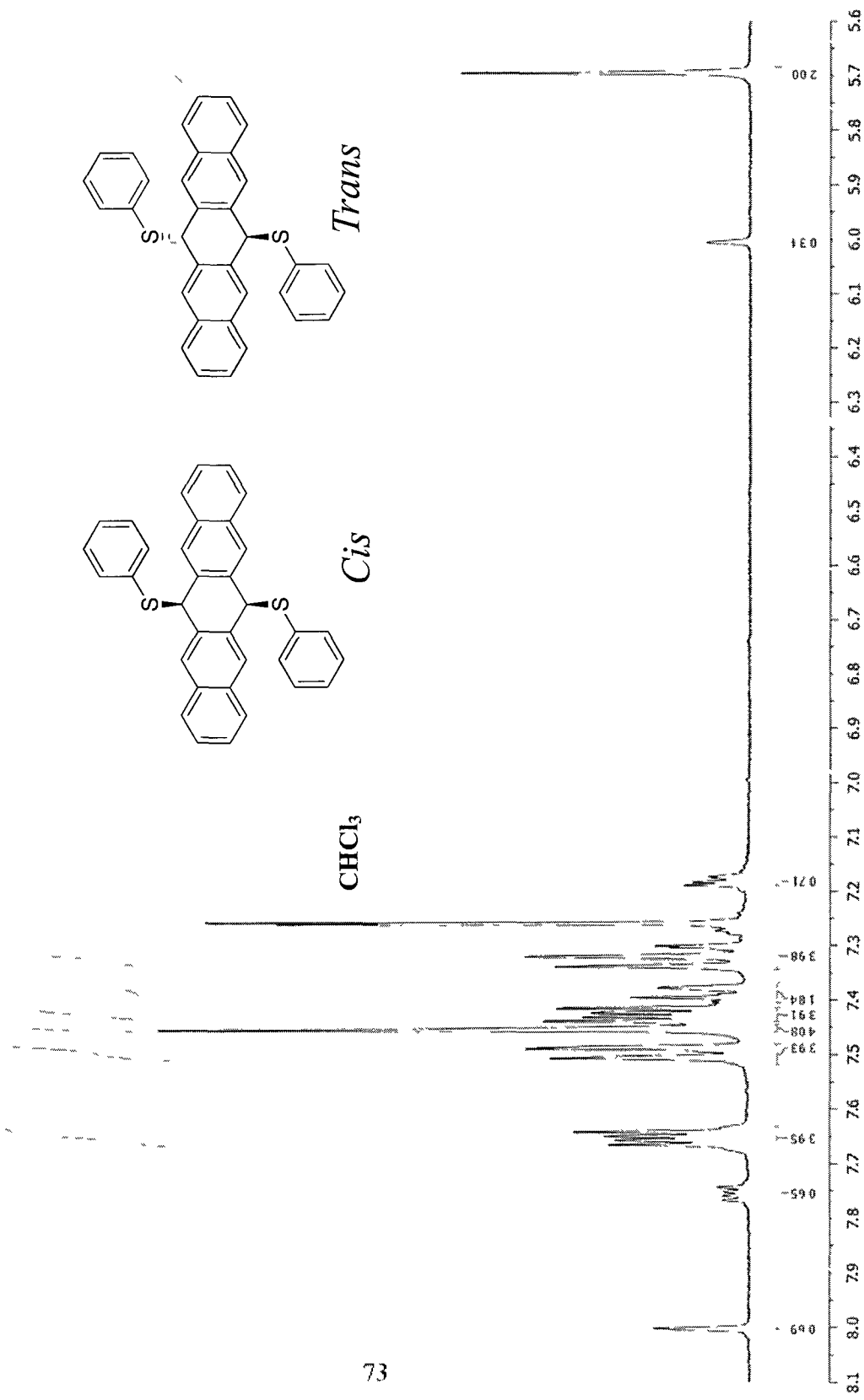
UV-Vis

6-Acetylthiopentacene (27)



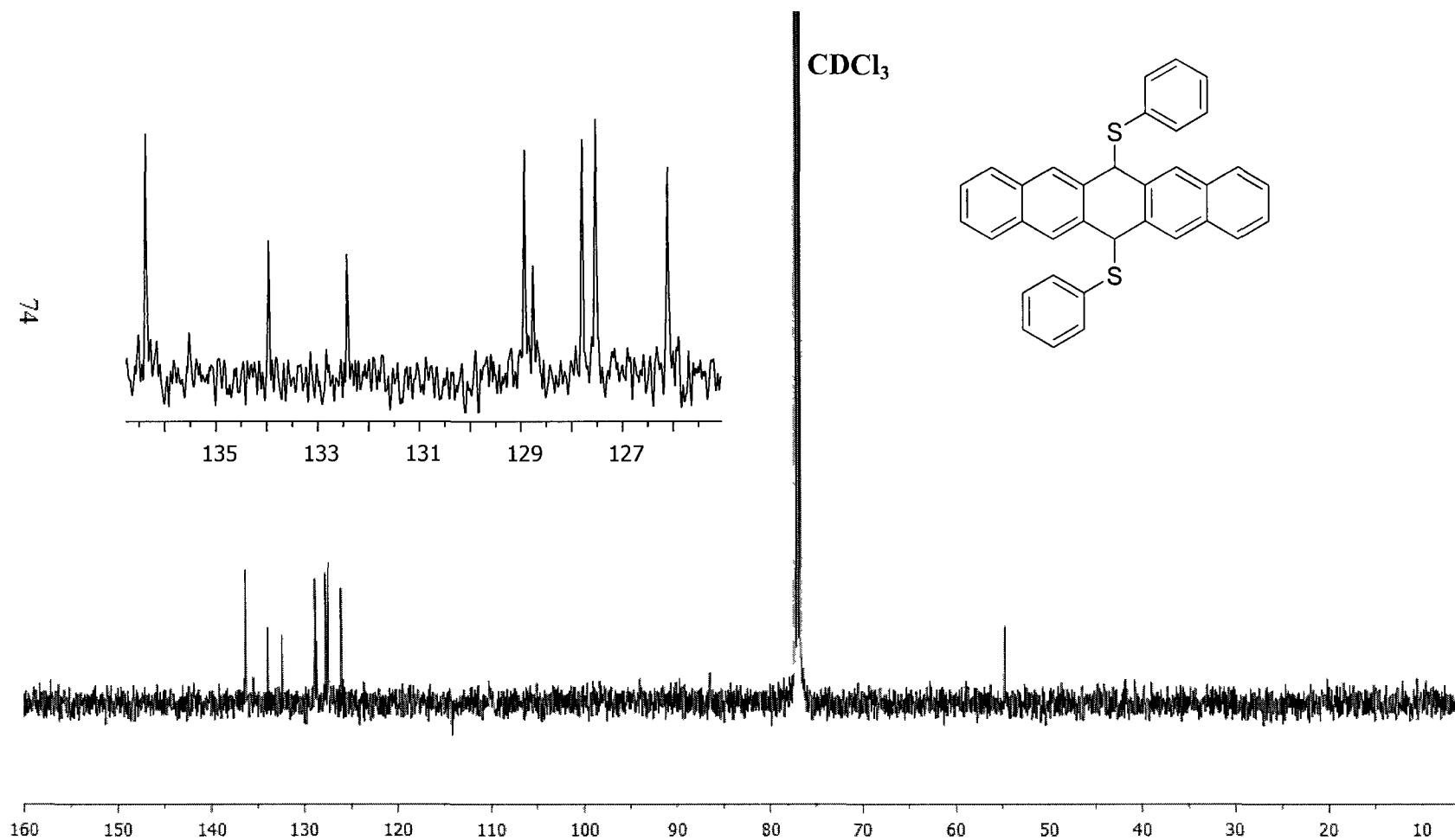
^1H NMR

Mixture of *cis* and *trans*-6,13-bis(phenylthio)-6,13-dihydropentacene (29)



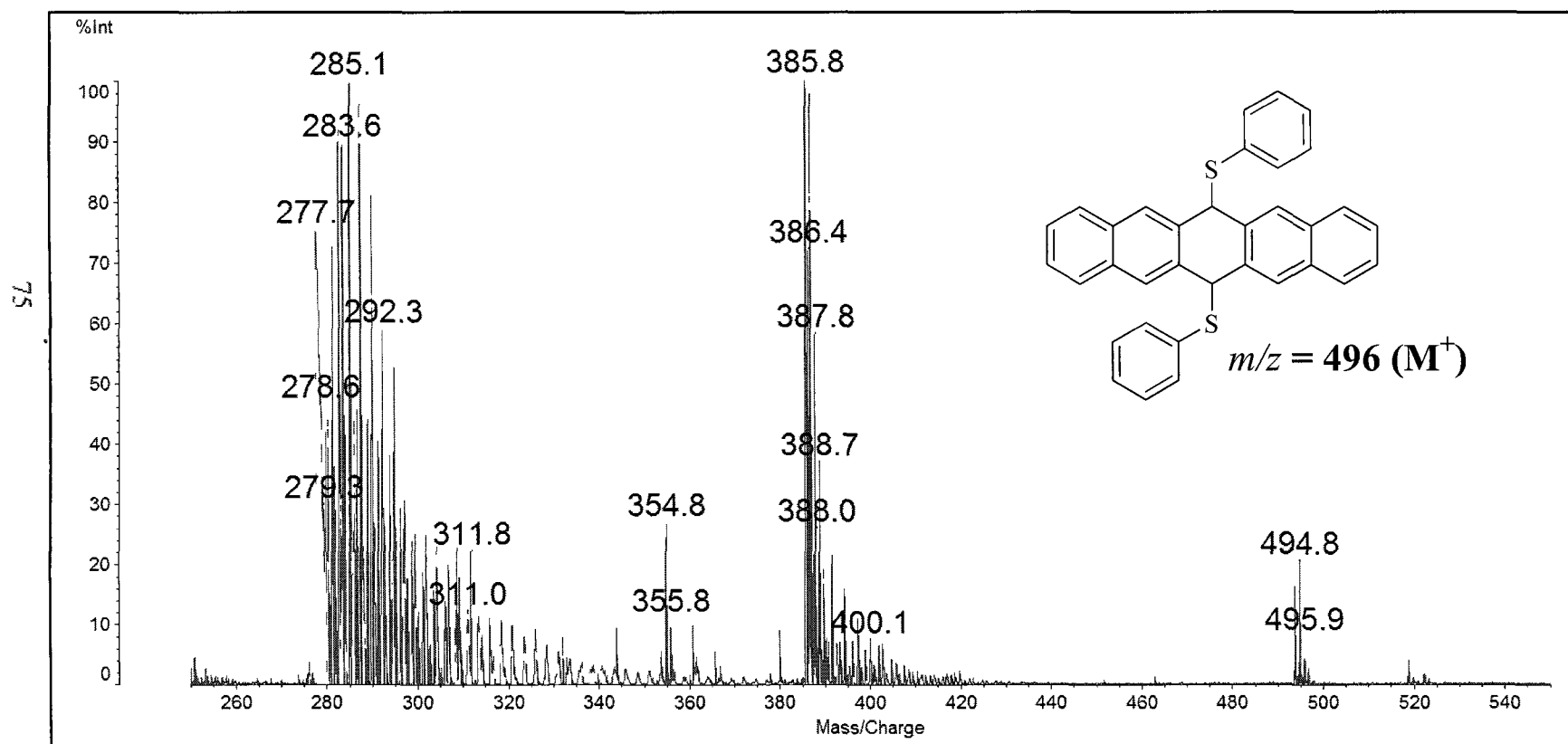
^{13}C NMR

6,13-Bis(phenylthio)-6,13-dihydropentacene (29) (single isomer)



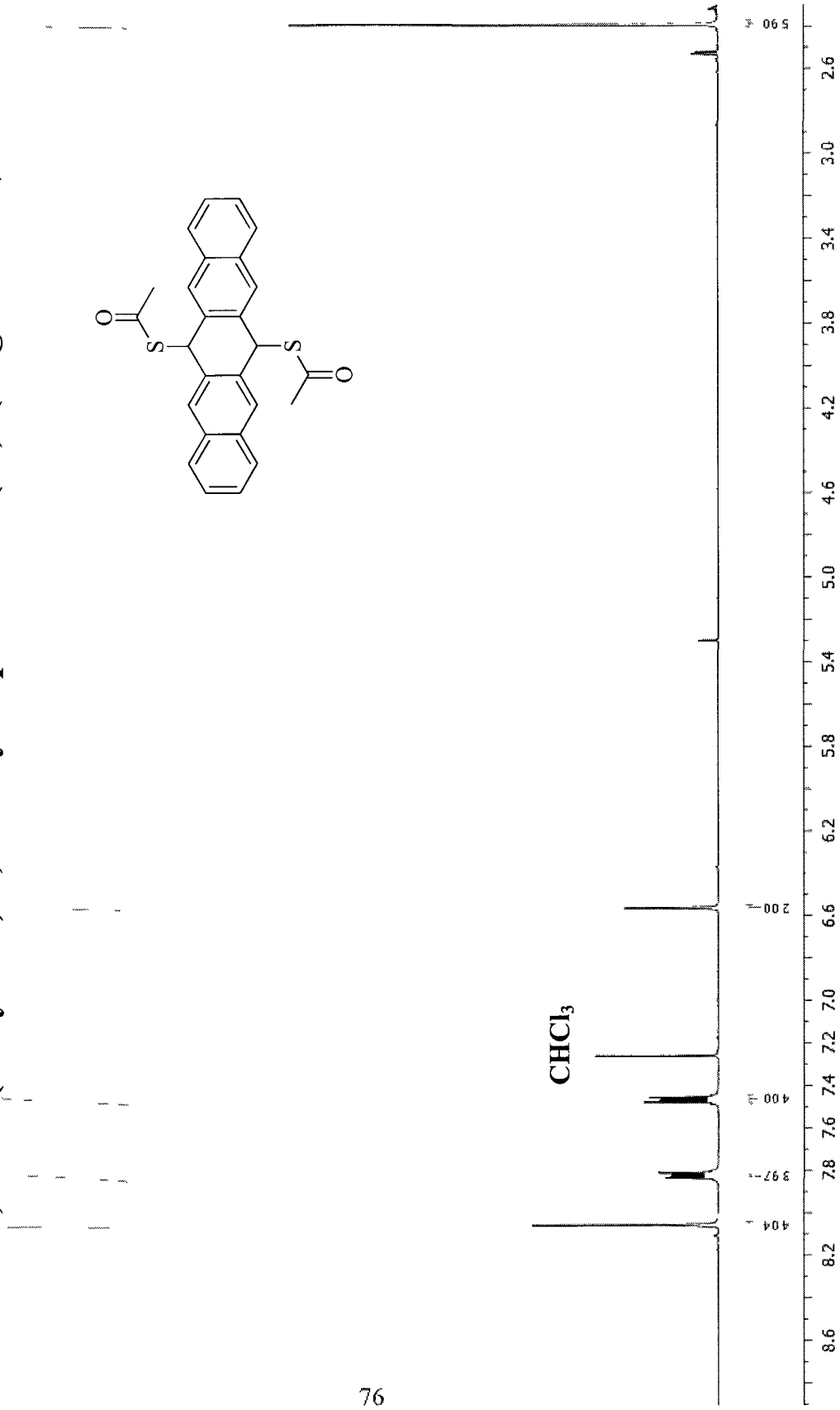
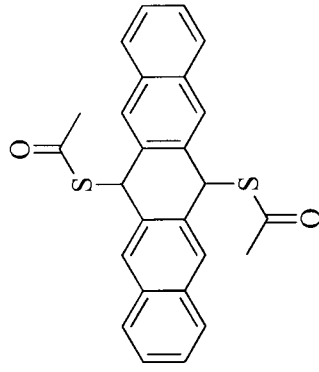
MALDI-MS

Mixture of *cis* and *trans*-6,13-bis(phenylthio)-6,13-dihydropentacene (29)



$^1\text{H NMR}$

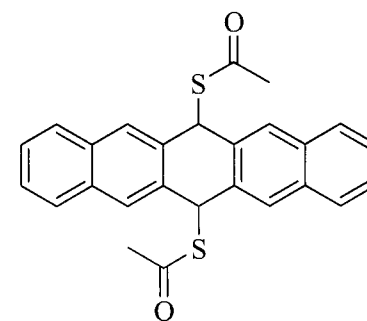
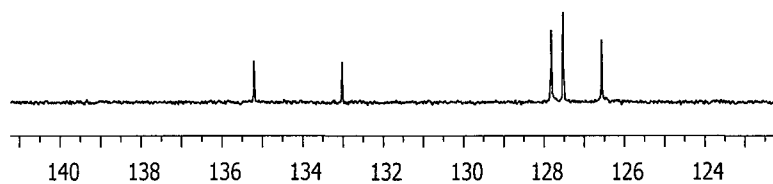
6,13-Bis(acetylthio)-6,13-dihydropentacene (30) (single isomer)



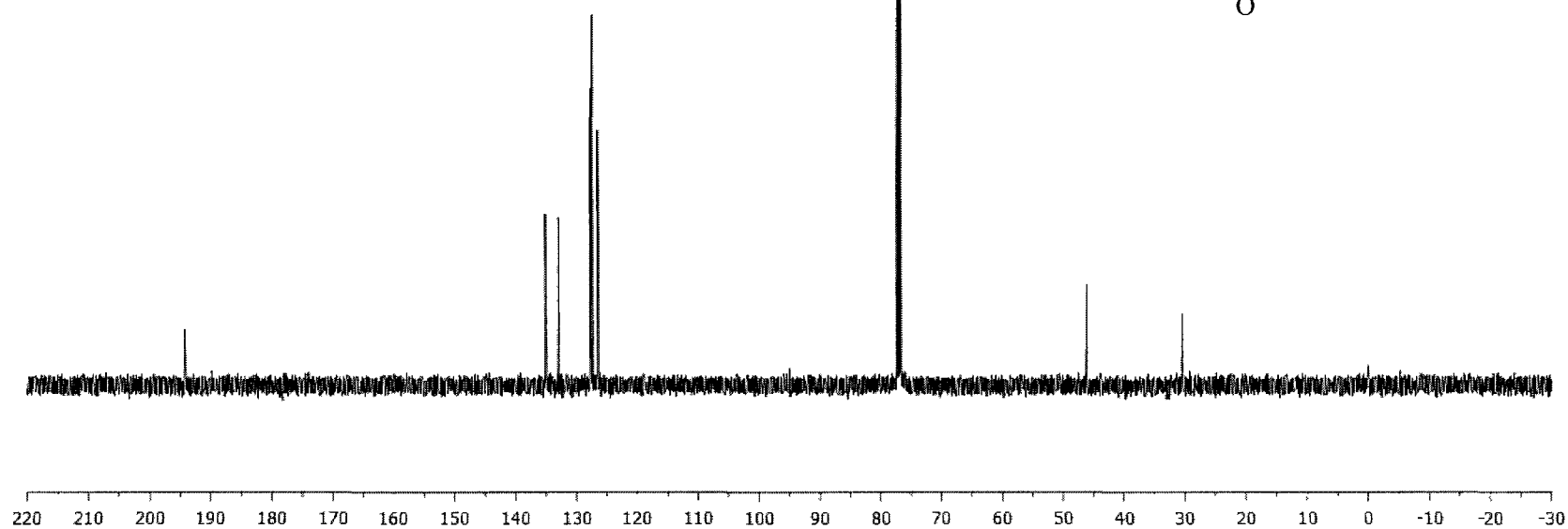
^{13}C NMR

6,13-Bis(acetylthio)-6,13-dihydropentacene (30) (single isomer)

CDCl_3

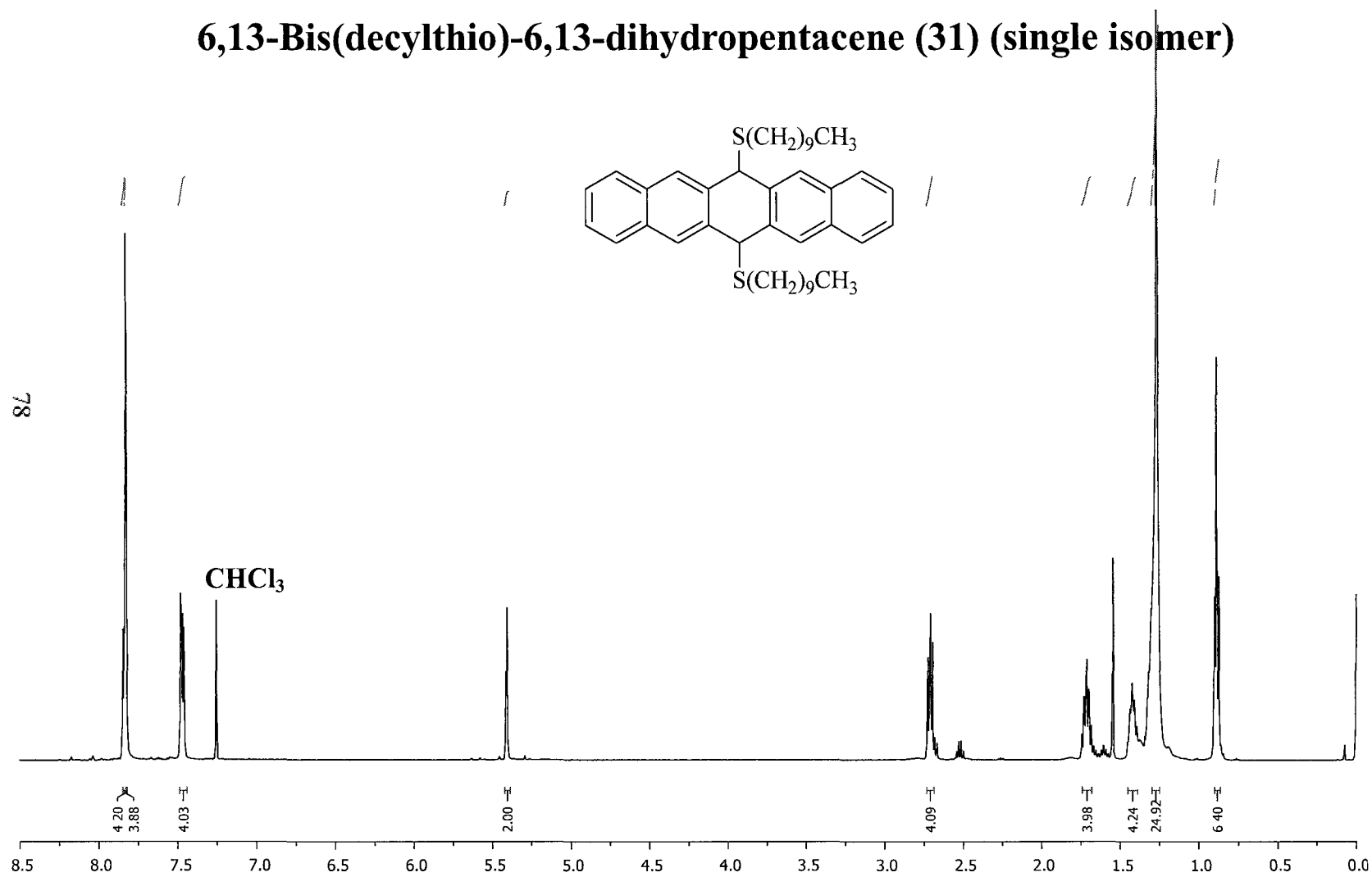


77



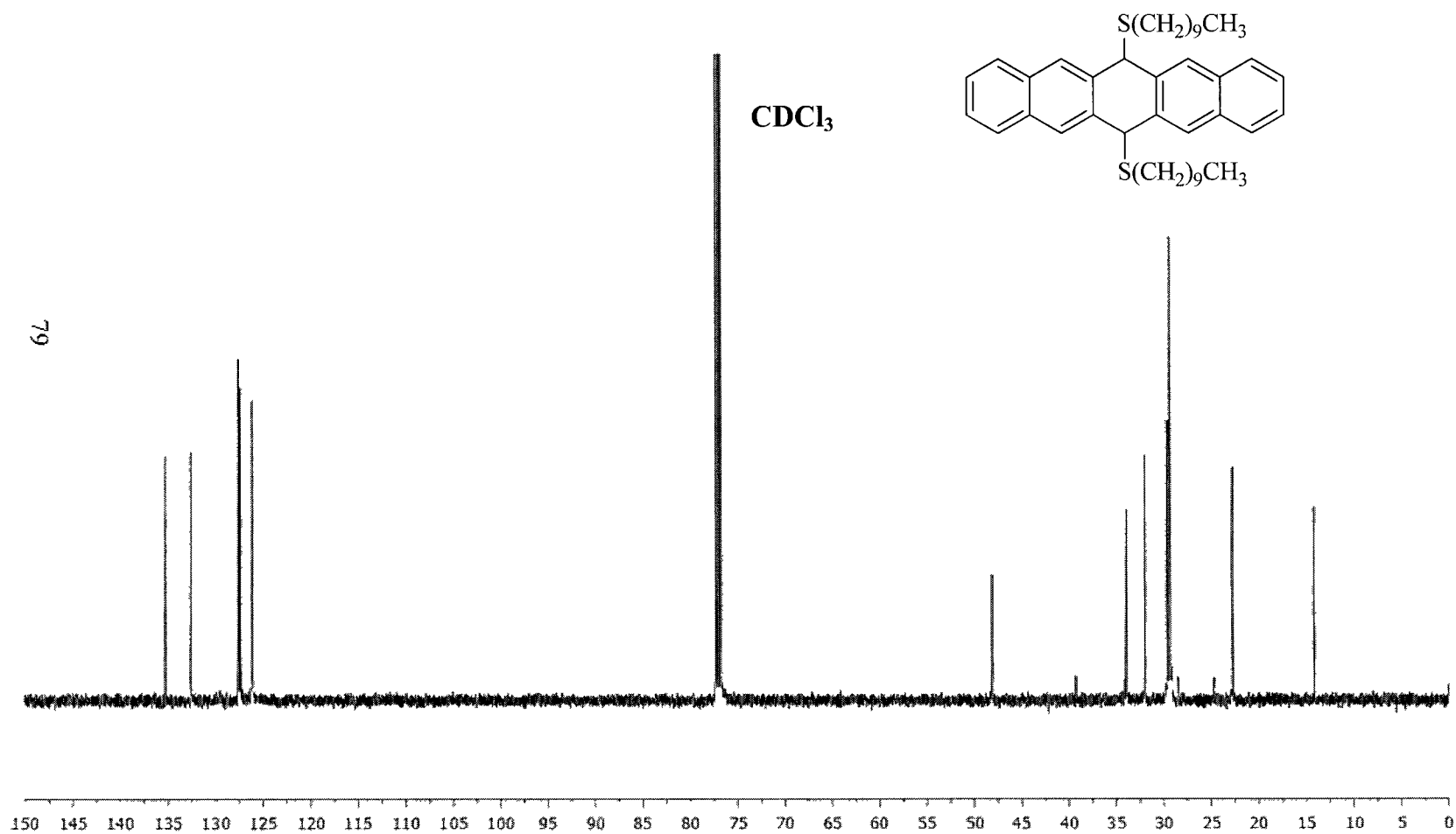
^1H NMR

6,13-Bis(decylthio)-6,13-dihydropentacene (31) (single isomer)



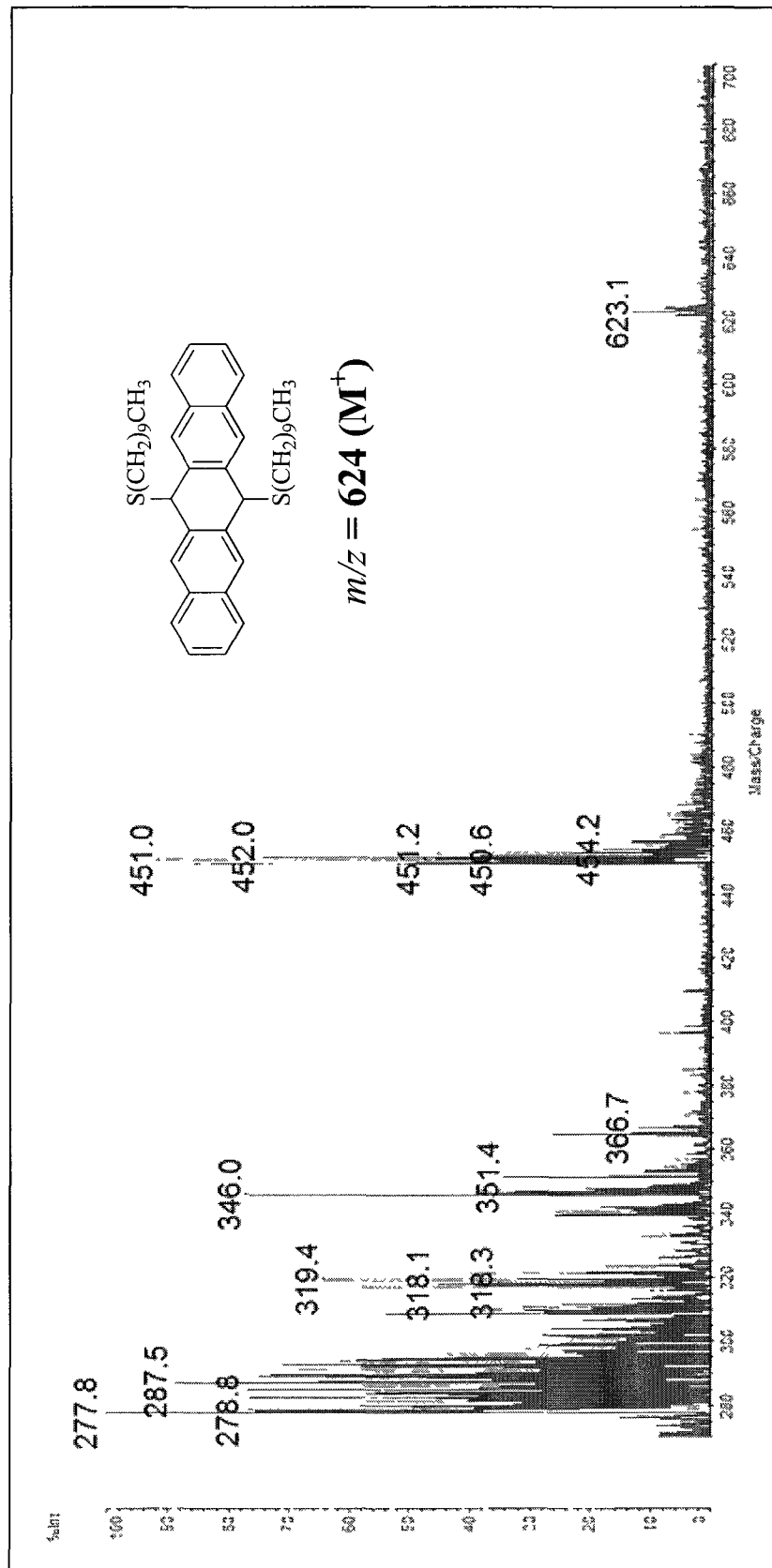
^{13}C NMR

6,13-Bis(decylthio)-6,13-dihydropentacene (31) (single isomer)



LDI-MS

6,13-Bis(decylthio)-6,13-dihydropentacene (31) (single isomer)



LDI-MS

6,13-Bis(phenylthio)pentacene (32)

81

